

**DEVELOPMENT OF AN ELECTRONIC VISUAL AID FOR MONOCULAR  
VISUAL IMPAIRED PATIENTS**

**By**

**NIRVENESH A/L RAVINDRAN**

**Thesis Submitted to the College of Graduate Studies, Universiti Tenaga  
Nasional, in Fulfilment of the Requirements for the Master of Mechanical  
Engineering**

**April 2020**

## **DECLARATION**

I hereby declare that the thesis is my original work except for quotations and citations which have been duly acknowledged. I also declare that it has not been previously, and is not concurrently submitted for any other degree at Universiti Tenaga Nasional or at any other institutions. This thesis may be made available within the university library and may be photocopied and loaned to other libraries for the purpose of consultation.

---

**NIRVENESH A/L RAVINDRAN**

31<sup>st</sup> April 2020

## ABSTRACT

The purpose of this research is to develop a working prototype of a visual aid for monocular visual impaired patients. Monocular visual impaired patients most commonly do not have the ability to obtain 3-dimensional visualization on their surroundings and have a reduced field of vision. The primary function of this prototype is to increase the field of vision by at least 20%, as it is the minimum gain of visual field based on previous studies and to enable them to have depth perception on their surroundings. The research was started by understanding the requirements of patients and healthcare professionals through surveys and interviews at Tun Hussein Onn Eye Hospital. A house of quality was then constructed to analyse the data that was obtained. A total of three phases of development of prototype was conducted to develop this prototype. Each phase of the development was separated into hardware and software, in terms of hardware, the designs were analysed and the suitable microcontrollers were developed. In terms of software, the algorithms for the field of vision and depth perception was focused. Each phase of development underwent feedback review from healthcare professionals. The final phase of the prototype was tested on real patients at the hospital with two setup apparatus to justify both the objective, it was found that the angle of field of vision has increased from an average of 110 degrees to an average of 176 degree, which is an increase in field of vision by 60% and the depth perception was evident for all 100% of patients that used the visual aid. A final cost analysis was also conducted to reduce and justify the current cost of the visual aid which costs less than RM750.00 which are cheaper than current treatment costs of monocular visual impairment in a year. In a nutshell, this research has successfully developed a cost-efficient visual aid for monocular visual impaired patients to have depth perception and a huge increase in the field of vision.

## **ACKNOWLEDGEMENT**

First, I am also truly grateful to my supervisor, Dr Hassan Mohamed, without whom it would have been impossible for me to complete my master's project. Thank you for showing such unceasing patience, guidance and sharing the knowledge. His guidance in this project was vital and he guided me the way to successfully complete this project.

I would like to also thank Yayasan Canselor Uniten (YCU) for granting me to complete my master's project financially. I would like to express my deepest gratitude to all the wonderful soul that stood by me and gave me all the support to complete this my master's project.

Also not forgetting my parents G.Ravindran and A.Mageswary who struggle hard to see me achieving my dream, my parents who have been supporting me endlessly with a touch of family love towards me. I owe a gratitude to my family and friends who give their unlimited moral support, guidance and encouragement.

Finally, I would like to thank all my lecturers and friends who have taught me and those who have assisted directly or indirectly throughout my studies. I owe it to all of them. THANK YOU.

## TABLE OF CONTENTS

	<b>Page</b>
<b>TITLE PAGE</b>	i
<b>DECLARATION</b>	ii
<b>ABSTRACT</b>	iii
<b>ACKNOWLEDGEMENT</b>	iv
<b>TABLE OF CONTENTS</b>	v
<b>LIST OF TABLES</b>	x
<b>LIST OF FIGURES</b>	xii
<b>LIST OF SYMBOLS</b>	xvi
<b>LISTS OF ABBREVIATIONS</b>	xvii
<b>LIST OF PUBLICATIONS</b>	xviii
<b>CHAPTER 1: INTRODUCTION</b>	1
1.1 Research Background	1
1.2 Problem Statement	7
1.3 Research Objectives	8
1.4 Research Scope	8
1.5 Thesis Overview	10
<b>CHAPTER 2: LITERATURE REVIEW</b>	11
2.1 Introduction	11
2.2 Medical Conditions	11
2.3 Existing Treatments for Monocular Visual Impaired Patients	14
2.4 Stereoscopic Cameras and Algorithms	21
2.5 Depth Maps	23
2.6 Application of Electronic Glasses	32
2.7 Previous Works Associated with the Development of the Monocular Visual Aid	36
2.8 Summary	38

<b>CHAPTER 3: METHODOLOGY</b>	39
3.1 Introduction	39
3.2 Research Design	39
3.3 Research Process	40
3.4 Design of Survey Questions	41
3.5 Extensive Survey with Healthcare Practitioners and Patients	41
3.6 Collecting and Analysing the Data (House of Quality)	43
3.7 Development of Working Prototype	44
3.7.1 <i>Development of Working Prototype Phase 1</i>	45
3.7.1.1 Hardware Development	45
3.7.1.2 Software Development	49
3.7.1.3 Preparing the Design of Prototype 1	51
3.7.1.4 Integrating Design into a Working Prototype 1	56
3.7.2 <i>Development of Working Prototype Phase 2</i>	57
3.7.2.1 Calibration of Stereo Cameras	58
3.7.2.2 Preparing the Design of Prototype 2	59
3.7.2.3 Integrating Design into a Working Prototype 2	62
3.7.3 <i>Development of Working Prototype Phase 3</i>	62
3.7.3.1 Preparing the Design of Prototype 3	64
3.7.3.2 Integrating Design into a Working Prototype 3	68
3.8 Testing of visual aid	69
3.8.1 <i>Field of Vision</i>	70
3.8.1.1 Visual Field Measurement	70
3.8.2 <i>The Depth Map on the Visual Aid</i>	72
3.8.3 <i>The Usability of the Visual Aid</i>	73
3.9 Cost Analysis	73
3.10 Summary	74

<b>CHAPTER 4: ANALYSIS AND DISCUSSION</b>	76
4.1 Introduction	76
4.2 Profile of Respondents and Related Details	76
4.2.1 <i>Visual Impaired Patient Respondents</i>	77
4.3 Feedback from Medical Professionals	81
4.3.1 <i>Feedback from Monocular Visual Impaired Patients</i>	82
4.3.2 <i>Analysis of the House of Quality</i>	84
4.4 Development of Working Prototype 1	86
4.4.1 <i>Design Analysis</i>	87
4.4.1.1 Von Mises Stress Study	88
4.4.1.2 Resultant Displacement Study	90
4.4.1.3 Equivalent Strain Analysis	91
4.4.2 <i>Integration of Visual Aid Design Structure and Stereoscopic Camera System</i>	93
4.4.3 <i>Cost Analysis</i>	94
4.4.4 <i>Visual Aid Output</i>	95
4.4.5 <i>User Feedback</i>	96
4.5 Development of Working Prototype 2	96
4.5.1 <i>Design Analysis</i>	97
4.5.1.1 Von Mises Stress Study	99
4.5.1.2 Resultant Displacement Study	101
4.5.1.3 Equivalent Strain Analysis	102
4.5.2 <i>Integration of Visual Aid Design Structure and Stereoscopic Camera System</i>	103
4.5.3 <i>Cost Analysis</i>	104
4.5.4 <i>Visual Aid Output</i>	105
4.5.5 <i>Result of Testing Prototype 2</i>	106
4.5.5.1 Results of Field of vision	106
4.5.5.2 Analysis of Field of vision	108
4.5.5.3 Results of Depth Perception	110

4.6	Development of Working Prototype 3	112
4.6.1	<i>Design Analysis</i>	112
4.6.1.1	Von Mises Stress Study	113
4.6.1.2	Resultant Displacement Study	115
4.6.1.3	Equivalent Strain Analysis	116
4.6.2	<i>Integration of Visual Aid Design Structure and Stereoscopic Camera System</i>	117
4.6.3	<i>Cost Analysis</i>	118
4.6.4	<i>Visual Aid Output</i>	120
4.6.5	<i>Result of Testing Prototype 3</i>	121
4.6.5.1	Results of Field of vision	121
4.6.5.2	Analysis of Field of vision	122
4.6.5.3	Results of Depth Perception	124
4.8	Summary	125
<b>CHAPTER 5: CONCLUSION AND RECOMMENDATION</b>		128
5.1	Overview	128
5.2	Conclusion	128
5.3	Recommendations	130
<b>REFERENCES</b>		132
<b>APPENDIX A INTERVIEW QUESTIONS (Patient)</b>		141
<b>APPENDIX B INTERVIEW QUESTIONS (Medical Professional)</b>		142
<b>APPENDIX C DETAILED INTERFACE OF THE WAVESHARE COMPUTE MODULE IO BOARD</b>		143
<b>APPENDIX D PRESET STUDY OF PROTOTYPE 1</b>		145
<b>APPENDIX E PRESET STUDY OF PROTOTYPE 2</b>		150
<b>APPENDIX F PRESET STUDY OF PROTOTYPE 3</b>		154

<b>APPENDIX G ORTHOGRAPHIC AND EXPLODED VIEW DRAWINGS OF PROTOTYPE 1</b>	158
<b>APPENDIX H FEEDBACK FORMS</b>	160
<b>APPENDIX I ORTHOGRAPHIC AND EXPLODED VIEW DRAWINGS OF PROTOTYPE 2</b>	162
<b>APPENDIX J RESEARCH PHOTOS AT TAIPING HOSPITAL</b>	164
<b>APPENDIX K ORTHOGRAPHIC AND EXPLODED VIEW DRAWINGS OF PROTOTYPE 3</b>	165
<b>APPENDIX L RESEARCH PHOTOS AT TUN HUSSEIN ONN EYE HOSPITAL (THONEH)</b>	167
<b>BIOGRAPHY OF AUTHOR</b>	168

## LIST OF TABLES

Table No.		Page
2.1	Summary of Existing Treatment For Monocular Visual Impaired Patients	16
2.2	Uncalibrated Parameters of Stereoscopic Cameras	22
2.3	Calibrated Parameters of Stereoscopic Cameras noting that Parameters $F$ , $T_y$ , And $T_z$ are the same	23
2.4	Summary of Depth Map Generation Techniques	32
3.1	Profile of Medical Professional Respondents in the Survey	42
3.2	Statistical Factors for survey sample size	42
3.3	Material Properties of Prototype 1	52
3.4	Fixtures Applied on Prototype 1	53
3.5	Loads Applied on Prototype 1	54
3.6	Material Properties of Prototype 2	59
3.7	Fixtures Applied on Prototype 2	60
3.8	Loads Applied on Prototype 2	61
3.9	Material Properties of Prototype 3	65
3.10	Fixtures Applied on Prototype 3	66
3.11	Loads Applied on Prototype 3	67
3.12	Visual Aid Testing Cause and Effect table	69
4.1	Profile of Visual Impaired Patient Respondents in a Survey	77
4.2	Customer and Corresponding Functional Requirements	82
4.3	Cost Analysis Table of Prototype 1	94
4.4	Cost Analysis Table of Prototype 2	104
4.5	Table of Results for The Field of Vision For Prototype 2	106
4.6	Results of Depth Perception for Prototype 2	110
4.7	Cost Analysis Table of Prototype 3	118
4.8	Table of Results for The Field of Vision for Prototype 3	121

4.9	Results of Depth Perception for Prototype 3	124
4.10	Comparison Table of Prototype 1, 2 And 3	126

## LIST OF FIGURES

Figure No.		Page
1.1	Causes of Visual Impairment	1
1.2	Intraocular Pressure Exerted on Eye Resulting in Glaucoma	3
1.3	Visual Field with Monocular Vision	4
1.4	Stereoscopic Vision Angles	4
1.5	Amblyopic Patient with an Eye Patch	5
1.6	Binocular Vision (Stereopsis) Used in Perceiving Depth	6
2.1	Anisometropic Amblyopia	12
2.2	Tree Diagram of Monocular Visual Impairment	13
2.3	Randot Circles Chart	13
2.4	(A) Game Participants use a Stereoscope to Attain Alignment of the Eye and play the Dichoptic Game. (B) Nonius Lines are used to Align the Eyes, The Participants Are Requested to Align the Two Images Until A Cross Is Seen (C) Screenshot of the Game During the Dichoptic Training	15
2.5	(A) Ultrasonic Spectacles (B) Ultrasonic Waist Belt	17
2.6	Microcontroller Flow Chart	18
2.7	A Graph of Probability Detection Against Obstacle Size	19
2.8	Stand Magnifier with Handle and A Lighted Hand-Held Magnifier	20
2.9	Low Vision Calculator and Low Vision Telephone with Emergency Remote Pendant	21
2.10	UBC3V Datasets	24
2.11	Given an Input Depth Map, the 3D Body Pose is Estimated As A Linear Combination of Prototype Poses, where the Convolved Neural Network (Convnet) is in charge of Computing The Weight of Each Prototype	24

2.12	An Overview of The Proposed Model	25
2.13	Process of Depth Map Processing	26
2.14	(A) Left Image; (B) Right Image; (C) Disparity Map (D) 3D Model	27
2.15	Block Diagram of The MVD System	28
2.16	Test Sequence ‘Balloons’: (A) Texture Image ;(B) Depth Map; (C) Difference Between Original and Code Depth Map; (D) Difference in Virtual View after Depth Map Coding	30
2.17	Transforming an Outdoor Photograph into a Model-Like Look	31
2.18	Spectacle with Hearing Aid	33
2.19	Spectacle Frame with Light and Prescribed Lenses	35
2.20	Visual Aid with Speaker	36
3.1	Project Flow Chart	40
3.2	Interface of Raspberry Pi 3B+ And Its Peripherals	46
3.3	Raspberry Pi Compute Module 3 (Cm3)	47
3.4	Waveshare Compute Module IO Board	48
3.5	Raspberry Pi Compute Module Integrated with The Waveshare Compute Module I/O Board	49
3.6	Algorithm Flowchart of ROS Stereoscopic Image Processing	50
3.7	Solid Works Design of Prototype Phase	51
3.8	5-Inch LCD Screen	55
3.9	Completed Phase 1 Prototype.	56
3.10	9 X 6 Checkerboard Used for Stereo Camera Calibration	58
3.11	Prototype 2 of the visual aid	62
3.12	StereoPi Microprocessor and Its Components	63
3.13	Solid Works Model of Prototype 3	64
3.14	Prototype 3 of the Visual Aid	68
3.15	Visual Field Measurement Apparatus (Top View)	70

3.16	Visual Field Measurement Apparatus (3D-View)	71
3.17	Test Conducted on Visual Field Measurement Apparatus	71
3.18	Depth Map Test Setup	72
4.1	Patient Respondents of Survey in Terms of Impairment	79
4.2	Visual Impaired Patient Respondents at Different Age Group.	80
4.3	Diabetic Retinopathy in Comparison with A Normal Eye	81
4.4	House of Quality of Developing A Visual Aid for Monocular Visual Impaired Patients	84
4.5	Slot Mechanism on Prototype 1	86
4.6	Mesh Analysis of Prototype 1	87
4.7	Stress Analysis Results of Prototype 1	88
4.8	Maximum Stress Point of Prototype 1.	89
4.9	Resultant Displacement Results of Prototype 1	90
4.10	Equivalent Strain Analysis of Prototype 1	91
4.11	Maximum Strain Points with Forces	92
4.12	Completed Assembly Prototype 1	93
4.13	(A.) Depth Map Generated from The Prototype of Visual Aid (B.) Field of Vision from Visual Aid of Prototype 1	95
4.14	Slot Design on Prototype 2	97
4.15	Mesh Analysis of Prototype 2	98
4.16	Stress Analysis of Prototype 2	99
4.17	Maximum Stress Area on Prototype 2	100
4.18	Displacement Analysis on Prototype 2	101
4.19	Equivalent Strain Study	105
4.20	Test Being Conducted on The Integrated Complete Visual Aid of Prototype 2 As Looked on By A Doctor at Taiping Hospital	106

	(A.) Depth Map Produced by Prototype 2 of the Visual Aid	
4.21	(B.) Grayscale Field of Vision Output by Prototype 2 Of the Visual Aid.	108
4.22	(A) Depth Map of Prototype 1 (B) Depth Map of Prototype 2	107
4.23	Analysis of The Blocks Seen with And Without the Visual Aid	108
4.24	Analysis of The Field of Vision (Angle) With and Without the Visual Aid	108
4.25	Percentage of Increase in The Field of Vision	109
4.26	The Depth Map Experimental Setup for Monocular Visual Impaired Patients	111
4.27	Mesh Analysis of Visual Aid Design Prototype 3	112
4.28	Stress Analysis on Prototype 3	113
4.29	Maximum Stress Area of Prototype 3 Of Visual Aid.	114
4.30	Static Displacement Fringe Diagram Results of Prototype 3	115
4.31	Equivalent Strain Analysis Prototype 3	116
4.32	Complete Prototype 3 of the Visual Aid	117
4.33	Comparison of Weight of Visual Aid from Prototype 1, 2 And 3	118
	(A.) Depth Map Produced by Prototype 3 Of the Visual Aid	
4.34	(B.) Field of Vision Produced by The Prototype 3 Of the Visual Aid	120
4.35	Analysis of The Blocks Seen with And Without the Visual Aid	122
4.36	Analysis of The Field of Vision (Angle) With and Without the Visual Aid	122
4.37	Percentage of Increase in The Field of Vision	123
4.38	(A.) The Depth Map Experimental Setup for Monocular Visual Impaired Patients (B.) Corresponding Depth Map	125

## LIST OF SYMBOLS

%	Percentage
$f$	Magnification Factor
$k$	Distortion Coefficient
$T_x$	Depth Axis (X-axis)
$T_y$	Depth Axis (Y-axis)
$T_z$	Depth Axis (Z-axis)
$R$	Rotation Matrix
$C_x$	Image centre point (X-axis)
$C_y$	Image centre point (Y-axis)
$S$	Uncertainty scale factor
cm	centimetre
$d_{ad}$	Additive Depth
$d_f$	Depth map (front)
$d_b$	Depth map (back)
°	Degree
g	Gram
Hz	Hertz
N/m <sup>2</sup>	Newton per metre square
mm	Millimetre
dB	Decibels

## LISTS OF ABBREVIATIONS

3D	Three Dimensional
ABS	Acrylonitrile Butadiene Styrene
AKPK	The Credit Counselling and Debt Management Agency
CM3	Compute Module 3
CM3L	Compute Module 3 Lite
FEA	Finite Element Analysis
GPIO	General-Purpose Input / Output
HDMI	High Definition Multimedia Interface
HOQ	House of Quality
IO	Input/output
LCD	Liquid Crystal Display
PE	Polyethylene
PLA	Polylactic Acid
PP	Polypropylene
PS	Polystyrene
RGB-D	Red Green Blue - Depth
THONEH	Tun Hussein Onn Eye Hospital
UKM	Universiti Kebangsaan Malaysia
UNITEN	Universiti Tenaga Nasional
UPM	Universiti Putra Malaysia

## LIST OF PUBLICATIONS

- 1 R. Nirvenesh, and H. Mohamed, “A Review on the Treatments for Monocular Visual Impairment for the Development of a Visual Aid”. *International Journal of Engineering and Technology (IJET)*, 7(4.35), 282-285.
- 2 R. Nirvenesh, and H. Mohamed, “Finite Element Analysis & Comfort Assessment Conducted on the Visual Aid Design for Monocular Vision Patients”. *International Journal of Advanced Trends in Computer Sciecne and Engineering (IJATCSE)*, Vol 9 (No 2.)

# CHAPTER 1

## INTRODUCTION

### 1.1 Research Background

Monocular vision impairment alludes to have no vision in one eye with enough vision in the other. Amblyopic eye and myopia are examples of monocular visual impairment. Amblyopia results from a condition that prevents the eye from focusing well thus allowing inadequate light to enter, sometimes amblyopia is also caused by a cataract or a clouding in the frontal part of the eye. Amblyopia is a medical condition where depth perception is lost due to the disability, thus the vision is only perceived in two-dimensional [1].

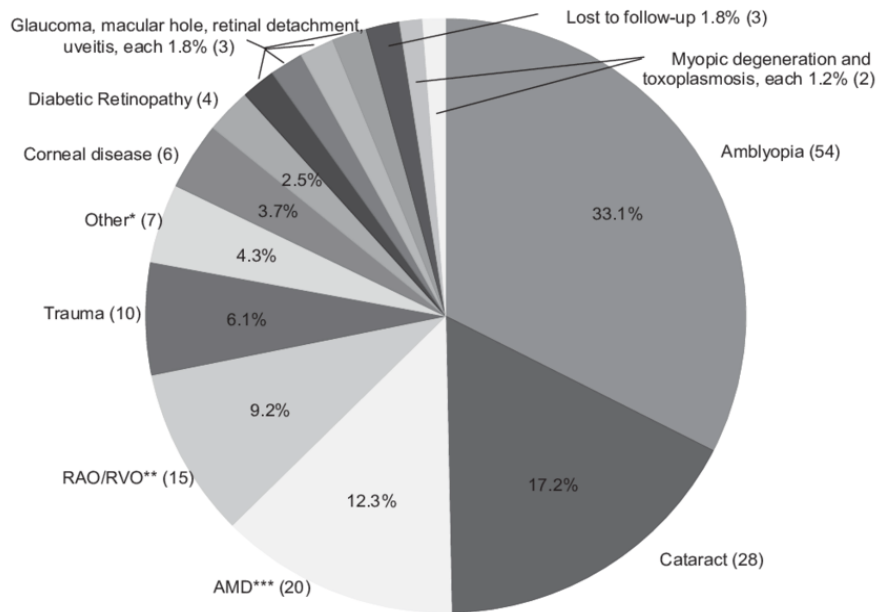


Figure 1.1: Causes of Visual Impairment [2]

From the pie chart in Figure 1.1, it is evident that amblyopia is the most cause of monocular visual impairment as 33.1% of people are affected by it.

Another type of monocular visual impairment is known as the amblyopic eye or lazy eye. It is also to be noted that amblyopic vision loss cannot be treated later on in life and thus adults with amblyopic visual impairment have no option of treatment but to live with the state they already are until the time of death [3]. Research in the United Kingdom also shows that the danger of genuine vision loss influencing the non-amblyopic eye is at a significantly more serious hazard than already expected [4]. Although various research does show the need for development in this field, only a very few research is being conducted to address this problem. This can be due to insufficient awareness in the field of ophthalmology or monetary sponsors which are rarely obtained to address a problem in this field [5].

Glaucoma is a disease which affects the optic nerve at the back of the eye as shown in Figure 1.2, the nerve is almost the size of a finger, this nerve is responsible for transmitting the images from a person's retina to the visual centre in the brain [6]. The pressure on these delicate optic nerves causes a reduction in the field of vision. There are namely two types of glaucoma, primary open-angle glaucoma and angle-closure glaucoma [7]. There is currently no treatment for glaucoma, however, there are methods that are imposed to decrease the rate of vision loss. The methods involve both invasive and medication [8]. This disease is most commonly associated with high levels of blood sugar levels however some non-diabetes patients with high intraocular pressure develop glaucoma as well. Glaucoma is also closely associated with family histories and is the second leading cause of monocular and stereoscopic blindness in the United States of America. Most patients with glaucoma experience monocular visual impairment [6].

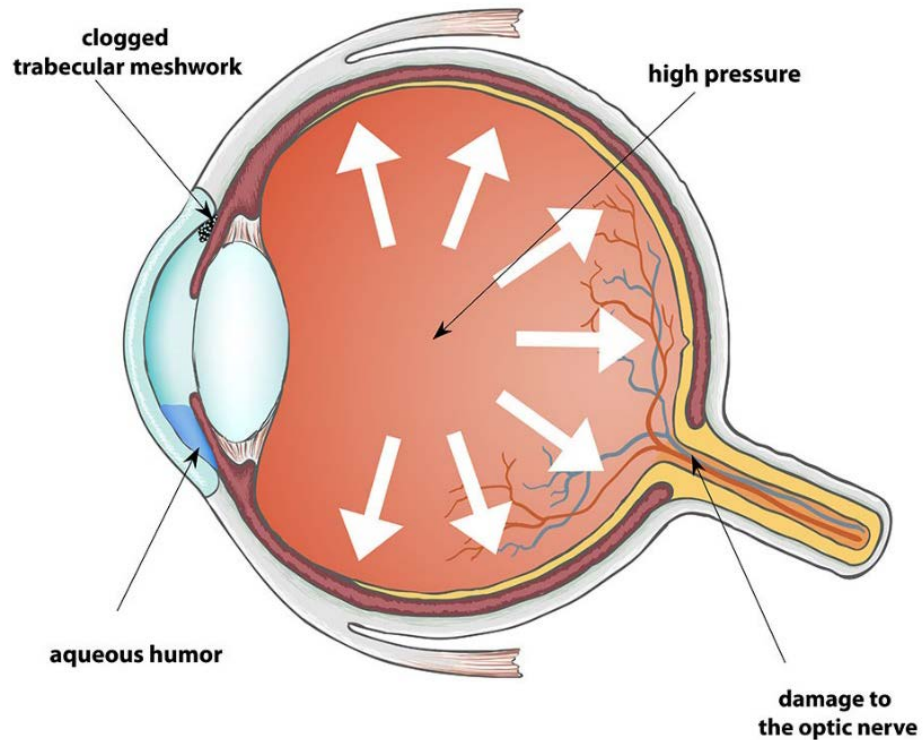


Figure 1.2: Intraocular pressure exerted on eye resulting in glaucoma [9].

These visual disabilities limit a person's ability to carry out daily tasks. A primary factor, which arises from these disabilities, is the reduction in the range of vision from stereoscopic to monoscopic vision (as shown in Figures 1.3 and 1.4) which reduces and eliminates the depth perception of a person's vision [10].

The distance and depth perception is very important for a human to carry out daily activities, The National Institute for Rehabilitation Engineering (NRE) has published a journal article on improving people's perception skills with optical aid for specialized occupation, safe driving and safe use for machinery. In this study, the institute encourages people to have a spatial perception of the workspace around for safer working environments. Visually impaired people, binocular or monocular, often but not always develop effective distance perception skills [11].

Depth perception is known as the capacity of the human eye to find 3-dimensional measurements and judge the separation of an object which are essential from numerous points of view. This capacity encourages us to maintain a strategic distance from impacts. Without it, humans would not have the capacity to know how far away a divider is or even the separation between a car and the car in front is. This is important in daily tasks, for example, crossing the street. This ability keeps a person safe in situations like these [11].

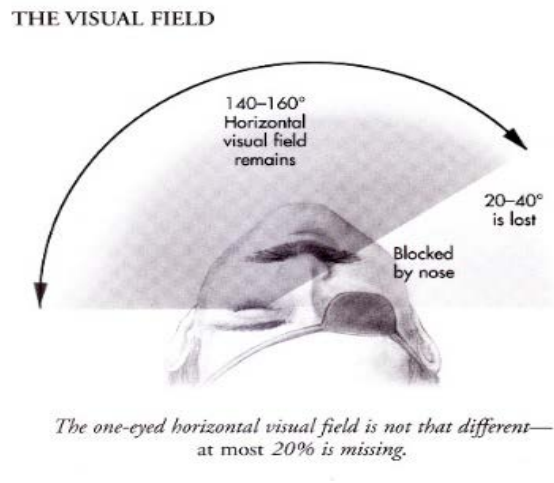


Figure 1.3: Visual Field with Monocular vision [12]

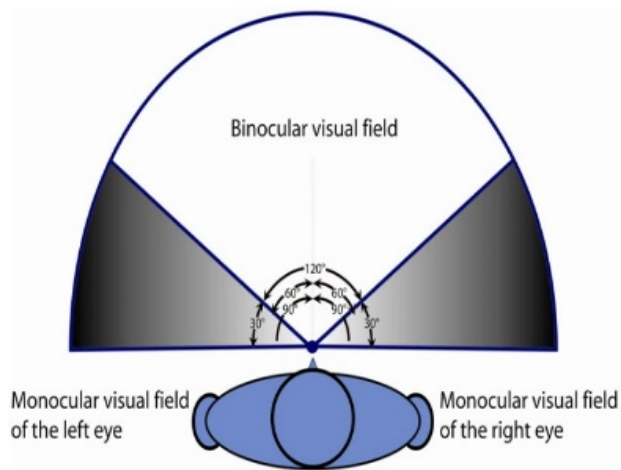


Figure 1.4: Stereoscopic vision angles [13]

Existing treatments for monocular visual impaired patients are not emphasized due to the population of these disabilities, which make up almost 2% of the population in America [14]. The existing treatment for monocular impairment is for amblyopic patients, a patch is placed on the sound eye to train the disabled eye to reactivate its optic nerve (as stated in Figure 1.5). Several other treatments also use the same principle of treatment which is to temporarily blind the sound eye, forcing the vision through the amblyopic eye. This form of treatment is however only valid for children of 7 to 10 years of life, as the visual system develops steeply during this period [15].



Figure 1.5: Amblyopic patient with an eye patch [16]

The usage of a single eye reduces the mind's ability to produce a depth perception or a clear 3-Dimensional (3D) image, which translates distance, and object. Both eyes are required to work coherently to perceive a piece of information about object size and distance, this condition is known as stereopsis [17]. Our eyes look at an object's images from two different angles as they are distant apart, this is known as retinal disparity, the visual centre in the brain then processes these images and merges them into a single image, this is clearly illustrated in Figure 1.6 [18]. Monocular visual impairment also leads to Strabismus or also known as cross-eye, which also has a hard time perceiving depth, due

to the disability. Because of this sensory impairment, fundamental daily activities such as driving and even navigating becomes a very tough task [18]. Our brain also uses depth cues to determine distance and sizes of an object. Interposition cues are used when an object is overlapped by another object [19]. Linear perspective is used when an object is seemed to get smaller and smaller as it travels further and further away, for example, when a ship is seen getting smaller and smaller as it travels across the ocean and seen from one stationary position. Shades and light shed on an object are also used as a depth cue, as it indicates the size of an object to an acceptable degree of accuracy [20].

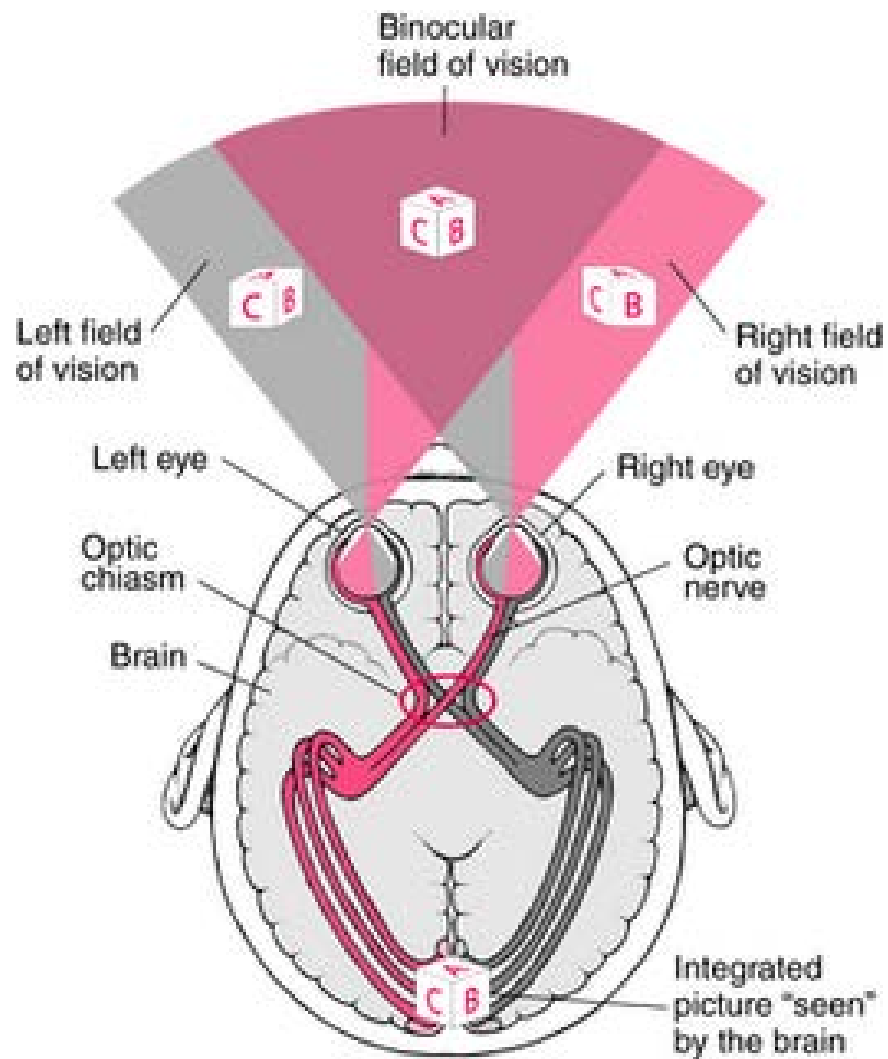


Figure 1.6: Binocular Vision (Stereopsis) used in perceiving depth [18]

It is important to note that patients with monocular visual impairment (low vision) are considered as one of the seven People With Disabilities (PWD or OKU) categories [21]. Therefore, this research is very significant and in-line with the Persons with Disabilities National Policy and the National Action Plan for Persons with Disabilities (2016-2022). This research will help to achieve some of the strategic cores of the National Action Plan as well as to fulfil the first objective of the Persons with Disabilities National Policy, which is to allow PWDs to have the same rights and opportunities as others.

However, it is to be noted, this treatment is only valid for children. Adults suffering from this disability have no form of treatment thus the development of a cost-efficient visual aid for monocular visual impaired patients is vital.

## **1.2 Problem Statement**

Globally, monocular visual impairment is an impairment that is rarely sorted. It is a visual impairment not commonly researched for a solution due to its lack of awareness [22]. One in ten children in Malaysia has an undiagnosed visual problem as researchers found serious vision issues among pre-schoolers, with 7.5 per cent (12 out of 161 youngsters with visual impedance) were distinguished with amblyopia (lazy eye) [23]. Patients with this visual impairment are most commonly a result of an accident or any other medical conditions such as amblyopia, myopia and glaucoma. This type of visual impairment lacks the success rate of treatment with age [24], and thus early detection is vital for the appropriate treatment of glaucoma. This also means adults with monocular visual impairment must live with a monocular vision indefinitely.

The existing treatments for monocular visual impairment are primarily focused on occluding the vision on the sound eye and hence improving the vision on the impaired eye. This type of treatment is conducted in various methods which include patching, lens occlusion and dichoptic training but all focused on to blocking the vision on the sound eye. Due to the success rate of this type treatment which decreases as a patient ages, a gap

is identified in developing a visual aid which focuses on external visualisation which caters for monocular visual impaired patients.

### **1.3 Research Objectives**

The primary purpose of conducting this research is to develop a visual aid for monocular visual impaired patients to overcome challenges in carrying out daily activities. With the fabrication of this visual aid prototype, monocular visual impaired patients not only have information on depth information of the objects ahead of them but also a wider field of vision as compared to having monocular vision. The design of the visual aid is also made to be simple and cost-efficient as it aims to be affordable by everyone.

This research was carried out with respect to the following objectives:

- I. To design and develop the prototype of a visual aid for monocular visually impaired patients using electronic components and existing spectacles
- II. To analyse the material properties of the prototype in terms of static analysis which include stress analysis, strain analysis and displacement analysis
- III. To assess the prototypes of patient for depth perception and increase in field of vision.

### **1.4 Research Scope**

The primary focus of this master's degree study is to develop a prototype of a visual aid for monocular visual impaired patients. With the visual aid, monocular visual impaired patients can now have a wider field of vision thus enabling them to have a better perspective of their surroundings. The visual aid also enables patients to better perceive distance with the depth maps embedded in the system, thus reducing the mishaps of carrying out daily activities such as picking up a glass of water on top of a table. Depth perception has been highlighted in this research as the survey suggests, during the early stages of this research which shows that depth and distance perception is the primary challenge for monocular visual impaired patients.

The first part of this research was commenced with obtaining background and in-depth information about monocular visual impairment and causes of low vision from ophthalmologist and opticians at The Tun Hussein Onn Hospital (THONEH). The sample size is taken based on the number of patients per day which were 16 patients who are monocular visual impaired, it will not represent the whole population of patients with low vision. With this information existing treatments on amblyopia and monocular visual impairment were further investigated to study the effectiveness in treatment. The second part of this research was conducted to identify the customer requirements and engineering requirements to construct the House of Quality. Based on the House of Quality, relevant information was considered for concept generation. A total of three concepts were generated to finalize the best design.

Relevant microprocessors and other electronic components were chosen with cost and quality taken into serious considerations to meet the objectives. Raspberry Pi is used as the primary processor to process images in this study. The image detection algorithm used for detecting depth is not discussed thoroughly in this work as it is an adapted algorithm from previous works.

This research is however limited to only the external visualization of depth, it does not include any modification of the lenses for the eyes to perceive the objects seen in a different manner. A total of two tests were conducted to assess the functionality of the visual aid which are the depth perception and field of vision test. The visual aid is produced with the assumption that the monocular visual impaired patients cannot perceive depth and possess narrow vision at close range of 2 metres as it is the distance at which most objects are at reach. This visual aid is also currently only intended for training purposes as it requires further modification to make it furthermore efficient. This study is also only limited to stationary objects and not dynamic or moving objects as the algorithm might differ.

## 1.5 THESIS OVERVIEW

This section summarizes the chapters of the thesis. A total of five chapters are covered in this thesis with references and appendices.

- a) Chapter 1 introduces the gist of the research by stating its background and discussing monocular visual impairment. The problem statement is then stated with reference to the background. The objectives of the research are then identified based on the problem statement.
- b) Chapter 2 provides a general conspectus and understanding about the monocular visual impairment, stereo cameras, depth maps as well as the review on the previous research. It also emphasizes all relevant practices currently used in the industry.
- c) Chapter 3 outlines the methodology from the research process. The research process states all the development processes in detail, which includes surveys, design, simulations, and testing of the visual aid. All the steps that were carried out to obtain results are mentioned in this chapter of the research
- d) Chapter 4 highlights the result and analysis of the surveys, design, simulations, and testing of the visual aid. The analysis was presented in graphs, Figures and tables for better explanations. The field of vision and depth perception test was clearly tabulated and examined. A final cost analysis was conducted based on the cost of every hardware used in each phase of the development process.
- e) Chapter 5 presents the conclusion of the entire research. The research is briefly discussed and summarized. The conclusion reaffirms the objectives that were initially mentioned in the introduction of this thesis as well as it addresses the problems stated during the initial phase. A recommendation section is also included in this chapter for future researchers to improvise and make this visual aid much more reliable and practical for monocular visual impaired patients.

## **CHAPTER 2**

### **LITERATURE REVIEW**

#### **2.1 Introduction**

This chapter discusses a wide variety of literature reviews which are associated with monocular vision impairment and its existing treatments, stereoscopic cameras, algorithms associated with stereoscopic cameras, the depth perception that is perceived by the stereoscopic cameras, and other relevant areas of studies related to the development of this visual aid.

#### **2.2 Medical conditions**

Monocular Visual Impairment is the leading cause of visual impairment in children around the world [25]. Among what is most affected in a person with amblyopia is the depth perception, and it is the most common deficit under ordinary. This development of visual aid for monocular visual impaired patients acts as a solution to the study by the department of psychology of the University of Pavia, Italy on the effects of complete monocular deprivation in visuospatial memory [26]. Subjects in this study were of monocular and binocular vision individuals. From the study, it was concluded that the monocular visual impaired patients performed worse than sight individuals indicating that the lack of binocular vision affects the visual information in visuospatial memory [26].

A medical condition highly associated with this type of monocular vision is known as amblyopia [27]. Amblyopia is a medical condition which most commonly happens in children and young adults. This condition arises due to brain development disorder which happens visual centre of the brain. vision. This causes complications by making them less

abled in sports and impairing proper locomotion. This also limits career options for people affected by amblyopia.

In children with amblyopia, having some quantifiable stereopsis (versus having none) altogether impacts the result of treatment. Stereopsis is the brain's ability to obtain vision from binocular vision and translate them into depth. Youngsters with no quantifiable stereopsis have a more than the two-fold increment in hazard for persevering amblyopia. The different levels of stereopsis influence the type of treatment required for a person with monocular visual impairment [25].

In people with amblyopia, the visual sharpness of one eye is undermined, the connection between the visual acuity of the amblyopic eye and stereo acuity is influenced by each other. By and large, the lower the visual acuity, the lower the stereopsis level. However, upon close review, the relationship between the visual acuity and the stereopsis level appears to be determined by subjects with different refractive power in each eye. This condition is known as anisometropic amblyopia as shown in Figure 2.1 [28]. The Figure 2.2 shows the types of monocular visual impairment.



Figure 2.1: Anisometropic amblyopia [28].

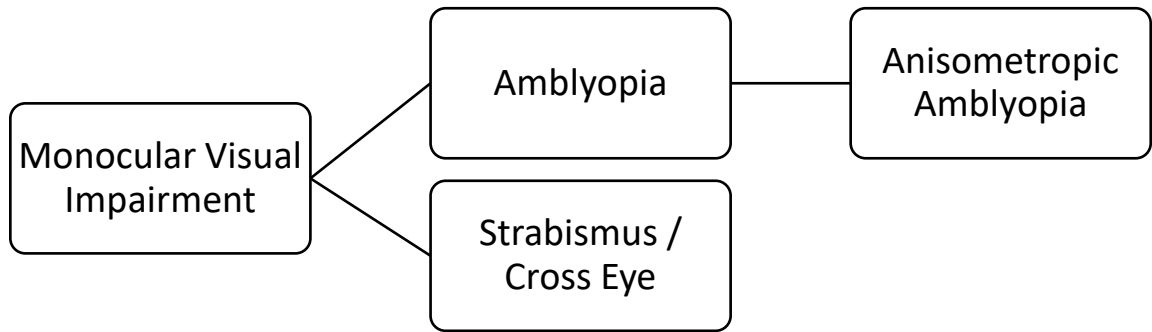


Figure 2.2: Tree Diagram of Monocular Visual Impairment

It is important to quantify stereopsis, as it is the proper way to measure binocular vision. The Randot “Circles” as shown in Figure 2.3 is the most common method used as a test for use with amblyopes. This test is used to benchmarks a person’s stereopsis ability by distinguishing the circle within the rectangle [29].



Figure 2.3: Randot Circles Chart [30].

The Randot's circle has a set of rectangles with three circles in each one. Monocular visual impaired patients perceive the circles as 2 dimensional, whilst people with normal stereopsis can distinguish one of the circles which are found to be nearer compared to the other two circles within the rectangle. The test is also conducted under polarized vision by the usage of a polarized spectacle. As a summary, it is highly important for us to properly understand the medical conditions associated with monocular visual impairment to actually provide a proper solution.

### **2.3 Existing Treatments for monocular visual impaired patients**

Monocular Visual impaired patients have always been a minority and seldom investigated. However, a study done by Schornack *et al.* [31] on the prescription and management of contact lenses in patients with monocular visual impairment discusses the occlusion method of treatment by contact lenses. This investigation shows that monocular visual disabled patients who wear contact lenses on the affected eye, ought to know about the danger of possibly debilitating them. Careful levels of cleanliness must to be rehearsed with the use of the contact lenses. It is additionally prescribed to wear proper spectacles to lessen the danger of damage to the sound eye. The application of contact lenses, however, does not solve the problems of reduction in the field of vision [31].

Most commonly, children with amblyopia aged 10 and below are treated by applying a patch on the sound eye to reactivate optic nerve on the affected eye [32], thus a study was carried out by Repka *et al.* [33] on the monocular oral reading performance after amblyopia treatment in children, the subjects were of 10 years and previously treated for amblyopia. The outcome of the study was based on the Gray Oral Reading Test (GORT-4). The results of the (GORT-4) turned out slightly worse when reading with previously treated amblyopic eyes compared with fellow patients with untreated amblyopic patients in terms of rate, accuracy and fluency but the reading comprehension was similar [33]. This is because amblyopic patients have difficulties with accommodations. The accommodative ability of amblyopic patients is much slower as compared to an ordinary person. An amblyopic patient takes more time to identify what

the word is instead of mentally capturing the word as a whole like a normal person would with ordinary comprehension.

A study by Yun Liu *et al.* [34] focuses on stereo acuity gain over monocular training by dichoptic training as shown in Figure 2.4 in adults with amblyopia. Stereo acuity is the ability of a person to detect the difference in depth while visual acuity is the clarity of vision [35] During the dichoptic training, the participants used the amblyopic eye to practice a contrast discrimination task, while a band filtered noise masker was simultaneously presented in the non-amblyopic eye. The results of the training have improved stereo acuity by 27% beyond 55% from previous monocular training. Thus, it is proven that with the dichoptic training, only stereo acuity is improved and not visual acuity [34].

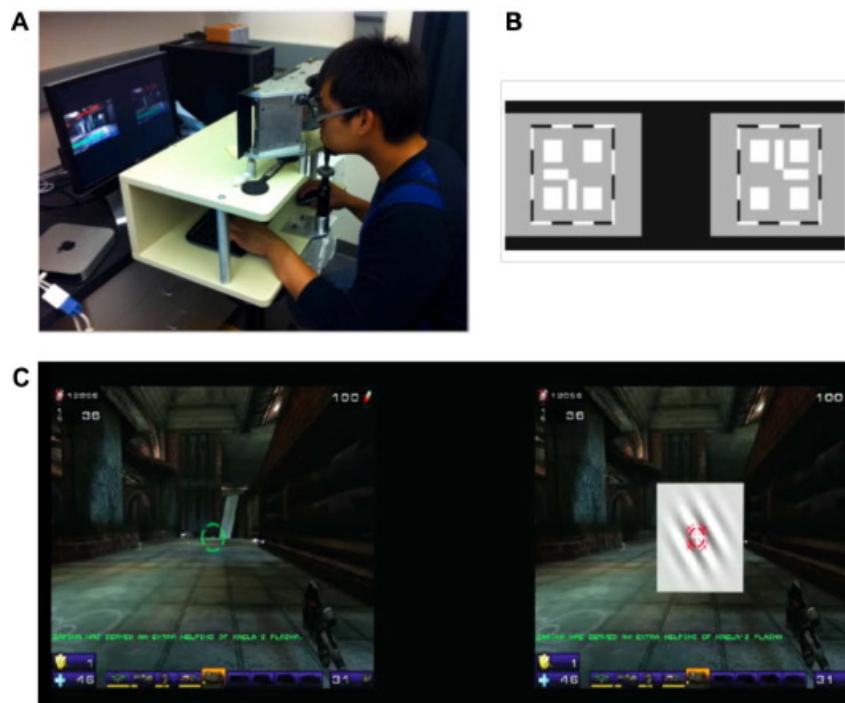


Figure 2.4: (A) Game participants use a stereoscope to attain alignment of the eye and play the dichoptic game. (B) Nonius lines are used to align the eyes, the participants are requested to align the two images until a cross is seen (C) Screenshot of the game during the dichoptic training [34].

The light level on the amblyopic side of the eye is much brighter. This is to overcome suppression and achieve fusion. The brighter light on the amblyopic eye requires the eye to be much adaptive to the lighting condition thus achieving fusion between both the eyes.

Table 2.1: Summary of existing treatment for monocular visual impaired patients

No.	Type of Treatment	Advantages	Disadvantages
1.	Occlusion by Contact Lenses	<ul style="list-style-type: none"> <li>• Aesthetically neat</li> <li>• Effective at a young age</li> </ul>	<ul style="list-style-type: none"> <li>• Cleanliness and maintenance of contact lenses are important</li> </ul>
2.	Dichoptic Training	<ul style="list-style-type: none"> <li>• Effective for middle-age patients aged between 11-17</li> </ul>	<ul style="list-style-type: none"> <li>• Does not imply for older age patients</li> </ul>
3.	Patching	<ul style="list-style-type: none"> <li>• Effective for young patients aged between 3-10</li> </ul>	<ul style="list-style-type: none"> <li>• Does not imply for older age patients</li> </ul>

Although treatments to improve the visual acuity of an amblyopic person with dichoptic training and patching is widely practised, there are certain monocular visual impaired cases where visual acuity conditions fail to improve. In this condition, the usage of electronic visual aid is a better option. Electronic visual aids are not something new and there have been several but not many studies into it. Ultrasonic spectacles and waist belt for the visually impaired and blind person by Shripad *et al.* [36] from the Indian Institute of Technology is one of the visual aid developed [36].

A very fundamental concept has been used to develop this prototype . This system detects obstacles from up to 500 cm in front, left and right of it. A network of ultrasonic sensors works coherently to detect obstacles around the blind person. An auditory feedback system is used to warn the person of the obstacles around them. A set of recorded voice from flash memory is played based on the direction of the obstacle [36].



Figure 2.5: (A) Ultrasonic Spectacles (B) Ultrasonic waist belt [36].

A total of five sensors are used for the application of this visual aid. A pair of ultrasonic sensors are mounted on the spectacle as shown in Figure 2.5 (A) and three ultrasonic sensors around the waist of the person on a belt as shown in Figure 2.5 (B). An AT89S52 microcontroller is used to compute all the data from the sensors [37]. The microcontroller then transmits a signal to the APR9600 flash memory to play a set of warning signals as shown in Figure 2.6. One week of training is enough to train a person to use this visual aid.

The prototype was tested under laboratory conditions with subjects that are monocular visual impaired. However, the author also states with rigorous training, this visual aid can also be used for outdoors [36]. With the development of this visual aid, it is evident that electronic visual aids does have a significant impact towards aiding the patient with monocular visual impairment. This development also aids in the current research by providing a framework of algorithms that can be used to develop the current prototype as shown in Figure 2.5.

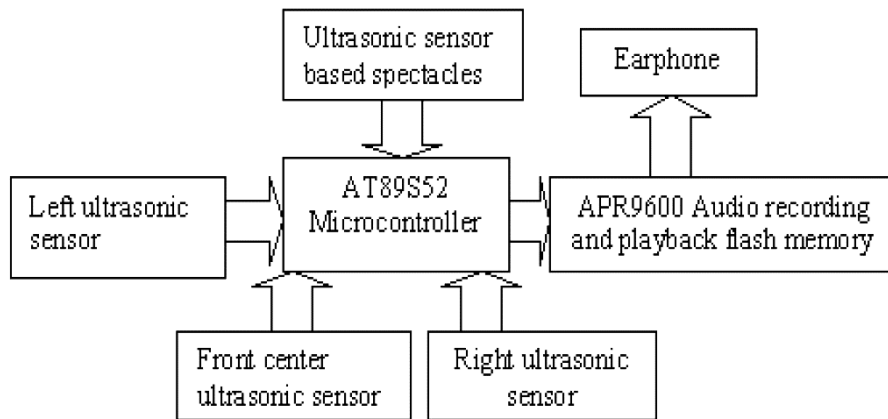


Figure 2.6: Microcontroller flow chart [36].

The ultrasonic visual aid is also known as a stand alone system due to its simplicity of design, a comprehensive navigation system is not achieved by the visual aid as it works based on the ultrasonic sensors. Thus a comprehensive navigation system is still vital for the visually impaired. An integrated navigation system for visually impaired and disabled was developed by Helal *et al.* and his team at the University of Florida [38]. The system is a wireless pedestrian navigation system.

This visual aid is known as Drishti, it utilizes the Global Positioning System (GPS) as well as the Geographic Information System (GIS) to guide a visually impaired (subject) to a destination. The GIS is used to understand the geography of the place that the subject is heading and GPS to compute the distance and route. The system also computes temporal constraints such as traffic congestion or roadworks and blockades on the route. This system also recognizes the voice of the subject and learns it in time [38].

This system acts as a supplementary visual aid to other existing navigational aids such as the long cane, or blind guide dogs. The system is also currently developed on to wheelchairs and integrated into a more user-friendly environment. The system currently runs on a low-end on-board computer which handles all the computing power with a battery pack. The weight of this system can be reduced if further developed on to a motorized wheelchair [38]. The GPS and GIS system can also be integrated in the

development of this visual aid to further understand the topography of a current area. The topography information would aid the person in understanding the depth in his field of vision.

The integration of GIS and GPS helps us perceive information that is obtained by normal stereo vision. Stereo vision has always been used for obtaining a 3-dimensional image of a surrounding, with that, a study by N. Molton from the Oxford University has worked on a stereo vision-based aid for the visually impaired [39]. This visual aid produced was primarily intended for the blind. The visual aid employs technology used in Automated Guided Vehicles (AGV). Recalibration of the system was done in order to accommodate the system to adapt a person's walking movement.

This system acts as an obstacle avoidance system. The stereo camera which uses the Ground Plane Obstacle Detection (GPOD) is a stereo matching system. The system contains ground plane data. It then compares these data with that obtained from the camera. This disparity seen is identified as an obstacle. Future models are known to equip with sonar and other relevant sensors to improve its robustness. The probability of detection is also high relative to the obstacle size as shown in Figure 2.7 [39]

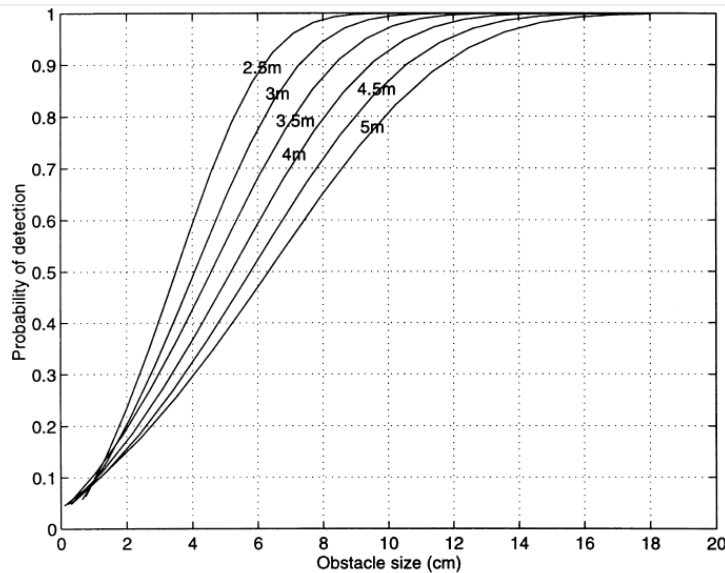


Figure 2.7: A graph of probability detection against obstacle size [39]

The movement of cameras during walking is also calibrated by several filters to adapt to this situation. The system is also currently modelled to improve the reliability and accuracy of the prototype. This type of visual aids developed for the visually impaired is the first of its kind to consist of sensors and stereoscopic imaging that is found to be useful [39].

Vision Aware is a low vision visual aid manufacturer. Although they do not provide direct solutions for depth perception and increased field of vision, they do provide optical devices such as reading glasses, loupes, and telescopes, non-optical devices such as reading stands, supplemental lighting, glare control sunglasses and electronic magnifiers (as shown in Figure 2.8) and magnifying systems. The current low vision devices are very specific to the tasks that are being conducted and designed for very near operation visual tasks. Depending on the type of tasks, several low vision visual aids might be required, to carry out a single task.



Figure 2.8: Stand magnifier with handle and a lighted hand-held magnifier [40].

Maxi Aid is another manufacturer that provides visual aids for low vision patients. Unlike the previous manufacturer, this company provides more task-specific products such as low vision calculators (Figure 2.9), low vision clocks, talking alarm clocks, low vision telephones (Figure 2.9) and many more. Although these devices are great for low vision patients, it is however not ideal for monocular visual impaired patients.



Figure 2.9: Low Vision calculator and low vision telephone with emergency remote pendant [40].

## 2.4 Stereoscopic cameras and algorithms

Depth perception is vital for monocular visual impaired patients, a study was conducted by the department of informatics at the University of Genoa on calibrated depth of field. In this study RGB-D cameras were used as a high degree of precision is required to identify a stereoscopic 3D environment. Calibration was also a vital procedure to improve the accuracy of the 3D measurements. Quantitative measurements were taken to validate the proposed approach [41] in terms of the reference distance (mm) and the kinect distance or also known as the calibrated distance (mm).

Misalignments in stereo images lead to a high level of discomfort to the viewer's eye, research by Di Zhang *et al.* on the 3D visual discomfort assessment by measuring the vertical disparity tolerance. The experiment was conducted with 17 subjects with varying vertical disparity, stimulus angular sizes and luminance. Based on the results of the experiment conducted, a regression was conducted to estimate the Vertical Disparity Tolerance (VDT) levels as a component of luminance and stimulus angular size. VDT is a perceived solid marker of visual solace because of vertical depth and the model can be utilized to foresee visual solace for given survey conditions [42].

The depth perception model also must be guided by visual comfort to obtain a clear visual salience, the perception of which an object stands out from the rest. The proposed saliency model by the study of Qiuping Jiang *et al.* composes of three components which are: 2D image saliency, depth saliency and visual comfort-based

saliency. The combination of colour, texture, and spatial saliency is processed and combined to derive a 2D image saliency. The global disparity is used to compute depth saliency, while the visual comfort level is distinguished by a stereoscopic image pair. The final 3D saliency map is obtained by computing all three components. This acts as a vital algorithm to obtain the appropriate saliency model for visual aid in this study [43].

Stereoscopic cameras or dual-camera systems are ideal for constructing 3D models. Stereoscopic cameras also require to be calibrated before application to avoid errors in readings. Kai Li from Shanghai University has investigated the calibration error for dual-camera digital image correlation at the microscale. There are several calibration parameters for dual cameras as shown in Table 2.2 below [44].

Table 2.2: Uncalibrated parameters of stereoscopic cameras [44]

	<b>Left Camera</b>	<b>Right Camera</b>
$f$	556.80	584.19
$k$	-0.000066	-0.000053
$T_x$	-10.81	-10.41
$T_y$	10.25	10.54
$T_z$	140.59	146.36
$R$	0.996445 -0.00512 -0.08409 -0.006434 0.99986 -0.01541 -0.083999 0.015893 -0.99634	0.99936 -0.00871 0.034692 -0.007658 -0.99951 -0.03024 0.034939 0.029954 -0.99894
$C_x$	873.75	688.00
$C_y$	732.32	517.50
$S$	0.99	0.99

For a stereoscopic camera to be error-free, the parameters  $f$  (magnification factor),  $T_y$ , and  $T_z$  must be the same as long as they are focusing on the same object as shown in Table

2.3. The ratio of  $f$  to  $T_z$  can also be used to determine if a camera is precisely calibrated or otherwise as the value should contradict to the magnification factor.

Table 2.3: Calibrated parameters of stereoscopic cameras noting that parameters  $f$ ,  $T_y$ , and  $T_z$  are the same [44]

	<b>Left Camera</b>	<b>Right Camera</b>
$f$	584.00	584.00
$k$	0.0	-0.0
$T_x$	-10.5	-10.4
$T_y$	10.5	10.5
$T_z$	146	146
$R$	0.996445 -0.00512 -0.08409 -0.006434 0.99986 -0.01541 -0.083999 0.015893 -0.99634	0.99936 -0.00871 0.034692 -0.007658 -0.99951 -0.03024 0.034939 0.029954 -0.99894
$C_x$	688	688.00
$C_y$	517.5	517.5
$S$	1	1

## 2.5 Depth Maps

Depth maps have coloured the image with a multicolour display that looks like a thermal image but distinguishes depth instead of heat [45]. Research by Jimenez *et al.*, where 3D human pose was estimated from depth maps using a deep combination of poses. His work inclines towards the human behavioural understandings, that is important in the ergonomic industry. The depth is obtained by depth sensors that are installed in an environment. The depth maps obtained by these sensors are used to translate the poses in 2D images [46].

This technology employs Deep Learning approach, where the sensors adapt and learn the more it is being used [47]. The proposed model that is used in this work is known as the Deep Depth Pose (DDP), which receives a depth map that has precompiled three-

dimensional prototype poses and outputs a 3-D position of the body connections of the subject as shown in Figure 2.10 below. The Deep Depth Pose has been completely evaluated on the challenging several datasets namely ‘ITOP and UBC 3 View (UBC3V) datasets as shown in Figure 2.11 which mimic realistic and plastic examples. These datasets are commonly used for evaluation of depth-based pose estimation techniques.

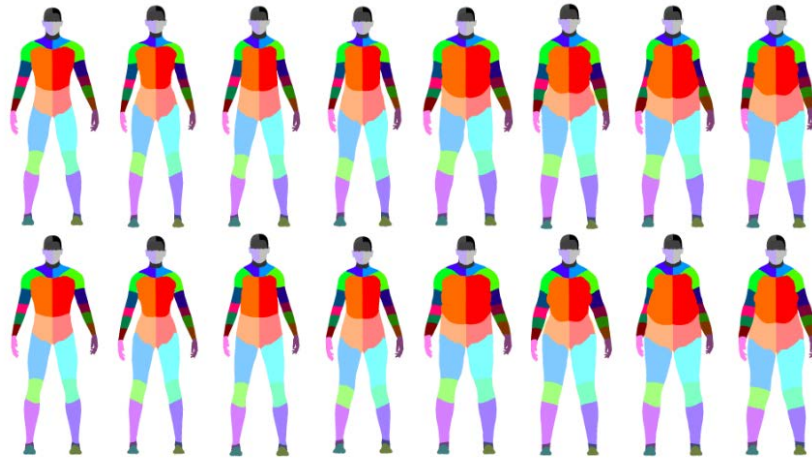


Figure 2.10: UBC3V datasets [48]

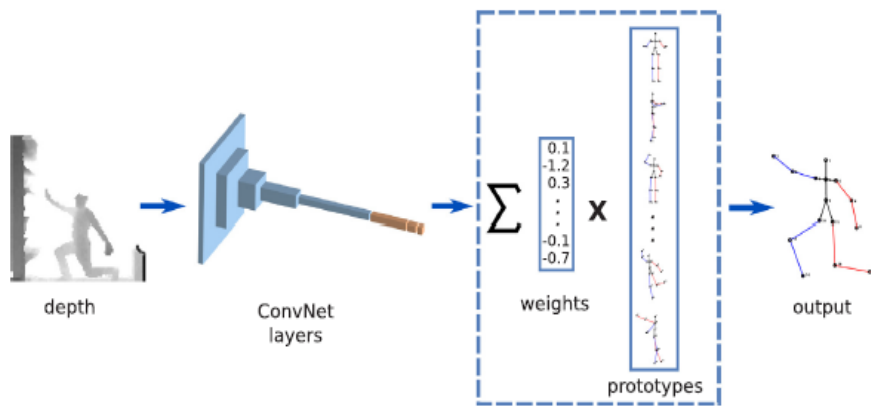


Figure 2.11: Given an input depth map, the 3D body pose is estimated as a linear combination of prototype poses, where the Convolved Neural Network (ConvNet) is in charge of computing the weight of each prototype[46]

Based on the datasets, and accuracy 100% and 98.8% were obtained for both ITOP and UBC3V respectively.

Although sensors are a great way of obtaining depth maps, Min-Gyu Park *et al.* has proposed a method that takes characteristic of manmade environments into account. The key commitment is to produce a piecewise planar difference map while anticipating the distortion issue in non-planar areas. To accomplish this, the process is broken down into three consecutive subproblems: beginning depth map estimation, plane theories building and worldwide streamlining with plane speculations. In the wake of finding an underlying depth map, it is discovered that local and global plane is derived from the depth map through division based local plane fitting, agglomerative various levelled grouping, and vitality based multi-model fitting systems [49].

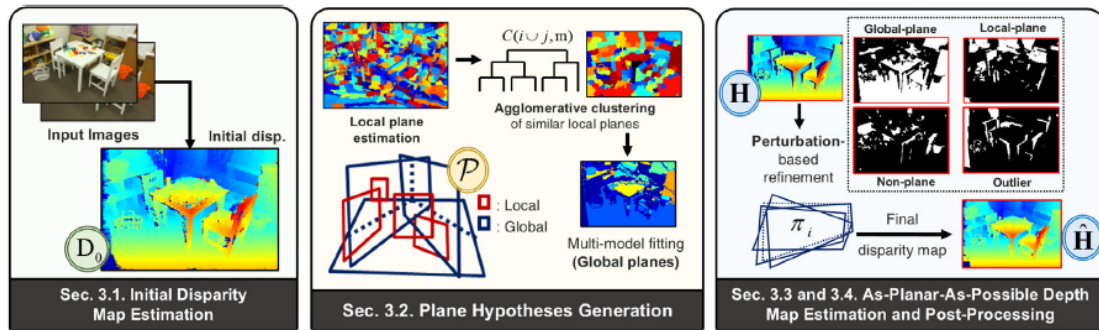


Figure 2.12: An overview of the proposed model [49]

This method is simply breaking a complex problem into simpler blocks that are much easier to compute and eases the load on a multicore processor. By simply breaking the complex structure of sample matching, clearer depth maps are obtained from global and local plane coordinates. Figure 2.12 shows the overview of the breakdown model proposed and conducted by Gyu-Park *et al.*

Deep learning and Artificial intelligence have much been associated with depth maps. Thus, Po Kong *et al.* have published research on an introduction to a 2D convolutional neural system (CNN) which uses the added additive depth map, for

recreating blocked segments of objects caught utilizing depth sensors. The added additive depth map serves as a measure of depth. This information is fed into the back depth taken by cameras located opposite of the primary input camera. An association of the information and back depth map is then the finished 3D shape. To achieve this assignment, they have utilized a leftover encoder-decoder with skip associations as the general design. They have trained and benchmarked their system utilizing existing engineered datasets just as true information caught from the aware depth sensor. Their analysis demonstrates that the added additive depth map, despite its insignificant 2D portrayal of volume, can deliver practically identical outcomes to existing cutting edge 3D CNN methodologies for shape fulfilment from single view depth maps [50].

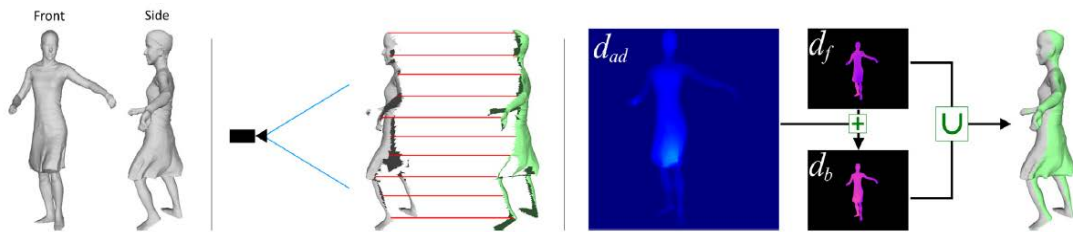


Figure 2.13: Process of depth map processing [50]

From Figure 2.13 above, on the left is the ground truth work seen from the front and side. Next is a camera imaging the work to create the preparation information. The added additive depth,  $d_{ad}$ , is pictured as the (overstated) red lines from the camera confronting network (in dark) to the back perspective on the work (in green). To the right is  $d_{ad}$  appeared as a picture just as the depth maps  $d_f$  and  $d_b$  which relate to the dark and green halfway networks, individually. The association of  $d_f$  and  $d_b$  creates the work result appeared in the extreme right. For all depth map pictures, more splendid hues suggest further separations [50].

Face recognition and depth maps have long been highly associated due to the accuracy of a face detection being highly dependent on the depths of the human face. A work by Krutikova *et al.* from Latvia has discussed on an idea to recreate 3D face model

from stereo depth images [51]. One of the current strategies for remaking 3D models of faces employs stereo cameras. The reproduction procedure, for the most part, comprises of a few stages: adjustment of cameras, securing the depth map and the making of the 3D model. In this paper, a strategy for securing a depth map is suggested that can later be utilized for the reproduction of a 3D model of a face. The proposed technique was tried in a virtual situation - a 3D supervisor "Autodesk 3Ds Max" was utilized to make a virtual scene containing stereo cameras and a human head. The proposed strategy was likewise tried utilizing two "VISAR" cameras, and an "Arduino Micro" microcontroller. "Arduino" programming permits to guarantee synchronization of cameras when utilizing the "Arduino Micro" microcontroller. The pictures are caught from the cameras by utilizing the "FlyCap" program. Since the beginning pictures contain mutilations, the initial step of the calculation is the alignments of cameras. For alignment, comparative focuses are found on both stereo pictures. These focuses are later used to compute the level of contortion, and the pictures are corrected accordingly. The redressed pictures are utilized to compute the depth map. The depth map is made from the front half-tone pictures of appearances [51].

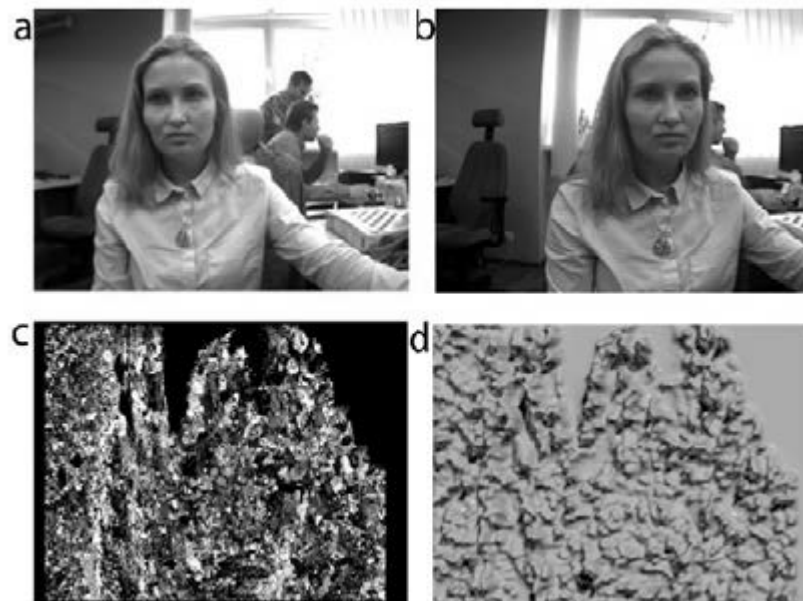


Figure 2.14: (a) Left image; (b) right image; (c) disparity map (d) 3D model [51].

From the experiment above in Figure 2.14, it was concluded to obtain a clear disparity map, a clear resolution camera is required to do the operation. In this experiment, the resolution of cameras is insufficient to perform the operation. It was also important to have cameras that are very precisely aligned with each other. It is also recommended to have bright conditions of light in order to have a clear reconstruction of the depth maps. Stereoscopic cameras for depth maps is also the most widely used technique. [51].

Although 3D technology has been widely discussed, it is not an area that has been mastered throughout the years. This paper by Lee *et al.* presents the pre- and present preparing plans to improve the coding execution of a Multi-View in addition to Depth map (MVD) framework, which is one of the key structures for cutting edge 3D video frameworks. In past work, depth maps have been considered as an alternate sort of video, and a traditional coding plan is just connected. The plan proposed here rather centres around one of a kind properties of depth maps and uses them to improve the coding execution of MVD frameworks as shown in Figure 2.15 [52].

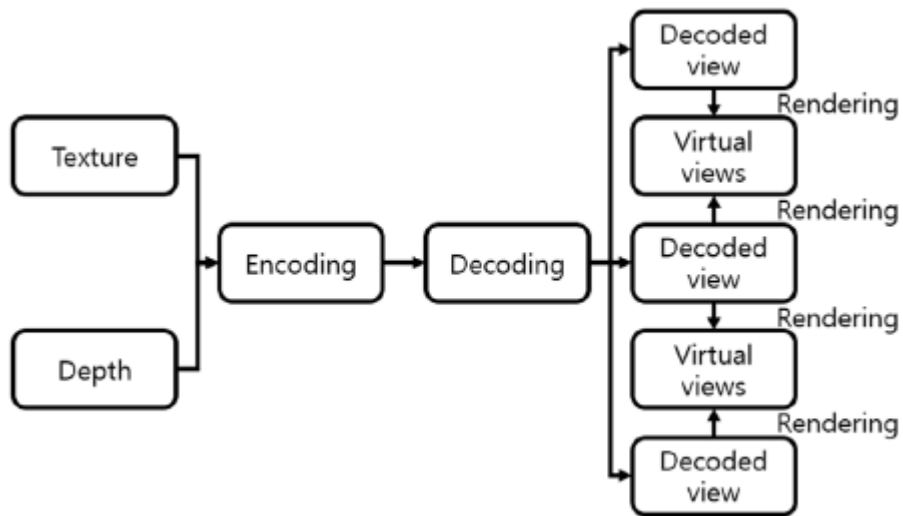


Figure 2.15: Block diagram of the MVD system [52].

In detail, the pre-preparing stage specifically channels the input depth map to decrease the bit-rate cost while limiting quality corruption, and the post-handling re-establishes the reproduced depth map with as much quality as possible. Moreover, the research also proposes an ideal filter selection by theoretic and experimental methods. The examinations demonstrate that the proposed methodology improves the exhibition of an MVD framework [52].

As discussed in the previous paper, Multiview video plus depth (MVD) format is a 3D video representation. This paper by Chao Yang *et al.* on fast depth map coding based on virtual view quality presents a new scheme to estimate virtual view distortion called Virtual View Distortion estimation (VVDE) induced by depth map compression. Based on the VVDE, a region-based Quantization Parameter (QP) adjustment scheme is introduced to improve the quality of the perceived video [53].

Since quantization parameter is conducted in regions, fast VVDE scheme is induced with Rate-Distortion Optimization (RDO) to improve the efficiency of the Coding Unit (CU) to reduce the complexity of the depth map coding. The results from this experiment show that the proposed algorithm can achieve 0.50 dB gain with 47.37% reduced in coding time [53]. The preliminary results of this study are shown in Figure 2.16.

Depth information can highly improve the quality of images and videos. Due to outdoor depth maps that are not easily obtained because of far and major object distances, it is not always an easy task to solve. A paper by Martin Cadik *et al.* on automated outdoor depth map generation and alignment discuss on a fully automated framework for model-based outdoor depth map. This is primarily conducted to improve the quality of images. The enhancement is conducted by leveraging the position of the cameras and 3D terrain models [54].

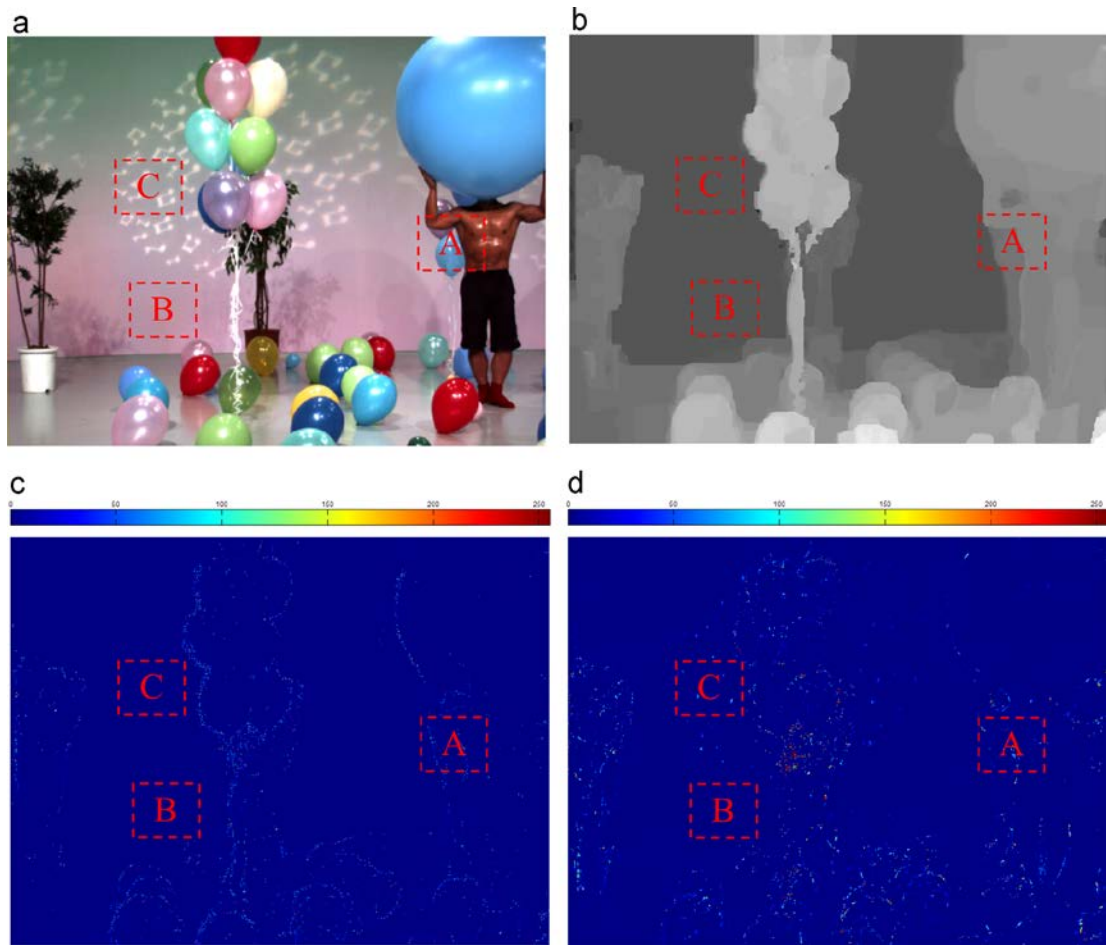


Figure 2.16: Test sequence ‘Balloons’: (a) texture image ;(b) depth map; (c) difference between original and code depth map; (d) difference in virtual view after depth map coding [53].

Figure 2.17 shows an automatically generated synthetic depth map is used to calculate plausible blur kernel size map (middle) to simulate shallow depth-of-field (right) in landscape images (left), where such an effect cannot be achieved using standard optics for physical reasons. Virtual camera: full-frame, f-number = 1.0, focal length = 1200 mm, focus distance = 5 km [54].

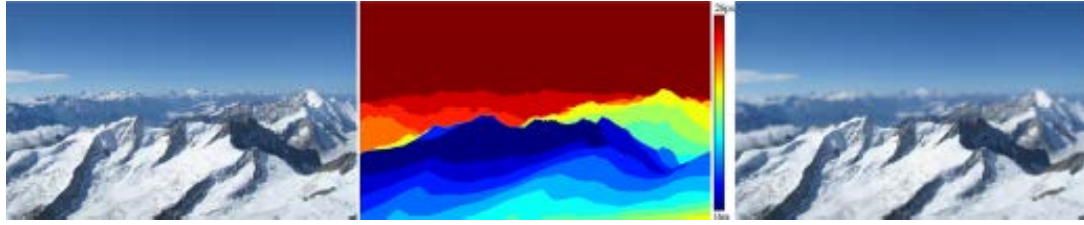


Figure 2.17: Transforming an outdoor photograph into a model-like look [54].

The authors have initially adjusted the manufactured profundity edges with photograph edges by utilizing a raw picture format and then further refining the edges. The subsequently manufactured profundity maps are exact, adjusted in the outright separation. The research findings exhibit their advantage in picture upgrade methods including re obscuring, profundity of-field reproduction, fog evacuation, and guided surface amalgamation [54]. The transformation of a normal image and an image after transformation is shown in Figure 2.16.

The Figure 2.18 below shows the source and synthesized texture with target depth and shading after minor processing of the obtained image sources.

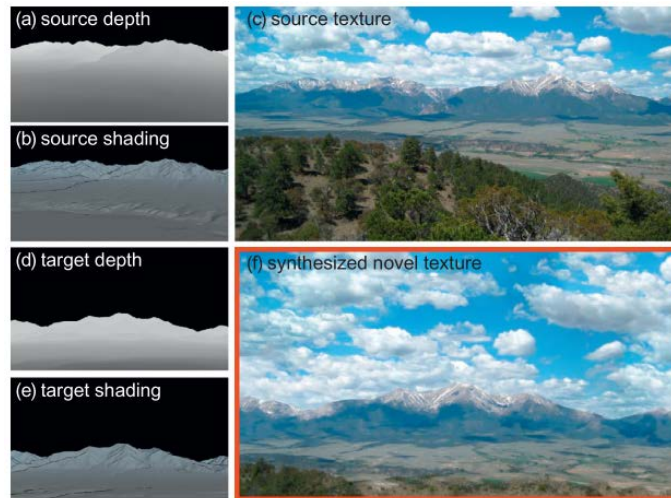


Figure 2.18 : Example of guided texture synthesis. From the source texture, its depth map and shading, we automatically synthesize a novel texture (the red box) for the target depth and shading.

As a summary of the types of techniques that can be used to generate depth maps are presented in Table 2.4. The different techniques are used for different applications as required by the objectives of the study.

Table 2.4: Summary of Depth Map Generation Techniques

No	Type of Depth Technique	Advantages	Disadvantages
1.	Deep Combination of Poses	<ul style="list-style-type: none"> <li>Utilizes machine learning technology which is adaptive to different poses</li> <li>The camera location is relatively unconstrained</li> </ul>	<ul style="list-style-type: none"> <li>Limited to human poses as the datasets used to train the systems are meant for human poses</li> <li>Requires high processing power.</li> </ul>
2.	Characteristics of manmade environments	<ul style="list-style-type: none"> <li>Separates man-made objects and natural environment</li> <li>Breaks down the complex process of obtaining depth</li> </ul>	<ul style="list-style-type: none"> <li>Slower processing time</li> </ul>
3.	Stereo cameras	<ul style="list-style-type: none"> <li>Widely used for the depth map application</li> <li>Relatively clear distinction of depth</li> </ul>	<ul style="list-style-type: none"> <li>Requires relatively bright light to operate</li> </ul>
4.	Virtual Estimation of Depth	<ul style="list-style-type: none"> <li>Requires a single camera application</li> </ul>	<ul style="list-style-type: none"> <li>Does not work in low light conditions</li> </ul>

## 2.6 Application of Electronic Glasses

The invention of highly advanced spectacles to aid us in our daily activities has helped us to carry out many things. The invention of the Google Glass, however, was not a success due to several downsides of which consists of inadequate information's and small and inefficient screen sizes [55]. An invention by Klaus Hoffmann from Hollywood on a binocular optical device is one step forward for electronic glasses [56].

This invention is aimed at producing a cost-effective glass which consists of microcomputers such as Raspberry Pi and Adafruit consoles and autofocus functions. The autofocus on this spectacle is intended to automatically focus on objects based on the exposure of light. The autofocus is also directly connected to the onboard camera which constantly does phase detection. Phase detection is a function which exists on all our handheld devices which allow the camera to automatically focus and allows us to take good pictures. This particular spectacle also consists of a hearing aid which can help those with auditory problems as shown in Figure 2.19 [56].

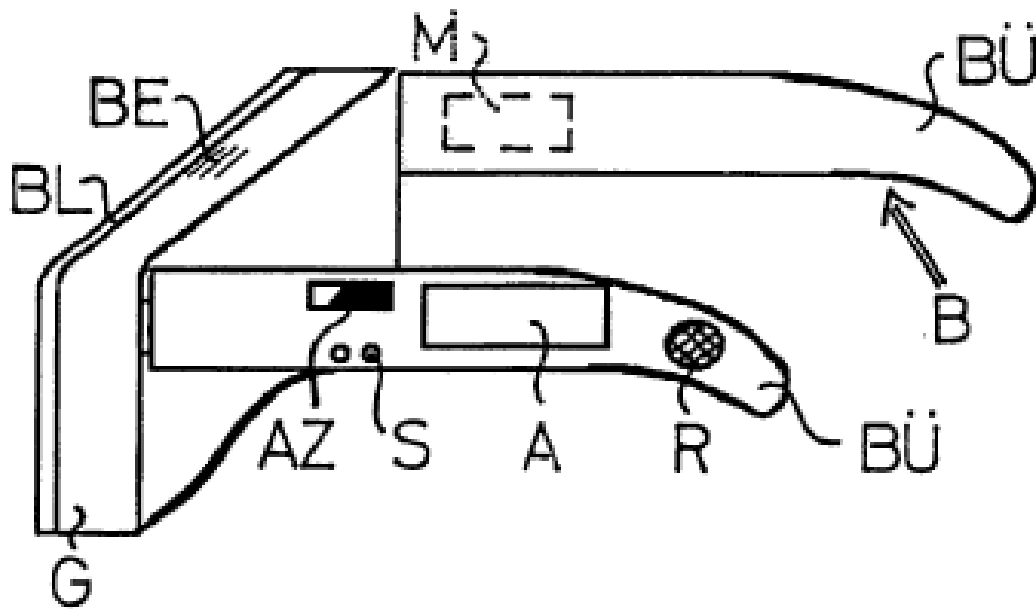


Figure 2.19: Spectacle with hearing aid [56]

Short and farsightedness or also known as hypermetropia and hyperopia are caused by the improper refraction of the eyeball and the lens. Thus, in the case of short-sightedness, the eyeball is short or also referred to as having low refractive power and vice versa for long-sightedness. This case is, however, being corrected by convex and concave lenses [56].

The principles of operation of a human eye are also very much the same as compared to a camera. In fact, the functionality of a camera is adopted from the human eye. Within our eyes, the lens is either flattened or thickened to produce a focused image the flattening and thickening process is controlled by the ciliary muscles which hold the lens in place. As we age, however, muscles get weaker, and they lose the tendency to contract and relax the lens properly. As compared to a six-year-old who can clearly focus on objects held close to him [56].

An invention by. Brady *et al.* on the combined spectacle frame and light have solved a fundamental problem with a simple solution. With the current trend and demand increasing for the need of every equipment to be at the reach of a fingertip, this solution enables a person to read in a dark with a personalized light. This is suitable for numerous people who live in different situations. For instance, an individual living with a roommate would not want to disturb him at night by turning on the light to do some reading [57].

Thus, this invention has a light suspended on the spectacle frame as shown in Figure 2.20. The spectacle is also well designed to allow those with prescribed lenses to be inserted within without interrupting the electromechanical components of the light and its frame. The power source of the light is also housed at the ends of the frame without disrupting the line of vision of the wearer. This design is also foldable for easy portability. The dual poles of the battery are interconnected in the middle of the spectacle frame. Two bulbs are provided at each end of the spectacle has a wider coverage area for the reader. This invention was patented in 1953, however, the same principles can still adhere much so with the current technology. With lithium-ion or cylindrical ion batteries, the system can be made much more compactly for much sleek look [57].



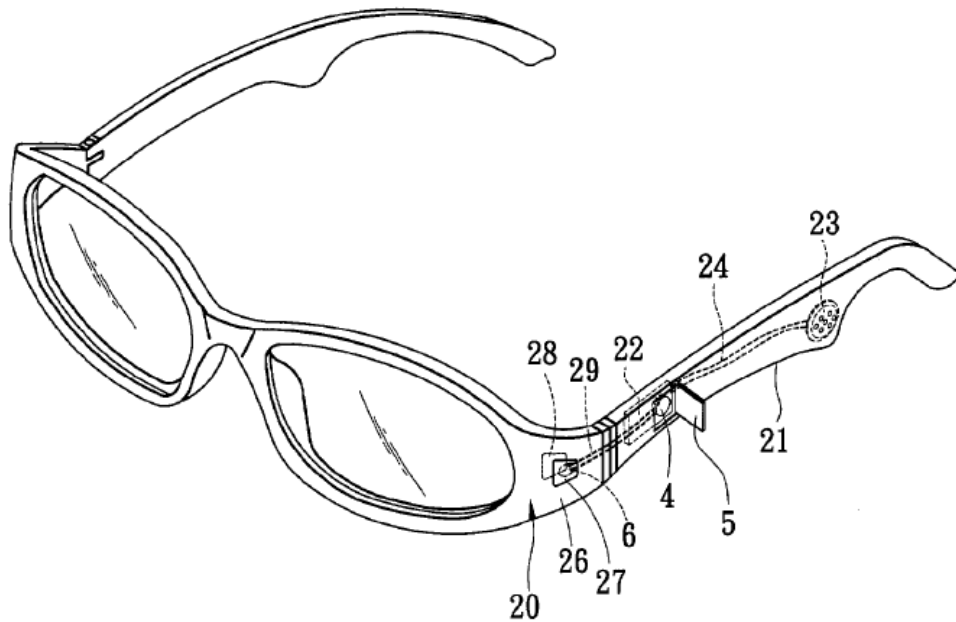


Figure 2.21: Visual aid with speaker [58]

The circuitry of the system is embedded within the frame and is thin in thickness. The information display device is connected by a low-frequency electromagnetic wave to the cell phone. With the integration of a speaker, this device also doubles as a media player [58].

### **2.7 Previous works associated with the development of the monocular visual aid**

A study by the Seoul National University on the monocular inertial navigation for mobile robots using uncertainty-based triangulation. The robots in this study use a monocular camera and an inertial measurement unit. The inertial measurement unit measures the surrounding objects, these measurements then associated the footage from the camera to produce uncertainty-based triangulation similar to how the Global Positioning System (GPS) works, which is able to provide an algorithm to differentiate the 3D objects and obtain a depth perception [59].

Another study on the variable view angioscopy was developed in a very simple way to enhance the field of vision using two faces angled graded-index (GRIN) lenses.

These lenses are miniaturized so much so that can enter through a blood vessel. The flexible angioscope is also able to measure the spatial resolutions in the blood vessel. Similar technology can be used to measure the spatial area of monocular visual impaired patients. The (GRIN) lenses can be used in accordance to enhance the field of vision [60].

Stereo vision systems are technologies that have become something that is used for navigation application due to its depth capability which has more control in terms of distance. A paper by Sankowski *et al.* on the uncertainty measurement in stereo vision system aims to estimate the uncertainty levels that are obtained from the saliency map that is generated by the stereo vision system. Practical application of the stereo vision system is very less studied until today, thus this paper studies the uncertainty measurement in the three axes (x,y,z) that is constructed by the stereo pair. The proposed method does not require any additional equipment besides the general two RGB sensors, calibration board and a laser distance meter. Sankowski *et al.* and his team have come with a test model and special mathematical formulas that are used for accurate measurement of the stereo vision system. The obtained measurements are known to be reliable and accurate due to the large amount of data obtained. Many experiments were conducted in order proof the application of this method in a real-life scenario. The proposed system can also be integrated into any current system as it does not require any alteration to the current system architecture and assessment process [61].

Technologies like Kinect uses a combination of RGB and an IR sensor to recognize depth based on range vision. This system works by the projection of infrared on to the visual field. The infrared ray that is reflected from the subject in the visual field is translated into depth information by measurement of the intensity of the infrared ray. The method used in this study is the typical stereovision technique where two cameras which known relative position and identifies the differences in the images by the cameras by the finding the correspondence between points that are viewed both the camera. Two important parameters namely the distance between the cameras, and type of camera is used to compute the three-dimensional location of the points.

## **2.8 Summary**

A research gap on the material used to manufacture the visual aids are not discussed properly in the previous prototypes, thus the material used to manufacture the current prototype is discussed in the following sections. As a summary, it can be said that existing treatments such as applying a patch for amblyopic patients on the sound eye and wearing lenses to correct refractive errors do not achieve the objective of the current study to improve on the field of vision or to obtain a depth perception on the things around them. Visual saliency is also vital in obtaining the appropriate level of clarity and comfort to the human eye. A study was also conducted for spatial recognition with monocular cameras by using Inertial Measurement Units (IMU). The misalignment of these cameras will also cause discomfort for the viewer; thus, it is vital to understand the disparity(mm) between stereoscopic cameras. These parameters are important in order to understand to produce a clear depth map. Based on the flexible angioscope, the field of vision an also is increased by compressing the image to form a fisheye image to highlight the front view.

## **CHAPTER 3**

### **METHODOLOGY**

#### **3.1 Introduction**

The purpose of this chapter is to explain the methodological framework used to conduct this research. This chapter underlines the steps taken to design, plan and to carry out the research. It will cover the methodological approach and methods used to identify the sample population and participants, the steps involved in designing and integrating the neurological framework behind the visual aid, and the experiments that were used to verify the objectives of the research. The methodology was chosen as relevant to the tasks of carrying out opinion surveys in the form of structured interviews and critically analysing and integrating the data from literature reviews from Chapter 2.

#### **3.2 Research Design**

A quantitative study approach was implemented, in this research and the priority is given to study the challenges faced by monocular visual impaired patients. The data collection also involves numeric information through questionnaires so that the final database represents quantitative information. Reviewing relevant articles on monocular visual impairment such as amblyopia helped limit the scope of the research, and several frameworks, models and theories by other writers and researchers.

### 3.3 Research Process

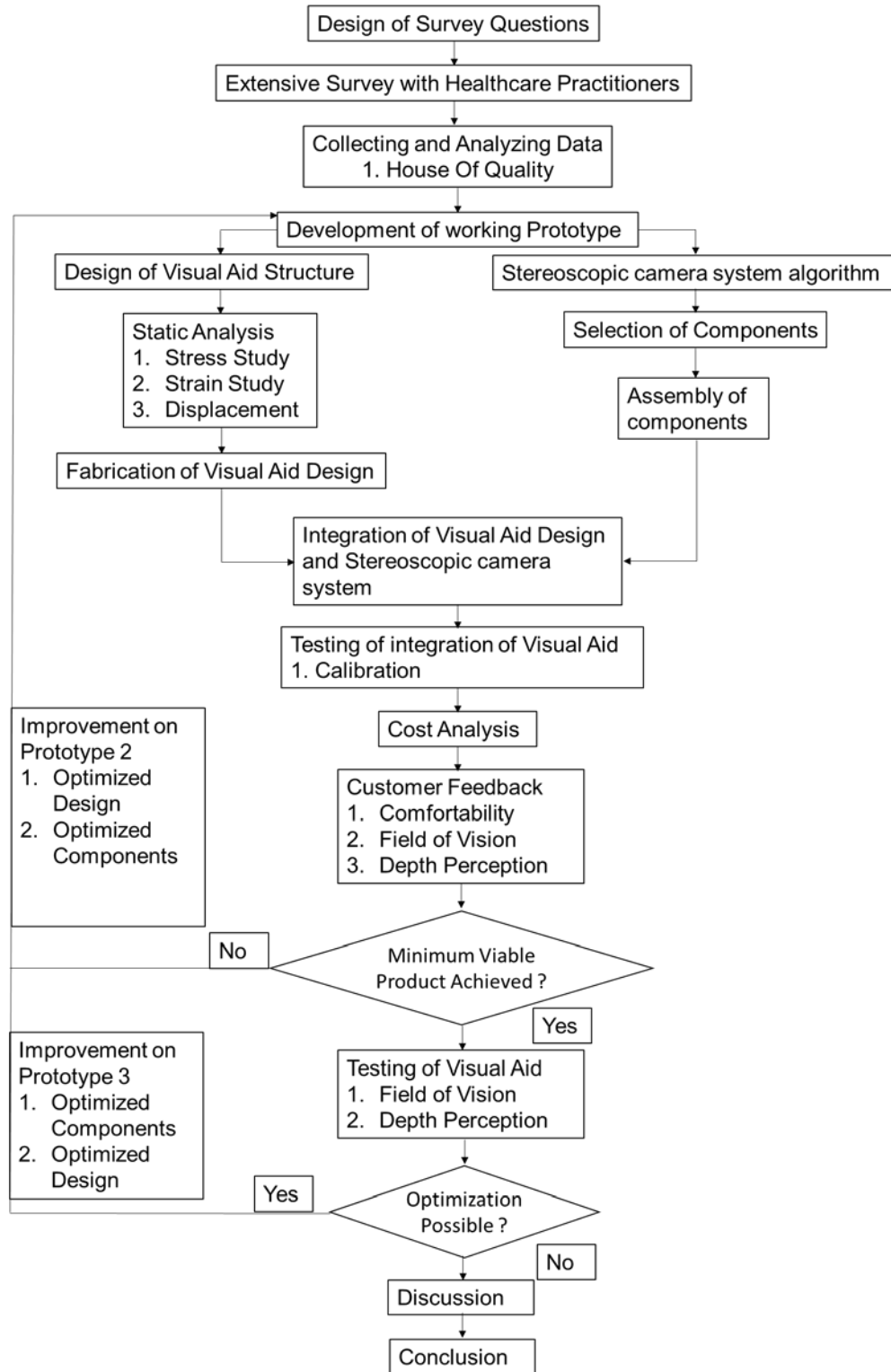


Figure 3.1: Project Flow chart

### **3.4 Design of Survey Questions**

The survey was conducted with ophthalmologist and patients to study more on how the monocular vision affects a person's daily activities. The interview was also conducted to deepen our understanding of the causes of this visual impairment. The main criteria of the questions that was interviewed with the monocular visual impaired patients and the medical professionals revolves around the main challenges faced the patients. Further statistics on the occurrence and treatment for these patients was also obtained with a personal interview (Refer Appendix A for Interview Questions) with an ophthalmologist.

The surveys were conducted as a personal interview survey or also known as a face-to-face survey. This method was chosen to be used as this research targets a specific population. This type of survey also enables us to explore the responses of the people to gather more and in-depth information about this research. They also have contributed to the requirements that needed to be embedded in the visual aid as they have a more broad and general perception of a monocular visual impaired patient.

The monocular visual impaired patients were interviewed personally to understand the challenges faced by them with the impairment. The patients also have contributed ideas and suggestions in order to have a visual aid made for them. They were also very delighted with the research and development on a visual aid that catered for their needs. Based on the feedbacks that were obtained from this survey a house of quality was constructed to understand the weight of the requirements to design the new visual aid.

### **3.5 Extensive Survey with Healthcare practitioners and patients**

The medical professionals that were interviewed for this study were all from the department Ophthalmology, two of the medical professionals were from the Tun Hussein Onn Eye Hospital, Ms Ramakrishnan who is an optometrist and Dr Lim who is an ophthalmologist have provided clear feedback and requirement from the care providers side of developing a monocular visual aid for the monocular visual impaired.

Table 3.1: Profile of medical professional respondents in the survey

<b>Name</b>	<b>Type of professional</b>	<b>Number of years of experience</b>	<b>Field of Expertise</b>
<b>Ms Geetha Ramakrishnan</b>	Optometrist	15	Low Vision
<b>Dr Lim Hsien Han</b>	Ophthalmologist	11	Low Vision
<b>Dr Lee Chee Wai</b>	Ophthalmologist	20	Monocular Visual Impairment

Both these professionals have more than 10 years of experience in their field of expertise of low vision. Low vision specialists are specialized in low vision testing, treatment and diagnosis and trained to conduct low vision evaluations to prescribe special devices for low vision as shown in Table 3.1. Most patients who referred to these specialist present with loss of visual field due to monocular visual impairment, loss of visual acuity, distortion, loss of colour vision, loss of depth perception or loss of contrast[62].

The patient respondents that have participated in this survey consists of patients from Hospital Taiping Ophthalmologist department and from the Tun Hussein Onn Eye Hospital in Petaling Jaya. A sample size of 16 respondents out of 50 patients per day were interviewed to obtain feedbacks and requirements for visual aid. This sample size represents about 32% of the low vision patients per day that visit the hospital. The sample size that was determined has the following statistical factors as shown in Table 3.2.

Table 3.2 : Statistical Factors for survey sample size

<b>1.</b>	Confidence Level	95%
<b>2.</b>	Confidence Interval	20.41
<b>3.</b>	Population	50

The confidence interval (also called margin of error) is the plus-or-minus Figure usually reported in newspaper or television opinion poll results. A confidence interval of 20.41 and 70% percent shows surety of the answer, if the question had been asked of the entire relevant population between 49.59% (80-20.41) and 90.41% (70+20.41) would have picked that answer.

The confidence level tells you how sure you can be. It is expressed as a percentage and represents how often the true percentage of the population who would pick an answer lies within the confidence interval. The 95% confidence level means you can be 95% certain. Most researchers use the 95% confidence level.

There were three main types of monocular visual impairment that were identified from the survey that was conducted. The three types of impairment were glaucoma, trauma and amblyopia.

Glaucoma is a visual impairment due to high ocular pressure which causes the retina to swell and thus vision is slowly lost. Glaucoma is most commonly associated with hyperglycaemia (Diabetes Mellitus) or high levels of glucose which causes the ocular pressure in our eye to regulate at an optimum level[63]. Trauma refers to patients who have lost their sight or vision due to accidents and mishaps. These types of patients are most commonly fitted with prosthetic eyes which function only as an aesthetic property to a patient and has no visual capabilities. Amblyopia, as discussed in the previous chapters, refers to having a vision in one eye or inadequate vision in the other eye. This impairment is reversible if treated at an early age and has an irreversible effect if left untreated at a later age.

### **3.6 Collecting and analysing the data (House of Quality)**

The data collected from surveys and interviews were then put into the House of Quality (HOQ) to determine the engineering and customer requirements of the final prototype. The data that was obtained were both qualitative and quantitative. The data that was obtained are coherent with the objective of this research. These parameters were reiterated in the development process of the visual to satisfy its objectives. With this, we were able

to understand the needs of a monocular impaired patient and was able to narrow down the concepts in the final design. The analysis of the data obtained from the HOQ by graphs and charts was then be further scrutinized to obtain a proper solution that was then integrated into the visual aid.

The House of Quality is a conceptual map that provides the means for inter-functional planning and communications [64]. The House of Quality is also known as the Quality Matrix. The matrix provides details such as customer requirements, technical descriptors, priority levels of the various descriptors, the relationship between the descriptors and target values for each descriptor amongst others [65]. This House of Quality is compared with existing visual aids in the market which was mentioned chapter 2. A total of 16 functional and customer requirements were assigned based on the interviews. The functional or engineering requirements were derived directly from the customer requirement. The functional requirements help to develop the prototype by directly focusing on a particular function on the visual aid's development. For example, a customer requirement of wide vision is mapped on to the field of vision (angle) in the functional requirement, thus angle being a measurable quantifier, is used to benchmark the prototype in the development process. This method aids in directly addressing the problem objectively.

### **3.7 Development of working prototype**

Based on the interpretations of data from the House of Quality, the development process was initiated. The analysis from the house of quality helps to directly address the customer requirement without developing on other areas of the visual aid which might not have helped to solve the challenges faced by the monocular visual impaired patients. In this research, increasing the visual range was the primary objective of the research, whilst increasing the field of vision. Developing a prototype is a very essential and rewarding step [66].

In terms of hardware, extensive work was put into designing and understanding the required hardware systems. Two cameras were arranged laterally and properly distant

on to the visual aid design mimicking the actual distance between a human eye [67]. The image produced from this camera were then processed in real-time on a microprocessor onboard to identify far and near an object.

The design specifications that were considered to be upgraded from each phase of the development are as stated below:

1. Weight of the visual aid
2. Type of microcontrollers used
3. Quality of Depth Map (clarity)
4. Visual field (angle of vision)

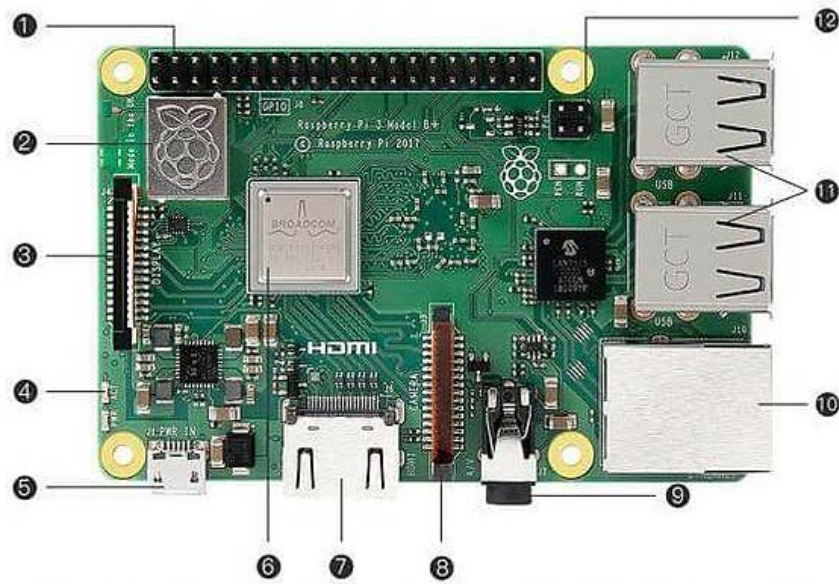
### **3.7.1 Development of Working Prototype Phase 1**

Development of this prototype in phase 1 focuses on bringing visual aid to a reality. Thus, the proper selection of hardware was vital for this project.

#### **3.7.1.1 Hardware Development**

It was decided in the stages of this research that a standard Raspberry Pi 3B would be used to conduct this study as it was very small and had the capabilities in terms of software to run the stereoscopic image processing.

However, although the Raspberry Pi 3B has the capabilities in terms of software. It does not contain the peripherals to attach a second camera on it [68]. The microcontroller only has one peripheral for camera input, this is because the microcontroller was not designed to handle stereoscopic image processing. It was designed simple specific purposes such as sensor and reaction functions [69]. Raspberry has developed other models of its products to conduct development projects as the stereoscopic image processing. The interface and peripherals that are available on a Raspberry Pi are shown clearly in Figure 3.2.



- |                                    |                        |  |
|------------------------------------|------------------------|--|
| ① 40-Pin GPIO Header               | ⑤ 5V MicroUSB          | ⑨ 4-Pole 3.5mm Audio & Composite Video |
| ② WiFi Antenna                     | ⑥ Broadcom CPU         | ⑩ Ethernet Port                        |
| ③ DSI Display Connector            | ⑦ HDMI Port            | ⑪ USB Ports                            |
| ④ MicroSD Card Slot (On Underside) | ⑧ CSI Camera Connector | ⑫ Power-over-Ethernet (PoE)            |

Figure 3.2: Interface of Raspberry Pi 3B+ and its peripherals [70]

Due to this constraint, another type of computing module is used. The Raspberry Pi Compute Module (Figure 3.3) was chosen to be used due to its extensive usage in the industry. The Raspberry Pi Compute Module also has all the capabilities of a Raspberry Pi 3 Model B+ but just very much more flexible. The compute module contains a Broadcom 1.2GHz ARMv8 64-bit processor and 1GB LPDDR2 SDRAM. This is all fitted onto a small (67.6mm x 31mm) board that fits into a standard DDR2 SODIMM connector [71].



Figure 3.3: Raspberry Pi Compute Module 3 (CM3) [72].

The compute module, however, is not a stand-alone device which works on its own. The raspberry pi requires an Input/output board or better known as IO or io board [73]. This is peripheral between an information processing system such as a processor and the outside world. Inputs are the instructions and signals received by the system and output is the reaction or data sent from it [74].

A simple example of an IO that is in abundance and is used by almost everyone daily is the motherboard of a computer. The processor that is embedded within the motherboard requires an IO board to interface itself for human input. For the Raspberry Pi Compute Module 3, there are two options for the IO boards [75].

The first option for the IO board that is produced by Raspberry itself, this board comes as a development kit together with the compute module. This IO board is intended for the sole purpose of using it with the IO board whereas the other board which is produced by a company called Waveshare. It is called as Waveshare Compute Module IO Board Plus, for Raspberry Pi CM3 / CM3L / CM3+ / CM3+L. The one thing that makes this IO board better than the previous board is that it is much more robust as it has an open-ended Arduino, standard and an add-on GPIO and other peripherals on it [76]. This makes this communications board have a wide range of functions. The interface of the Waveshare compute module is as shown in Figure 3.4

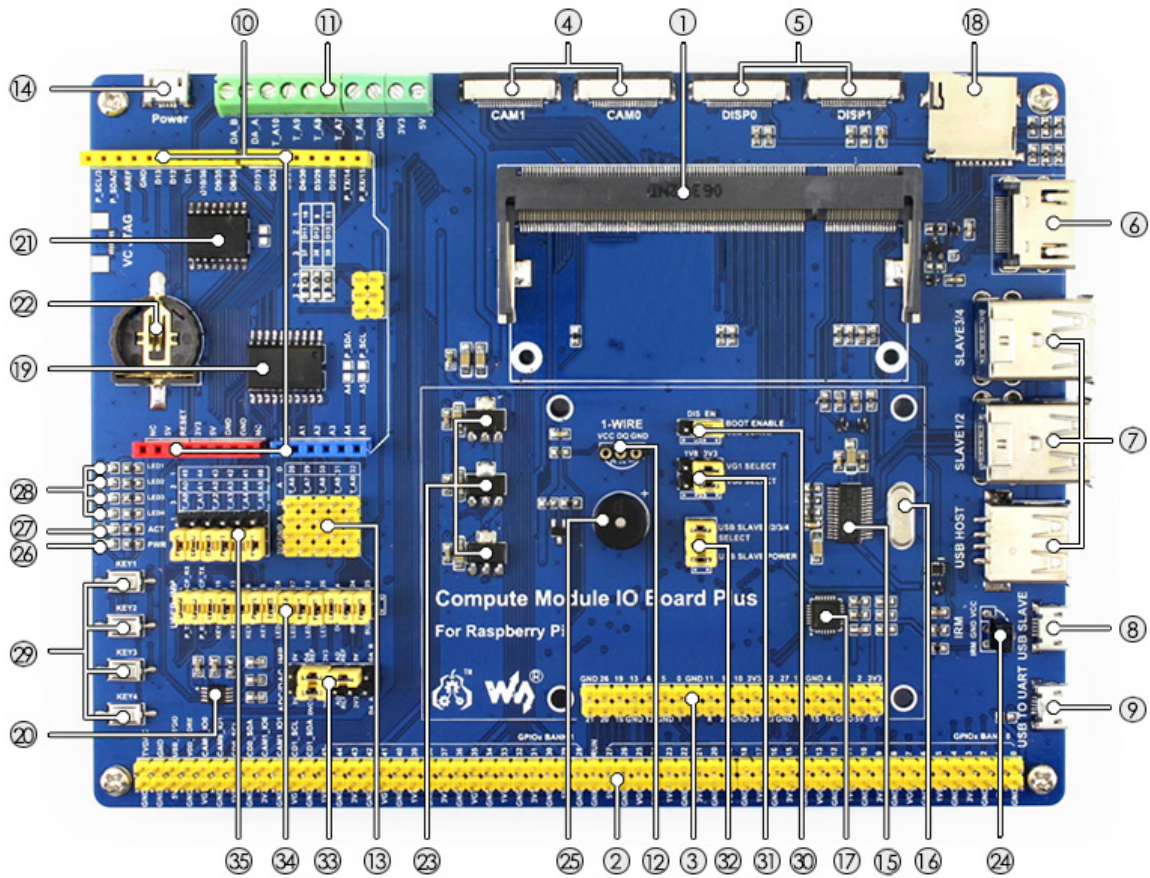


Figure 3.4: Waveshare compute module IO board [77]

The detailed interface of the Waveshare compute module IO board is shown in Appendix C which corresponds to the numbers on Figure 3.4.

Concluding the hardware of development of working Prototype phase 1, where the compute module and IO board are integrated together as shown in Figure 3.5. The software development was begun in terms of the coding process.

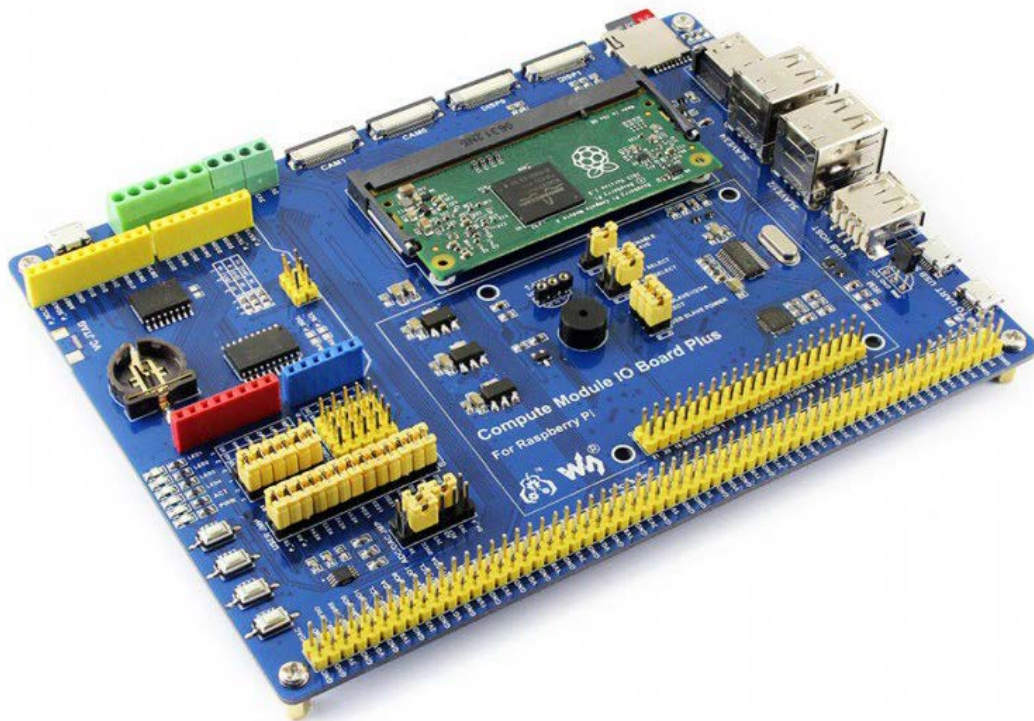


Figure 3.5: Raspberry Pi Compute Module Integrated with the Waveshare compute module I/O board

### 3.7.1.2 Software Development

In terms of software, the program is written in the Python language on a raspberry pi microprocessor running ROS (Robot Operating System) [78]. The Robot Operating system is not actually an operating system, but just a framework and set of tools that provide the functionality of an operating system on a different type of microcomputers or computer clusters [79]. The advantage of this system is not only limited to robots but most of the tools provided here are focused on working with peripheral hardware such as the Raspberry Pi or the Compute Module. The key feature of ROS is that it provides a way to connect a network of processes (nodes) with a central hub [80]. The main way of creating the network is by defining a publisher connection with other nodes. As the processes for a major process is broken into smaller processes. The load on the physical processor is reduced, thus the results obtained is much better in terms of frame rate and latency. This

eliminated the need for a calibration process [81]. The algorithm flowchart is shown in Figure 3.6.

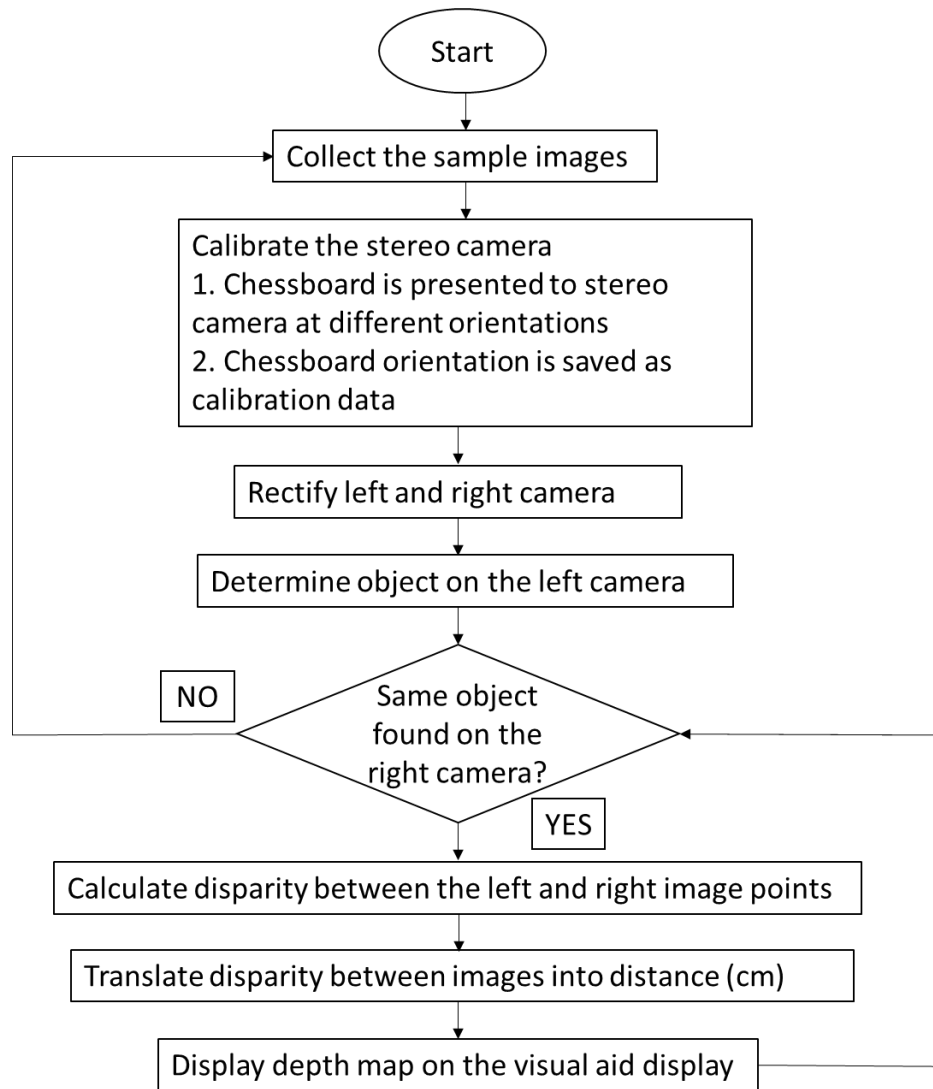


Figure 3.6 Algorithm flowchart of ROS stereoscopic image processing

### 3.7.1.3 Preparing the Design of Prototype 1

The design of the prototype as shown in Figure 3.7 was designed to accommodate the hardware of the compute module and the two stereoscopic cameras. Static studies were also conducted on this design to ensure it does not have a heavy structure and does not apply too much force to discomfort the user. As per current international standard for spectacle frames weighing over 25 g, a contact area of more than 250mm<sup>2</sup> is recommended [82]. The study was conducted on Solidworks 2019.

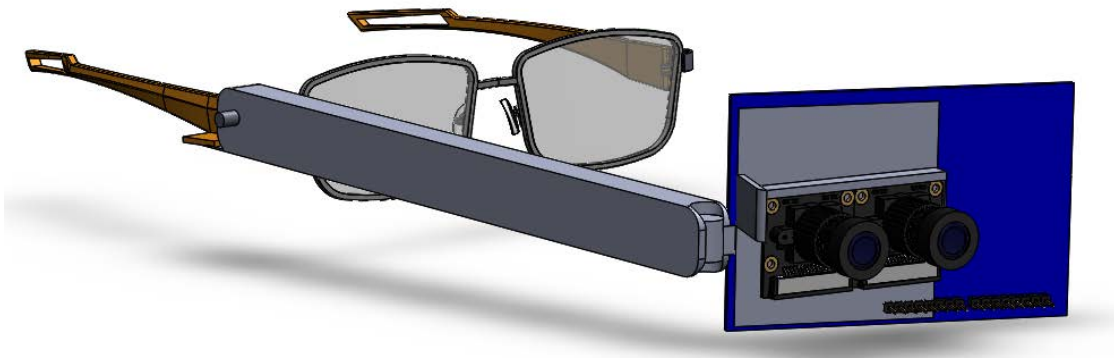
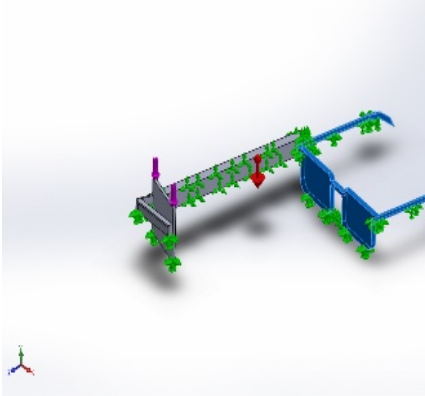
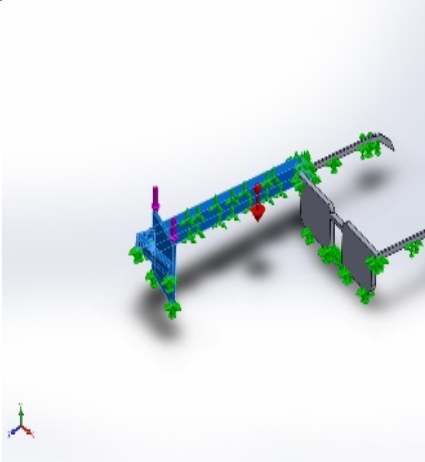


Figure 3.7: Solid works design of prototype phase

To ensure the proper outcome of any static study, it is important to ensure the pre-sets on the model are as accurate as possible dimensionally. There are many pre-sets that determine the result of a study. However, for this study, only three main pre-set criteria are focused namely material properties, loads and fixtures. The complete pre-sets of the study are attached in Appendix B.

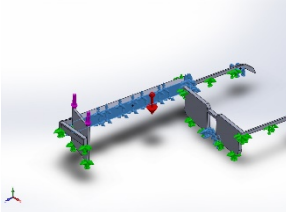
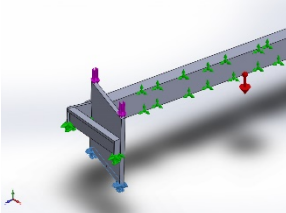
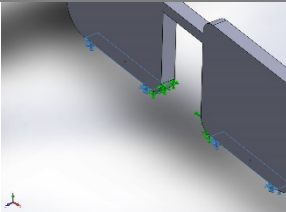
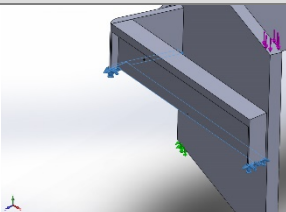
## 1. Material Properties

Table 3.3: Material Properties of Prototype 1

Model Reference	Properties	
	Name:	<b>ABS PC</b>
	Model type:	<b>Linear Elastic Isotropic</b>
	Tensile strength:	<b><math>4 \times 10^7</math> N/m<sup>2</sup></b>
	Elastic modulus:	<b><math>2.41 \times 10^9</math> N/m<sup>2</sup></b>
	Poisson's ratio:	<b>0.3897</b>
	Mass density:	<b>1070 kg/m<sup>3</sup></b>
	Shear modulus:	<b><math>8.622 \times 10^8</math> N/m<sup>2</sup></b>
	Name:	<b>PLA</b>
	Model type:	<b>Linear Elastic Isotropic</b>
	Default failure criterion:	<b>Max von Mises Stress</b>
	Yield strength:	<b><math>3.59 \times 10^7</math> N/m<sup>2</sup></b>
	Tensile strength:	<b><math>5.0332e \times 10^7</math> N/m<sup>2</sup></b>
	Elastic modulus:	<b><math>3.51633 \times 10^9</math> N/m<sup>2</sup></b>
	Poisson's ratio:	<b>0.35</b>
	Mass density:	<b>1249.44 kg/m<sup>3</sup></b>
	Shear modulus:	<b><math>2.41317 \times 10^9</math> N/m<sup>2</sup></b>

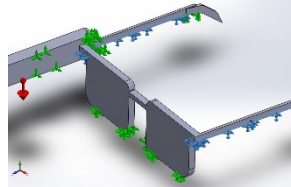
## 2. Fixtures

Table 3.4: Fixtures Applied on Prototype 1

Fixture name	Fixture Image	Fixture Details		
Fixed-1		Entities: <b>5 face(s)</b> Type: <b>Fixed Geometry</b>		
Resultant Forces				
<b>Components</b>	<b>X</b>	<b>Y</b>	<b>Z</b>	<b>Resultant</b>
<b>Reaction force(N)</b>	<b>0.000273586</b>	<b>0.414493</b>	<b>-0.00309878</b>	<b>0.414505</b>
Fixed-2		Entities: <b>1 edge(s), 1 face(s)</b> Type: <b>Fixed Geometry</b>		
Resultant Forces				
<b>Components</b>	<b>X</b>	<b>Y</b>	<b>Z</b>	<b>Resultant</b>
<b>Reaction force(N)</b>	<b>-0.00913319</b>	<b>0.51055</b>	<b>-0.0241037</b>	<b>0.5112</b>
Fixed-3		Entities: <b>2 face(s)</b> Type: <b>Fixed Geometry</b>		
Resultant Forces				
<b>Components</b>	<b>X</b>	<b>Y</b>	<b>Z</b>	<b>Resultant</b>
<b>Reaction force(N)</b>	<b>0.000777361</b>	<b>0.165315</b>	<b>-0.00281183</b>	<b>0.16534</b>
Fixed-5		Entities: <b>2 face(s)</b> Type: <b>Fixed Geometry</b>		

Resultant Forces				
Components	X	Y	Z	Resultant
Reaction force(N)	0.00215938	0.108642	0.00160813	0.108675

Fixed-6

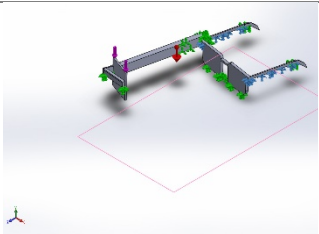
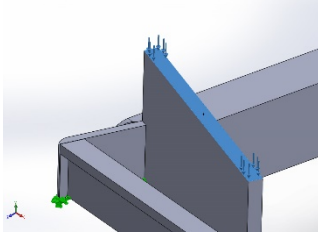


Entities: 2 face(s)  
Type: Fixed Geometry

Resultant Forces				
Components	X	Y	Z	Resultant
Reaction force(N)	0.000983265	0.04085	0.00637382	0.041356

### 3. Loads

Table 3.5: Loads Applied on Prototype 1

Load name	Load Image	Load Details
Gravity-1		Reference: Top Plane Values: 0 0 -9.81 Units: m/s <sup>2</sup>
Force-1		Entities: 1 face(s) Type: Apply normal force Value: 0.48 N

This design also features a 5.0-inch 1280 x 720 pixels LCD screen with an HDMI input as shown in Figure 3.8 to display the depth map and the extended range of vision.

The HDMI screen was chosen in contrast with the standard GPIO screen due to its impressive simplicity which reduces the number of components and looks very neat in terms of aesthetics. The HDMI output is used to transmit the video feed between the processor and the screen. The HDMI cable was also replaced with an HDMI pin instead of the cable.

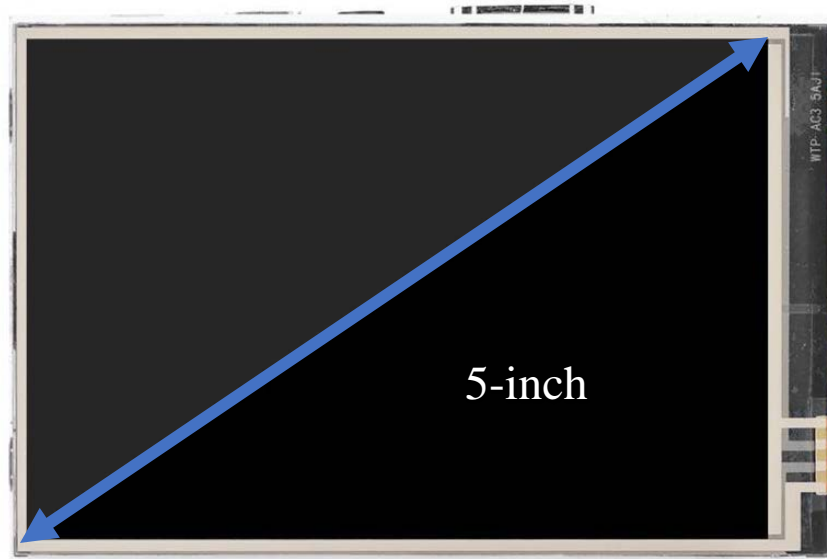


Figure 3.8: 5-inch LCD screen [83]

The Visual Aid was printed with a 3D printer, loaded with Polylactic Acid (PLA) material with 20% infill. PLA was chosen as it is very much different than most thermoplastic polymers, this material is derived from renewable resources like corn starch or sugar cane. PLA is also known as a common type of bioplastics due to its derivation from biomass resources, thus making it biodegradable [84].

The cost of PLA is also relatively low due to its characteristic being like common types of plastics such as polystyrene (PS), polypropylene (PP), polyethylene (PE), thus does not require any new manufacturing equipment to produce it [85]. The huge benefit of PLA as a biodegradable material is its versatility and the fact it naturally degrades when exposed to the environment. As the visual aid has slight contact with human skin and

interfaces itself directly with the user, it was a concern if the plastic material would cause any form of harm such as rash or any form irritation [86].

PLA in its solid form is not toxic. As a matter of fact, PLA is commonly used in medical implants that biodegrade within the body over time and the food handling industry. As most of any other plastic materials, it does have a threat of toxicity if inhaled or absorbed into skin or eyes in its liquid or vapour form (most commonly during the manufacturing process) [87].

#### **3.7.1.4 Integrating Design into a Working Prototype 1**

The components that help in the function of the visual aid such as image processing algorithms and the placement of cameras was then integrated with the design of the prototype. With the integration of both the frame and the internal components, the prototype was then completed for further testing that was conducted to optimize the design into its final and complete state. The completed prototype is shown with all its components embedded together in Figure 3.9.

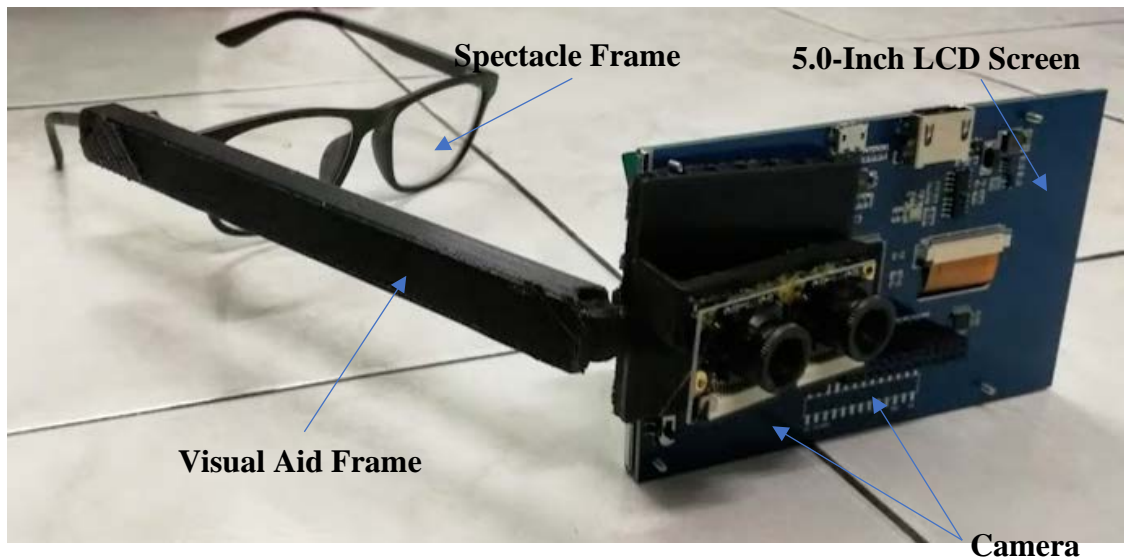


Figure 3.9: Completed Phase 1 prototype.

### **3.7.2 Development of Working Prototype Phase 2**

Phase 2 of the development process was begun after receiving feedbacks and critics from the development of a prototype conducted in Phase 1. This phase of development focused more on optimizing the product based on user ergonomics.

In terms of hardware, the compute module and its accompanying IO board remain as the brain of the whole visual aid. However, phase 2 has focused more on the aesthetics and improving the quality of the depth map produced previously making it more accessible to the user.

In terms of software, prototype 2 was installed with the Raspbian OS, Raspbian OS is a free operating system designed and optimized for the Raspberry Pi hardware. The advantage of a Raspbian OS is that it comes with over 35,000 packages, pre-compiled software packed in a simple format for easy installation on a Raspberry Pi [88].

As Raspberry Pi is a well-known platform for development, an image processing library was used for this purpose. The Open Source Computer Vision library or better known as OpenCV library was used in prototype 2. This programming library is mainly for real-time computer vision. The library was originally developed by Intel [89]. As this library is cross-platform, thus can be used on a simple microprocessor such as the raspberry pi or a complex machine such as a table top computer and on various operating systems such as Windows, macOS, FreeBSD, NetBSD, OpenBSD and Linux. It is also a very versatile library as it is open-sourced under the open-source BSD license [90].

However, calibration was required with the OpenCV library to produce a depth map. Calibration was conducted with 9 x 6 checkerboard as shown in Figure 3.10.

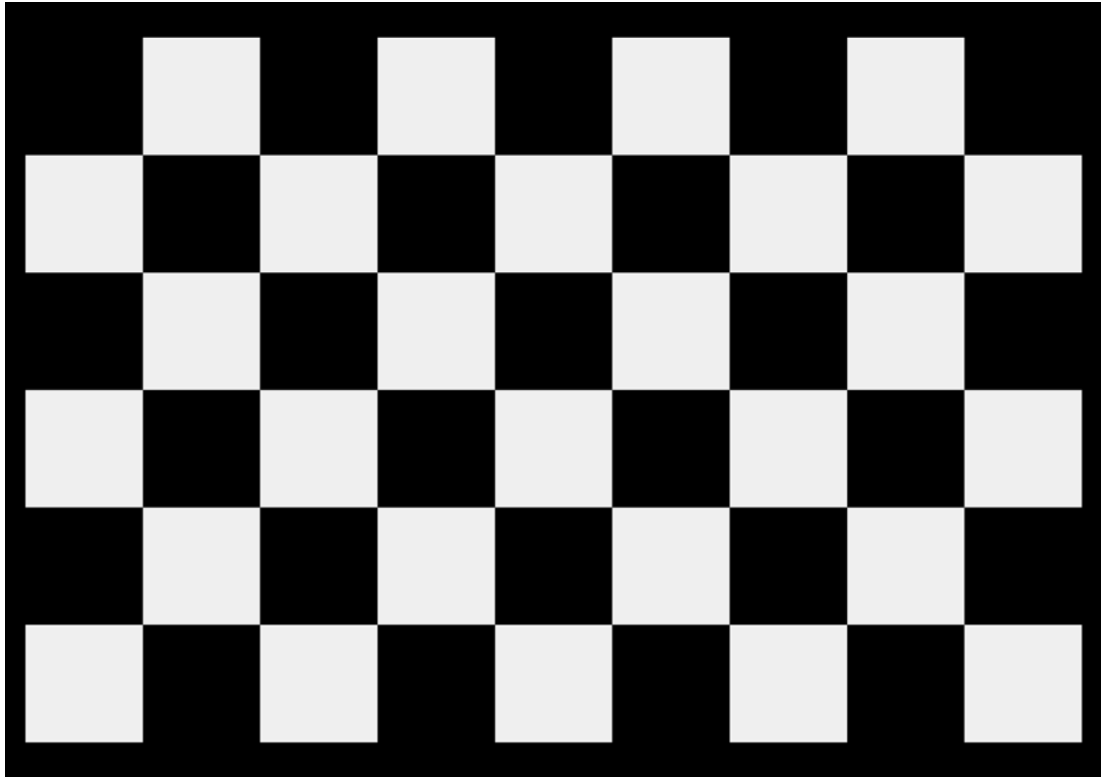


Figure 3.10: 9 x 6 checkerboard used for stereo camera calibration [91].

### 3.7.2.1 Calibration of Stereo Cameras

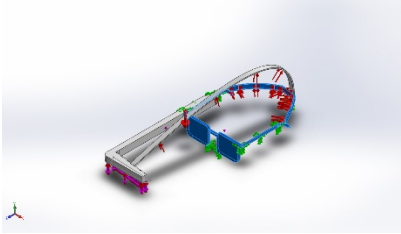
The calibration process is initiated by the program by snapping 30 sets shots of the checkerboard at 5 seconds interval. The program then cuts the pairs and separates it between left and the right image with user input to discard any blurred images. This process of discarding any one of the sets of images does not interrupt with calibration as there are enough images taken before. The program then calibrates itself using the sets of images to produce a rectified left and right image of the calibrated checkerboard. The flowchart of the algorithm used with OpenCV is the same as shown in Figure 3.6.

### 3.7.2.2 Preparing the Design of Prototype 2

A new design for the visual aid was designed on the Solidworks 2019 platform. This design as like the previous designs have undergone static failure analysis to analyse the stress and strain points of the design as the preloads are as shown in Table 3.6 to Table 3.8. Support structures were also added in this design to aid in the load-bearing aspect to the user. The complete presets of the study are attached in Appendix C.

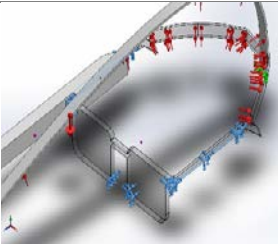
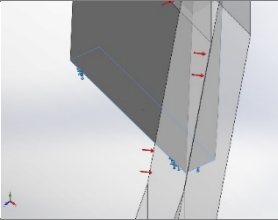
#### 1. Material Properties

Table 3.6: Material Properties of Prototype 2

Model Reference	Properties
	Name: <b>PLA</b> Model type: <b>Linear Elastic Isotropic</b> Default failure criterion: <b>Max von Mises Stress</b> Yield strength: <b><math>3.59e \times 10^7 \text{ N/m}^2</math></b> Tensile strength: <b><math>5.0332 \times 10^7 \text{ N/m}^2</math></b> Elastic modulus: <b><math>3.51633 \times 10^9 \text{ N/m}^2</math></b> Poisson's ratio: <b>0.35</b> Mass density: <b><math>1249.44 \text{ kg/m}^3</math></b> Shear modulus: <b><math>2.41317 \times 10^9 \text{ N/m}^2</math></b>
	Name: <b>ABS PC</b> Model type: <b>Linear Elastic Isotropic</b> Default failure criterion: <b>Max Von Mises Stress</b> Tensile strength: <b><math>4 \times 10^7 \text{ N/m}^2</math></b> Elastic modulus: <b><math>2.41 \times 10^9 \text{ N/m}^2</math></b> Poisson's ratio: <b>0.3897</b> Mass density: <b><math>1070 \text{ kg/m}^3</math></b> Shear modulus: <b><math>8.622 \times 10^8 \text{ N/m}^2</math></b>

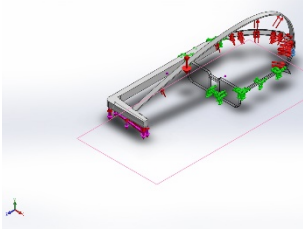
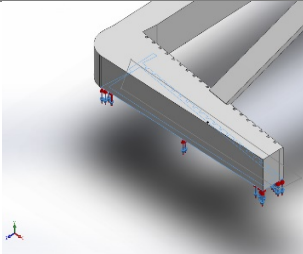
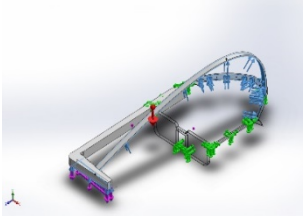
## 2. Fixtures

Table 3.7: Fixtures applied on Prototype 2

Fixture name	Fixture Image	Fixture Details		
Fixed-1		<b>Entities: 5 face(s)</b> <b>Type: Fixed Geometry</b>		
Resultant Forces				
<b>Components</b>	<b>X</b>	<b>Y</b>	<b>Z</b>	<b>Resultant</b>
<b>Reaction force(N)</b>	<b>0.0101519</b>	<b>1.37803</b>	<b>-0.0333347</b>	<b>1.37847</b>
Fixed-2		<b>Entities: 1 face(s)</b> <b>Type: Fixed Geometry</b>		
Resultant Forces				
<b>Components</b>	<b>X</b>	<b>Y</b>	<b>Z</b>	<b>Resultant</b>
<b>Reaction force(N)</b>	<b>-0.0102752</b>	<b>0.0504436</b>	<b>0.0349908</b>	<b>0.0622454</b>

### 3. Loads

Table 3.8: Loads applied on Prototype 2

Load name	Load Image	Load Details
Gravity-1		<b>Reference:</b> Top Plane <b>Values:</b> 0 0 -9.81 <b>Units:</b> m/s <sup>2</sup>
Force-1		<b>Entities:</b> 1 face(s) <b>Type:</b> Apply normal force <b>Value:</b> -0.48 N
Pressure-2		<b>Entities:</b> 9 face(s) <b>Type:</b> Normal to selected face <b>Value:</b> 1 <b>Units:</b> N/m <sup>2</sup> <b>Phase Angle:</b> 0 <b>Units:</b> deg

### 3.7.2.3 Integrating Design into a Working Prototype 2

As compared to the previous prototype, this prototype was intended to be much more flexible and robust to use. As the design was 3D printed with PLA. The design was then fitted on existing spectacles. This design also included a smaller bracket on the other side of the spectacle to be used as a support structure as shown in Figure 3.11.

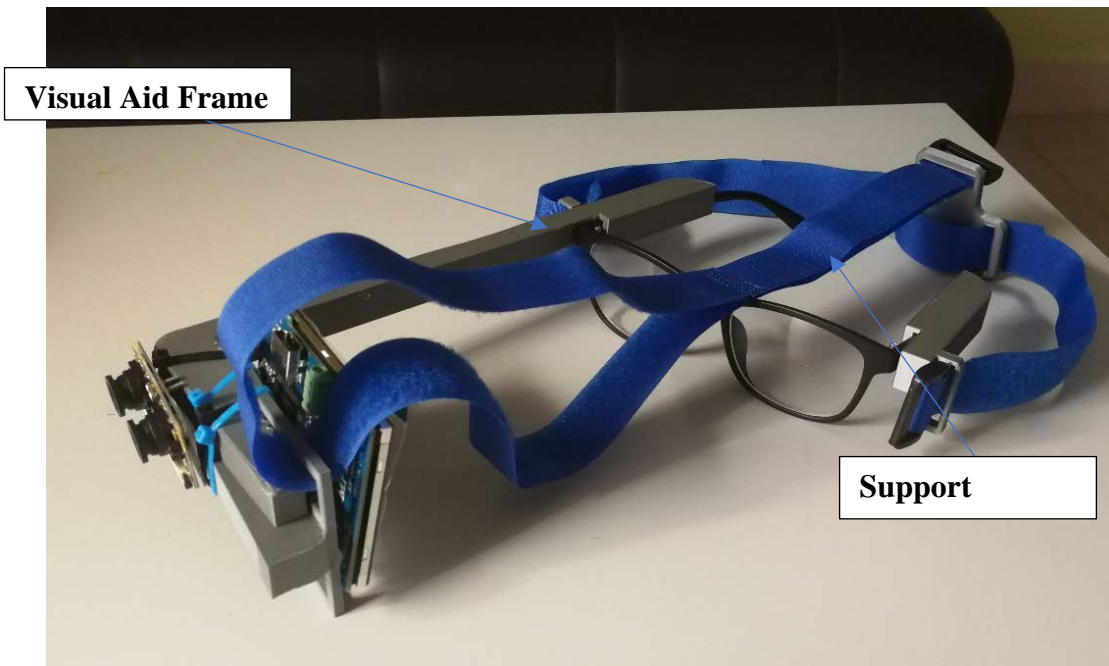
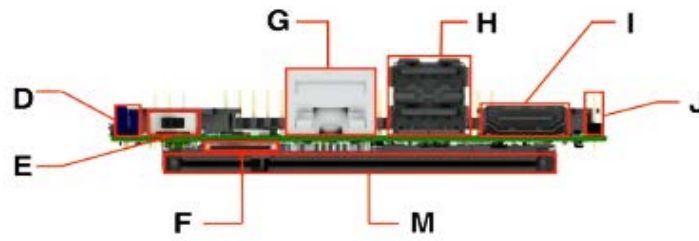


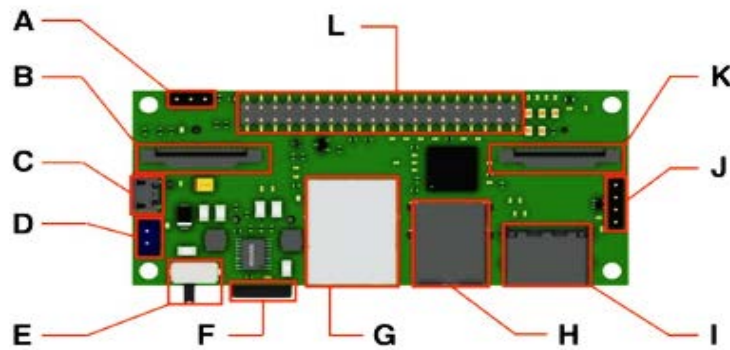
Figure 3.11: Prototype 2 of the visual aid

### 3.7.3 Development of Working Prototype Phase 3

Development of Phase 3 began with integrating the StereoPi microprocessor. The StereoPi microprocessor is a microprocessor which is developed for stereo camera usage as the typical Raspberry pi microprocessors do not support stereo camera setup. Figure 3.12 shows the detailed components onboard the StereoPi microprocessor.



Front view



Top view

A. boot mode jumper	H. dual USB Type-A connector
B. camera 1 CSI-2 connector	I. HDMI out
C. micro USB (for firmware upload)	J. USB port pin header
D. 5 VDC power connector	K. camera 2 CSI-2 connector
E. power switch	L. 40-pin RPI GPIO header
F. microSD slot	M. RPI Compute SO-DIMM connector
G. RJ45 Ethernet jack	

Figure 3.12: StereoPi microprocessor and its components [92]

The results of the processed image are then projected on to a 3.5-inch screen on the visual aid. . The screen used on the visual aid is an LCD 3.5-inch TFT touch screen. A touch screen interface was used as it is much more user-friendly and ease of access to the users. The 3.5 inch LCD screen is the smallest size that is available in the market, this size is chosen because it optimal for monocular vision and light in weight compared to the 5 and 7 inch size of LCD screen

### 3.7.3.1 Preparing the Design of Prototype 3

The design of prototype 3 (Figure 3.13) began with input gained from the testing conducted at Hospital Taiping. From the testing, many design flaws such as the weight of the visual aid which was expected and was identified by both patients and medical practitioners. These were addressed in the design of prototype 3. The stereoscopic cameras were also adjusted to obtain further clearance of field of vision by articulating the frame.

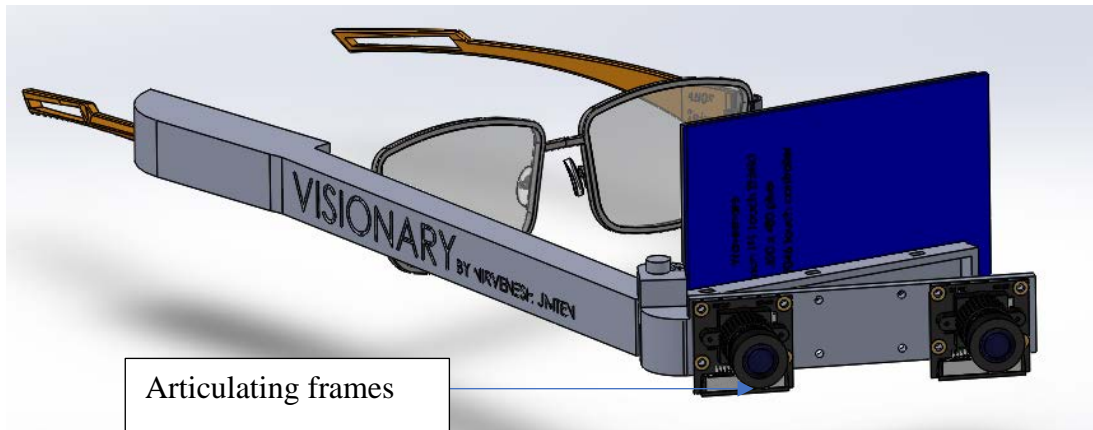


Figure 3.13: Solid works model of Prototype 3

The design was also undergoing static failure analysis to understand further on his behaviour during practice. For the analysis, however, as of all the models, this model was also simplified by reducing the curved surfaces making the design more linear and rigid for quick and precise processing [93]. However, the design was not compromised to the extent of interfering with the results as dimensionally the models are precise. The complete presets of the study are attached in Appendix D.

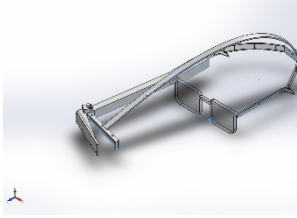
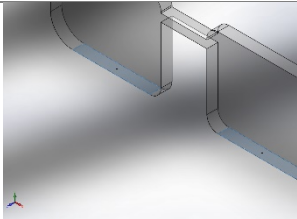
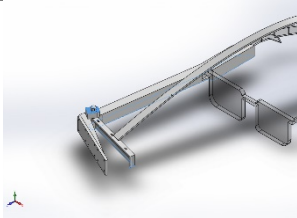
## 1. Material Properties

Table 3.9: Material Properties of Prototype 3

Model Reference	Properties
	<p>Name: <b>PLA</b>            Model type: <b>Linear Elastic Isotropic</b>            Default failure criterion: <b>Max von Mises Stress</b>            Yield strength: <b>3.59e+07 N/m<sup>2</sup></b>            Tensile strength: <b>5.0332e+07 N/m<sup>2</sup></b>            Elastic modulus: <b>3.51633e+09 N/m<sup>2</sup></b>            Poisson's ratio: <b>0.35</b>            Mass density: <b>1249.44 kg/m<sup>3</sup></b>            Shear modulus: <b>2.41317e+09 N/m<sup>2</sup></b></p>
	<p>Name: <b>ABS PC</b>            Model type: <b>Linear Elastic Isotropic</b>            Default failure criterion: <b>Unknown</b>            Tensile strength: <b>4e+07 N/m<sup>2</sup></b>            Elastic modulus: <b>2.41e+09 N/m<sup>2</sup></b>            Poisson's ratio: <b>0.3897</b>            Mass density: <b>1070 kg/m<sup>3</sup></b>            Shear modulus: <b>8.622e+08 N/m<sup>2</sup></b></p>

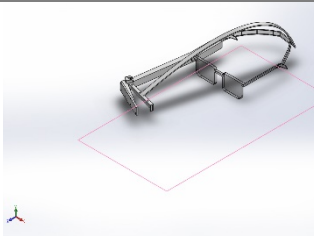
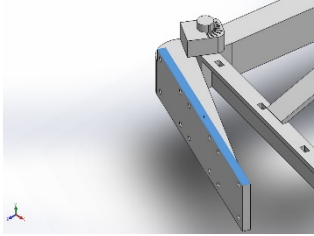
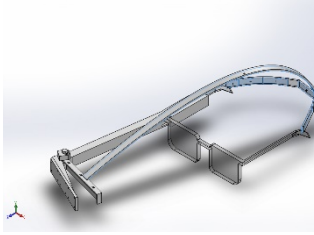
## 2. Fixture

Table 3.10: Fixtures applied on Prototype 3

Fixture name	Fixture Image	Fixture Details		
Fixed-1		<b>Entities:</b> 2 edge(s), 6 face(s) <b>Type:</b> Fixed Geometry		
Resultant Forces				
<b>Components</b>	<b>X</b>	<b>Y</b>	<b>Z</b>	<b>Resultant</b>
<b>Reaction force(N)</b>	<b>0.000296797</b>	<b>0.698461</b>	<b>0.00127503</b>	<b>0.698462</b>
Fixed-2		<b>Entities:</b> 2 face(s) <b>Type:</b> Fixed Geometry		
Resultant Forces				
<b>Components</b>	<b>X</b>	<b>Y</b>	<b>Z</b>	<b>Resultant</b>
<b>Reaction force(N)</b>	<b>0.000250275</b>	<b>0.164303</b>	<b>4.54109e-05</b>	<b>0.164303</b>
Fixed-3		<b>Entities:</b> 2 face(s) <b>Type:</b> Fixed Geometry		
Resultant Forces				
<b>Components</b>	<b>X</b>	<b>Y</b>	<b>Z</b>	<b>Resultant</b>
<b>Reaction force(N)</b>	<b>0.00692157</b>	<b>1.09893</b>	<b>-0.0337913</b>	<b>1.09947</b>

### 3. Loads

Table 3.11: Loads applied on Prototype 3

Load name	Load Image	Load Details
Gravity-1		<b>Reference:</b> Top Plane <b>Values:</b> 0 0 -9.81 <b>Units:</b> m/s <sup>2</sup>
Force-1		<b>Entities:</b> 1 face(s) <b>Type:</b> Apply normal force <b>Value:</b> 0.48 N
Pressure-1		<b>Entities:</b> 7 face(s) <b>Type:</b> Normal to selected face <b>Value:</b> 1 <b>Units:</b> N/m <sup>2</sup> <b>Phase Angle:</b> 0 <b>Units:</b> deg

### 3.7.3.2 Integrating Design into a Working Prototype 3

As compared to the previous prototype, this prototype was intended to be a much more mature product as it has undergone rigorous testing and feedback. This was also intended to be the final product of the visual aid. As the design was 3D printed with PLA the design was then fitted on an existing spectacle. This design also included a smaller bracket on the other side of the spectacle to be used as a support structure as shown in Figure 3.14.



Figure 3.14: Prototype 3 of the visual aid

### 3.8 Testing of visual aid

The visual aid is tested on both qualitative and quantitative methods. The visual aid is tested on amblyopic patients, monocular visual impaired patients and binocular versioned patients with one eye patched.

The testing of the visual aid was conducted in multiple medical and visual impaired institution such as the Society of Blind Malaysia, Taiping Hospital and Tun Hussein Onn Eye Hospital. A proper proposal for visual aid testing was submitted to the Human Resource department of each institution with detailed procedures as in the following on the testings that were conducted.

A risk (cause & effect) assessment was conducted to identify to potential risks in conducting the tests on the patients.

Table 3.12 : Visual Aid Testing Cause and Effect table

No	Cause	Effect	Mitigation
1.	Improper mounting of visual aid on patient	Hazard to patient (might cause small scratches)	Proper mounting of visual aid was conducted
2.	Sharp edges on visual aid	Hazard to patient (might cause small scratches)	Sharp edges will be chamfered

The visual aid is first tested on its primary objective which is to increase the field of vision and display on the monacle. This test is vital in ensuring an increment of vision from the current amblyopic vision angle of 100 ° to 160 ° and above. The visual aid is then tested for depth perception, this feature aims to distinct far and near objects and display notes on the projected image to recognize and focus on objects.

The developed integrated prototype of the visual aid is tested with few patients with the supervision of an ophthalmologist. Three main aspects will be tested which are field of vision, visual field measurement and depth map.

### 3.8.1 Field of Vision

The field of vision is one of the important objectives of this developmental research. Thus two important criteria's are to be highlighted in terms of conducting the test for the field of vision.

- a. To check whether the horizontal vision range can be regained at least 20%.
- b. To study and record the actual gained visual range.

#### 3.8.1.1 Visual Field measurement

The normal visual field for a normal human vision with stereoscopic vision is  $180^{\circ}$ . However, this field is further decreased to only  $95-100^{\circ}$  on a monocular vision. Nine objects were placed in a visual angle of  $180^{\circ}$  with an interval 22 degree apart from each object as shown in Figure 3.16 and 3.17. Subjects were requested the identify the number of objects that is in front of them, before and after wearing the visual aid. The number of objects was placed at 22-degree interval to incrementally asses the visual field in front of them.

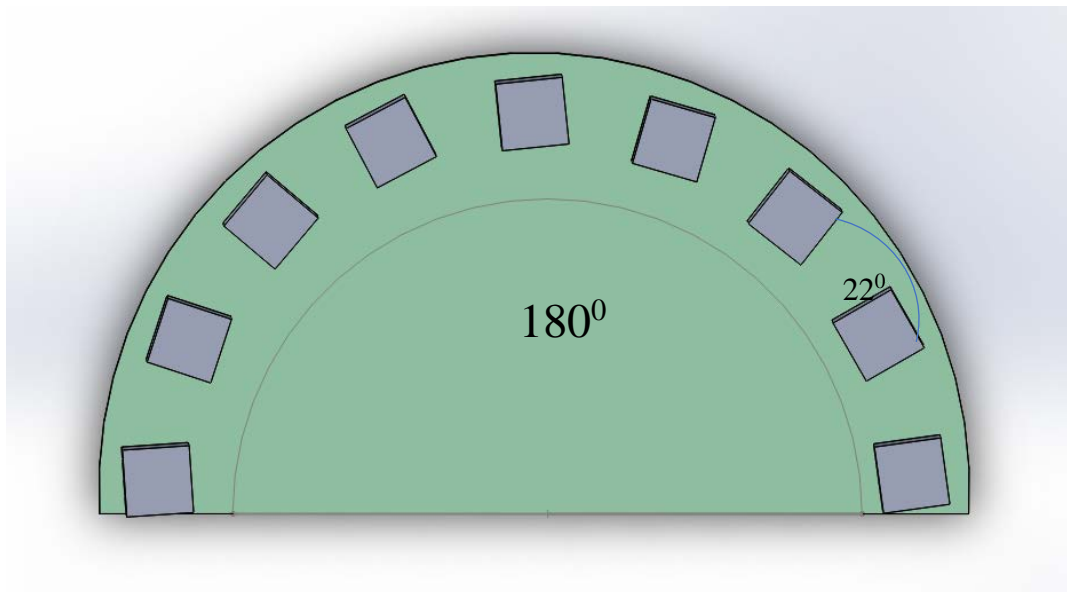


Figure 3.15: Visual Field measurement apparatus (top view)

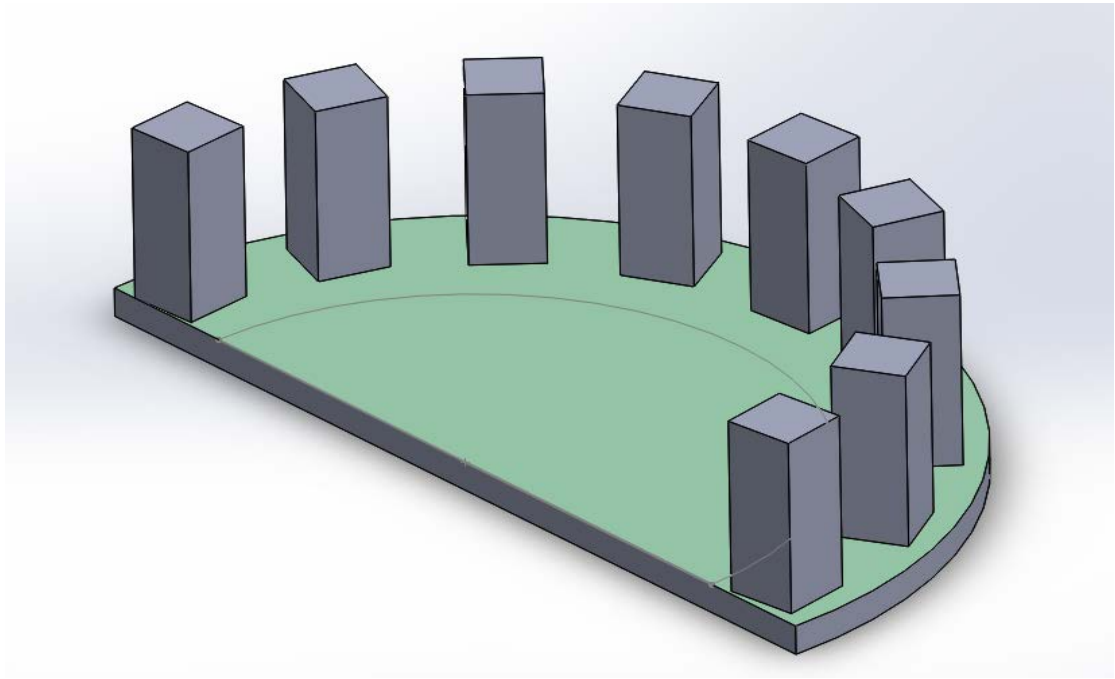


Figure 3.16: Visual Field measurement apparatus (3D-view)

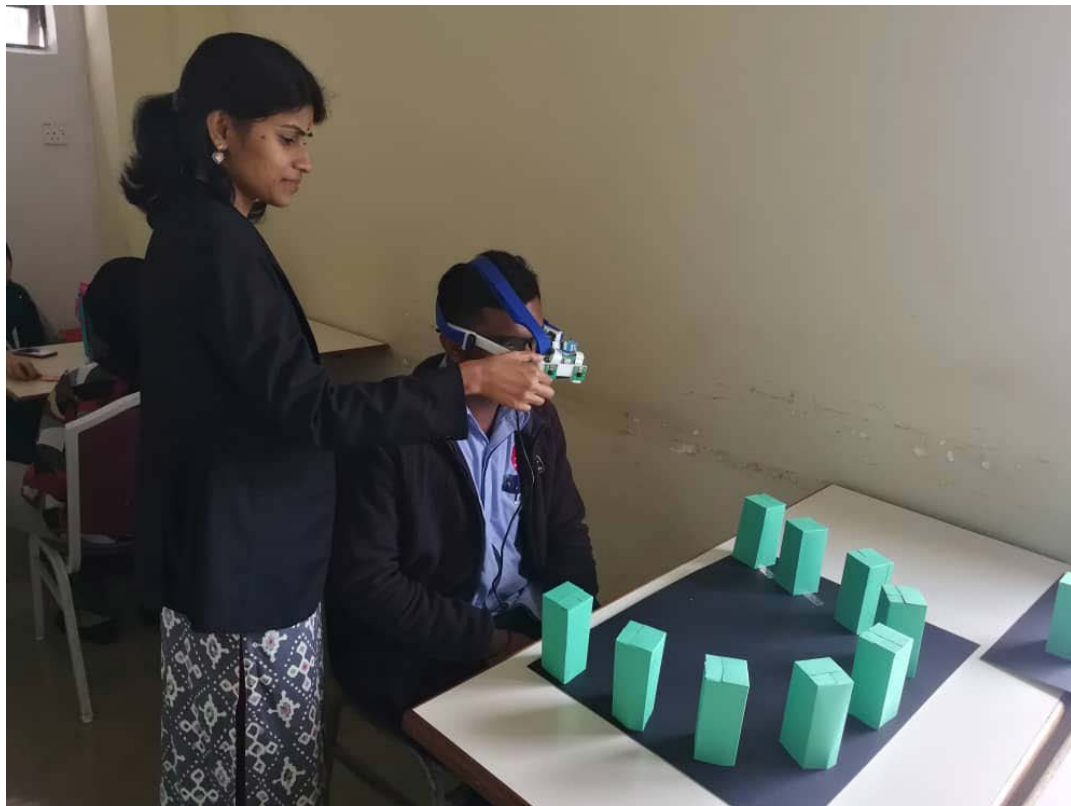


Figure 3.17: Test Conducted on Visual Field Measurement apparatus

The arrangement of the objects was arranged in a semi-circular pattern which also adds the depth perception on the visual field that is seen by the patient. The number of objects that are seen by the patient acts as a visual field indicator. The distance between each object is  $22^\circ$  in angle.

### 3.8.2 The Depth Map on the visual aid

The objectives of this test is to differentiate the distance between objects based on the depth map produced onboard the visual aid.

Depth cues were presented to patients on a table. Objects were placed on the table 20 cm, 15 cm, 10 cm and 5 cm apart. Thus 4 objects were placed at different distances on the table as shown in Figure 3.19.

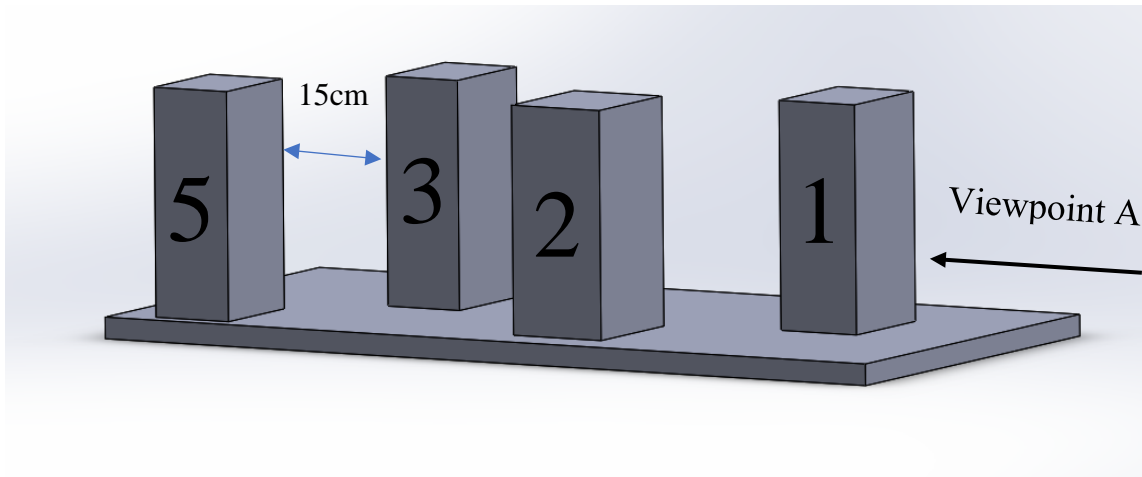


Figure 3.18 : Depth Map test setup

The monocular visual impaired subjects were required to identify the objects based on the order of the numbers from viewpoint A. The results were obtained before and after using the visual aid.

### **3.8.3 The usability of the Visual Aid**

The usability of the visual aid is a qualitative research as it emphasises on the patients comfort from using the visual aid. This test was conducted each the above tests for field of vision and depth perception were conducted. The criteria that were emphasised during this test are:

- a. To analyse the ease of use and practicality of the Visual Aid with actual patients for certain time periods.
- b. To examine whether the use of Visual Aid can cause extra fatigue or other negative effects on the patients

Feedback and comments received from the users were used to continuously improve the prototype's hardware and software. As this product has developed from each phase, the feedback on the design and feasibility of the visual aid was obtained at each stage of the development. The testing on real subjects was however conducted on the final prototype. The results were then tabulated and analysed based on the number boxes seen in the field of vision test, which translate into the angle of vision and the sequence of numbers in the depth of field test.

### **3.9 Cost Analysis**

Based on the final improved prototype, a cost analysis was to be performed to ensure that the product was affordable as stated in the objective of this research, which is to produce a cost effective visual aid for monocular visual impaired patients. The cost breakdown analysis was conducted on the final prototype.

Table 3.12: Sample of Cost Analysis Table

Cost Driver	Quantity	Unit Price (RM)	Price (RM)	Percentage of the total cost (%)
<b>Total Prototype Cost</b>				

Cost Breakdown Analysis breaks down the capital cost involved in the supplier's cost summary into its individual pieces [94]. Each piece is then scrutinized to minimize the cost of the final product. There are many types of cost involved in cost breakdown analysis some of which are labour cost, material cost, conversion costs, logistics cost, subcontracting cost and overhead cost. The costs that were considered in this research are primarily the material cost only, as it is not meant for any commercialization for now. The components of the cost are known as the cost driver and the percentage of the total costs for each component is identified. From there, it is a matter of reducing the percentage of cost and obtain a balance in terms of cost and quality of the final product. The analysis was performed based on Table 3.12 [95]. Based on the analysis that were performed at each stage of the cost analysis, a reduction in terms of material cost was considered in the following stages of development. The final cost of the visual aid was to be lower than RM750.00, as it is an affordable price for even for lower income group in Malaysia as suggested by The Credit Counseling and Debt Management Agency (AKPK) [96].

### 3.10 Summary

As a summary, this chapter has explains the methods taken in order to obtain the necessary data in order to initiate the development process. The questionnaire building and interview process were the first steps taken, followed by the data obtained being structured into the House of Quality. Further analysis on the house of quality enabled us to focus on the objectives of this research and address the challenges faced by monocular visual impaired patients. Each phase of the development process was started by the static analysis of the

respective designs, with this the design was justified to be feasible during actual fabrication of the prototype.

A total of 3 phases of development was initiated with factors such as the visual field and depth, weight and type of microcontrollers being the variable for each phase of development. At the end of each phase of development, cost analysis was conducted based on main cost drivers such as microcontrollers and materials customer feedback from various institutions were obtained for the following development phase. At the end of the third phase of development, test on the field of vision and depth perception was conducted.

## **CHAPTER 4**

### **ANALYSIS AND DISCUSSION**

#### **4.1 Introduction**

Chapter 3 has discussed the main framework that required to acquire the results and to validate this research. This Chapter 4 presents the results which includes of the survey data that was conducted on medical professionals and monocular visual impaired patients. Based on the survey, the house of quality was constructed and analysed meticulously. A total of three phases of development are discussed in this chapter where the final phase is the product of this research, each phase discusses the designing process, static study results, cost analysis and the visual aid output. Testing of the visual aid was conducted on the final prototype of the visual aid based on the experimental setup discussed in Chapter 3.

#### **4.2 Profile of Respondents and Related Details**

The profile of the selected range of respondents in this study is focused mainly on two groups of people namely the ophthalmologists and opticians which comprise of medical professionals in the field of ophthalmology and the patients who have visual impairment which mostly comprise of those with monocular visual impairment either through trauma or since the time of birth. The two main groups of respondents have helped achieve the primary objective of this survey in gaining a broad spectrum of perspectives and views from across two ends of the impairment. Table 4.1.

#### 4.2.1 Visual Impaired Patient Respondents

Table 4.1: Profile of visual impaired patient respondents in a survey

<b>Respon dent No.</b>	<b>Age</b>	<b>Type of monocular visual impairment</b>	<b>Years with impairme nt</b>	<b>Any Visual Aid Used</b>	<b>Type of treatment</b>	<b>Challenges faced</b>
<b>1</b>	72	Glaucoma	7	No	Rehabilitation	Unable to walk with stability
<b>2</b>	66	Trauma	40	No	Prosthetic eye	Unable to drive at night
<b>3</b>	67	Glaucoma	8	No	Rehabilitation	Difficult to grab objects on table
<b>4</b>	82	Glaucoma	10	No	Rehabilitation	Unable to walk independently
<b>5</b>	34	Trauma	11	No	Rehabilitation (sealed eyelids)	Unable to drive
<b>6</b>	15	Amblyopia	5	No	Patching	Difficulty in reading
<b>7</b>	32	Trauma	10	No	Sealed eyelids	Difficult to grab objects on table with

<b>8</b>	12	Amblyopia	2	No	Acupuncture	Double vision
<b>9</b>	78	Glaucoma	7	No	Rehabilitation	Unable to drive
<b>10</b>	77	Glaucoma	7	No	Rehabilitation	Unable to climb stairs independently
<b>11</b>	58	Glaucoma	1	No	Rehabilitation	Unable to walk unattended
<b>12</b>	22	Trauma	4	No	Sealed eyelids	Unable to adapt to monocular vision due to double vision
<b>13</b>	22	Amblyopia	6	Yes	Patching	Difficult to grab objects on table
<b>14</b>	84	Glaucoma	11	No	Rehabilitation	Unable to walk independently
<b>15</b>	10	Amblyopia	2	No	Patching	Difficulty in reading
<b>16</b>	21	Trauma	4	No	Rehabilitation (Prosthetic eyes)	Unable to drive

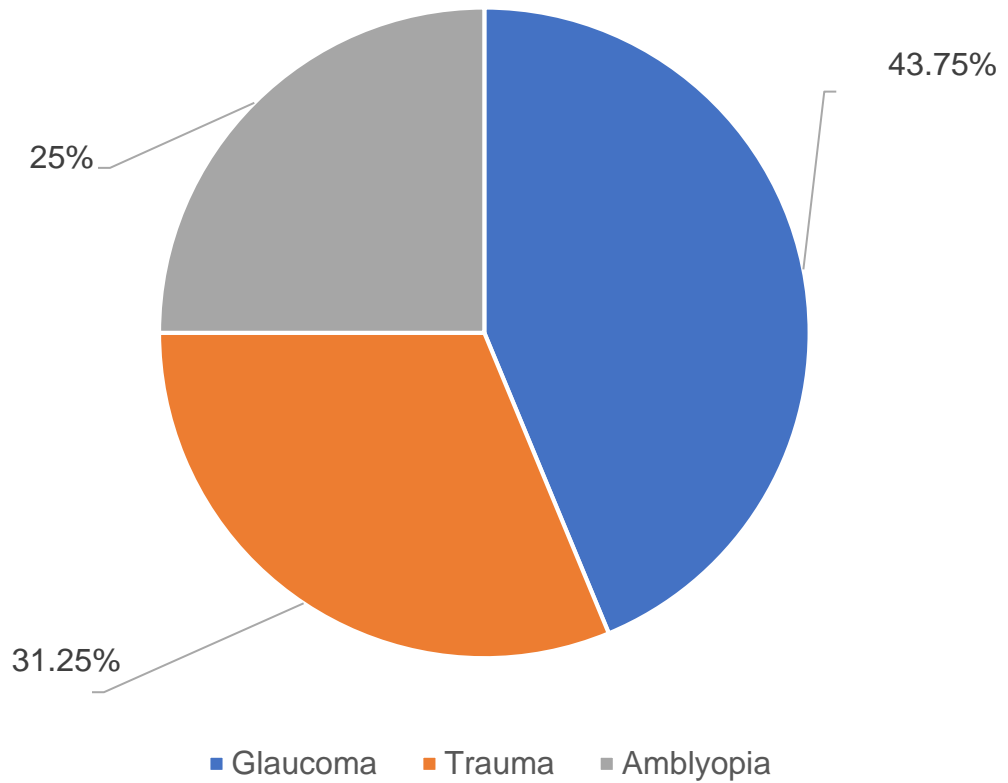


Figure 4.1: Patient Respondents of survey in terms of impairment.

Based on Figure 4.1 above, 43.75% of the patients that have participated in this survey consisted of glaucoma patients who have undergone who have lost their sight of vision either partially or completely on one side. The second most common monocular visual impairment is found to be patients who have undergone trauma or mishaps which consists of 31.25% and the remaining of 25% consists of patients who have amblyopia.

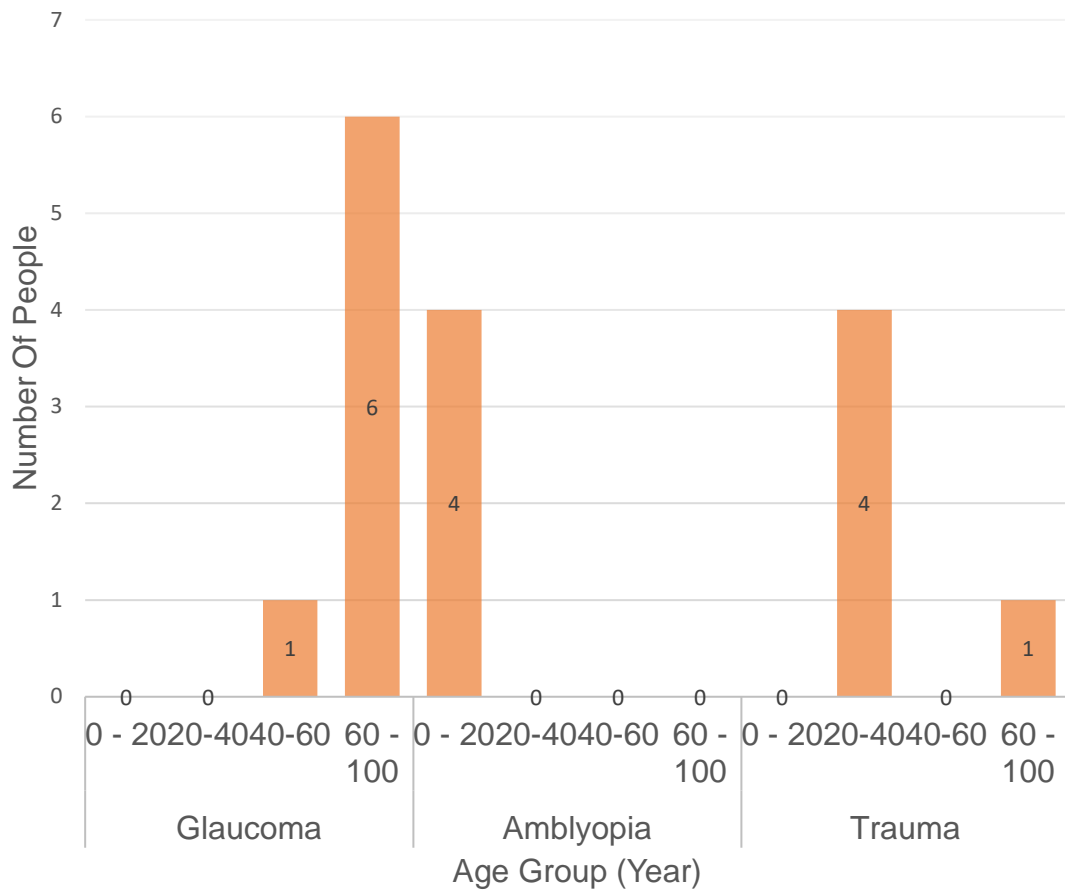


Figure 4.2: Visual Impaired patient respondents at different age group.

From the analysis in Figure 4.2, glaucoma patients consist of mostly between the age group of 60-100, as this impairment is associated with diabetes. As diabetes is most commonly prominent at a later age, the data that is obtained is found to be in line with the expected survey group which consists of mostly glaucoma patients. This is seconded by patients who have undergone trauma or accidents and the remaining numbers are from amblyopia. We can also conclude that most monocular visual impaired patients consist of glaucoma patients as they are no other solution for this impairment besides rehabilitation.

### 4.3 Feedback from Medical Professionals

Medical professionals explained the main causes of monocular visual impairment. Glaucoma is known to be the most prominent cases of this type of impairment due to the increasing number of hyperglycaemic patients in the country. The prevalence of diabetes type 2 which is most general in patients of older age has increased to 20.8% in adults above age 30 affecting 2.8 million individuals [97]. Individuals with diabetes are twice as likely to develop glaucoma compared to non-diabetic patients. Neovascular glaucoma is the most common type of glaucoma associated with other abnormalities, with diabetes being the most common [98]. This is also known as diabetic retinopathy as shown in Figure 4.3 where blood vessels on the retina are damaged and the retina manufactures new, abnormal blood vessels. Sometimes the new blood vessels grow on the iris (coloured part of the eye) shutting off the fluid flow in the eye and increasing the ocular pressure (eye pressure). This disease is also difficult to treat, and most commonly only analgesics are prescribed [99].

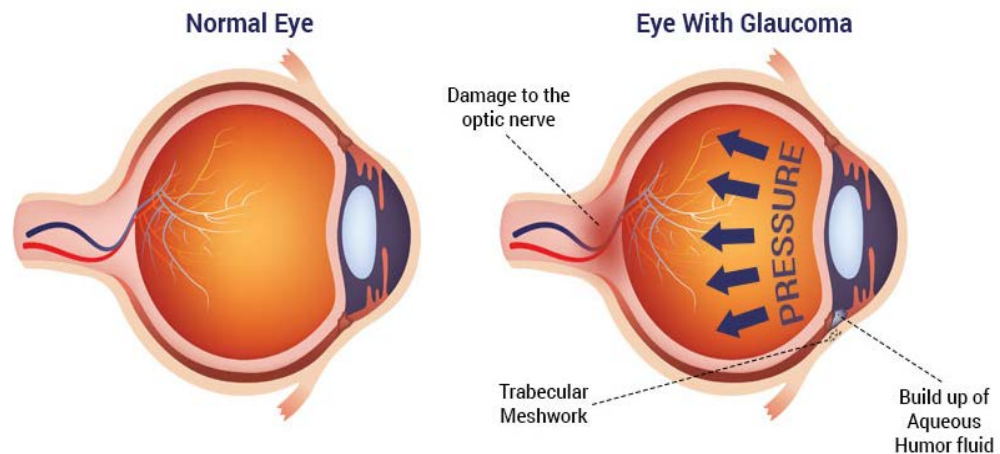


Figure 4.3: Diabetic retinopathy in comparison with a normal eye [100]

Thus, it was evident that this problem needed a solution with interventions outside of the medical industry. The ophthalmologists and optometrist that have been interviewed

have suggested the visual aid to overcome the main objectives of this research which are to provide depth perception and increase the visual field range of the user. They have also suggested the visual aid to be used as a training aid initially as it would help in the rehabilitation exercise for new patients. Patients, however, have common depth issues with grabbing common things on the table and while climbing stairs.

#### 4.3.1 Feedback from Monocular Visual Impaired Patients

The visually impaired patients were intrigued with the development of the visual aid for them, as there is less effort taken in developing a visual aid for them. The patients had a similar objective of developing visual aid with the medical professionals as it was their main challenge. However, as a user, they did not want the visual aid to be very bulky and heavy as like olden spectacles where marks are left by the nose pads on the nose if used for a longer duration of time. Some also suggested the visual aid like a virtual reality (VR) box. As most of these patients are of older age, they wanted the ease of access user interfaces for easy usage of the visual aid.

Table 4.2: Customer and corresponding functional requirements

<b>Customer Requirements</b>	<b>Functional Requirements</b>
<b>Wide Vision</b>	Field of Vision
<b>Differentiate distance</b>	Depth Perception
<b>Comfortable to wear</b>	Type of Material
<b>Ease of functionality</b>	Weight
<b>Simple Outlook</b>	Ultraviolet
<b>Fashionable</b>	Screen Brightness
<b>Work Faster</b>	Processing Time
<b>Low Weight</b>	Water Resistance
<b>New in Market</b>	Length
<b>Long Lastingness</b>	Width
<b>No external disruption</b>	Durability

<b>Portability</b>	Hardness
<b>Ultraviolet protection</b>	Camera Resolution
<b>Flexibility</b>	Battery Capacity
<b>Simple interface</b>	LCD size
<b>Weather proof</b>	Number of components

### 4.3.2 Analysis of the House of Quality

The Figure 4.4 shows the analysis of the house of quality.

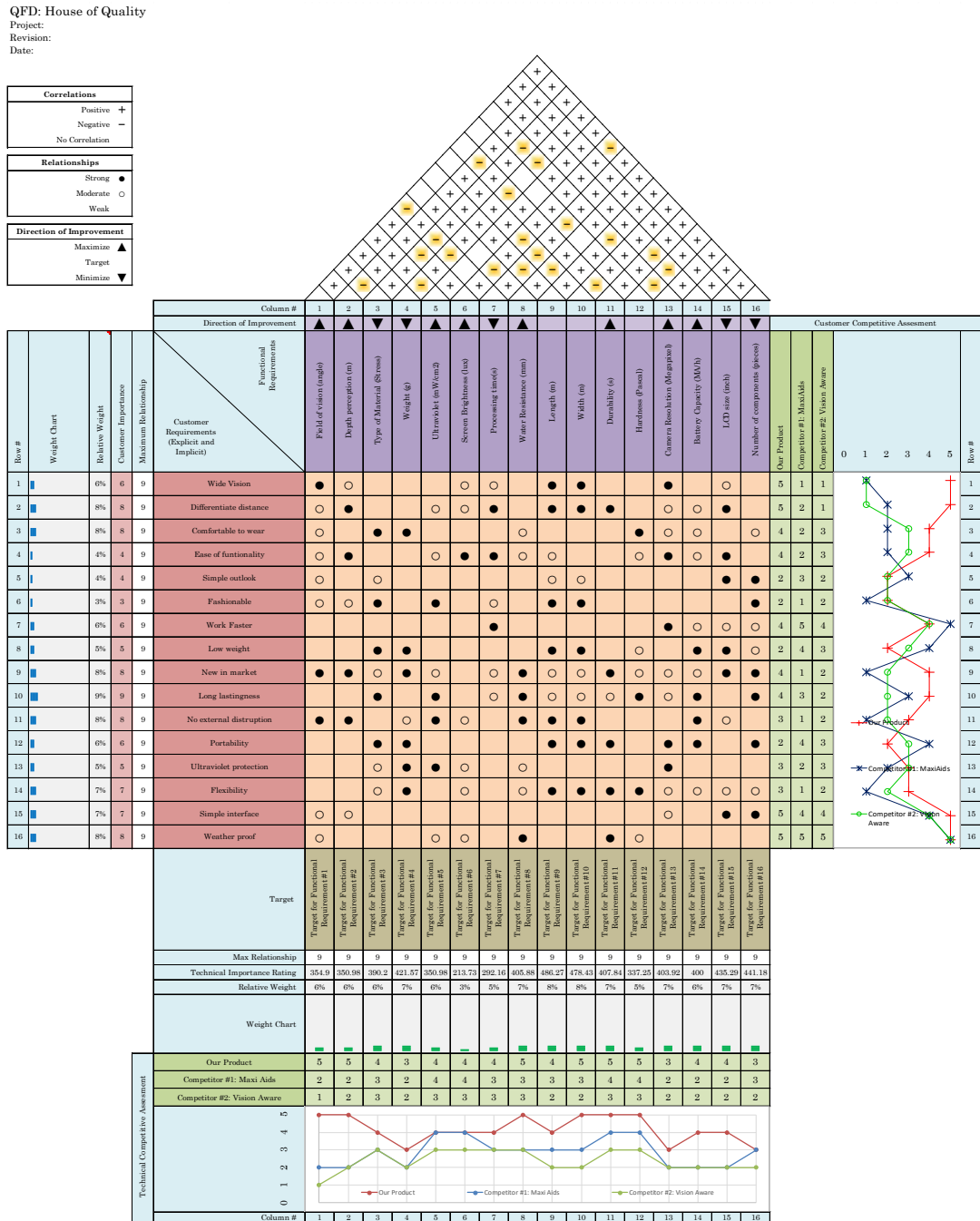


Figure 4.4: House of Quality of developing a visual aid for monocular visual impaired patients

The House of Quality was constructed with the feedbacks obtained from the personal interview survey conducted. The customer requirements of the House of Quality were deduced from the feedbacks provided by the visually impaired patients and the medical professionals in the ophthalmological department. The functional requirements are from the customer requirements but more quantified and measurable. Both requirements were crossed to obtain the relationships between them, it can be said that most of the customer requirements have a strong relationship between them. This justifies that the factors that have been derived in the functional requirements are accurate [64]. The functional requirements also allow us to benchmark our design with feedback from the customers perspective.

Benchmarking was also made based on the current products that were available on the market. There were only two products that were available on the market which caters for monocular visual impaired patients, which were Vision Aware and Maxi Aide.[40]

The top or roof of the house of quality indicates the relationship between the functional requirements. From the analysis above, it can be seen that a very strong relationship can be seen among the requirements. This indicates that the development is in clear sight of its objectives and targets.

#### 4.4 Development of Working Prototype 1

The development of the first prototype began with the idea of producing a visual design with a screen to project all important information which includes the depth map on to it. The first prototype was a spectacle specific design which has a long bar which extends across to hold the LCD panel and the microcontroller unit of the LCD panel onboard. The slot was used to attach the LCD screen frame to the bar that connects to the spectacle as shown in Figure 4.5. An orthographic and exploded view drawings with dimensions of Prototype 1 are attached in Appendix E

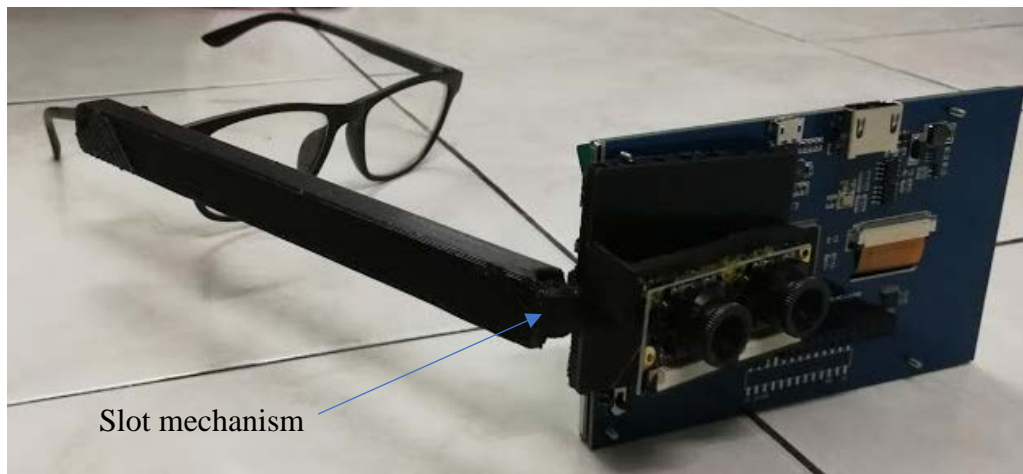


Figure 4.5: Slot mechanism on prototype 1

This prototype held the controller unit in a separate containment as the Waveshare I/O board was very big and not suitable to be fixed on to the visual aid design. The design that was used to conduct the analysis is real scale in size but not in details, this ensures smoother processing of the study at a much faster rate.

#### 4.4.1 Design Analysis

The design analysis in Figure 4.6 shows the mesh analysis that was conducted on the design of prototype 1. A solid mesh type was used to conduct this analysis. The element size that was used to conduct this analysis is 4.0249mm with a tolerance of 0.2012mm. The size of the mesh element determines the accuracy of the study. A total of 89780 nodes were found on this model resulting in a total element of 56263.



Figure 4.6 : Mesh analysis of Prototype 1

In finite element analysis or FEA, the mesh density plays a critical role in determining the accuracy of the study, a fine element size would result in a more accurate result but may consume high computing power and a lot of time which is inefficient especially for projects like this, where model is tweaked and remodelled multiple times in a single design. It is also because of that the models used in the study are simplified models of the real design. The element that is chosen is also an in the mid-range element size.

#### 4.4.1.1 Von Mises Stress Study

Figure 4.7 below shows the fringe diagram results of the stress analysis results that were conducted on Prototype 1

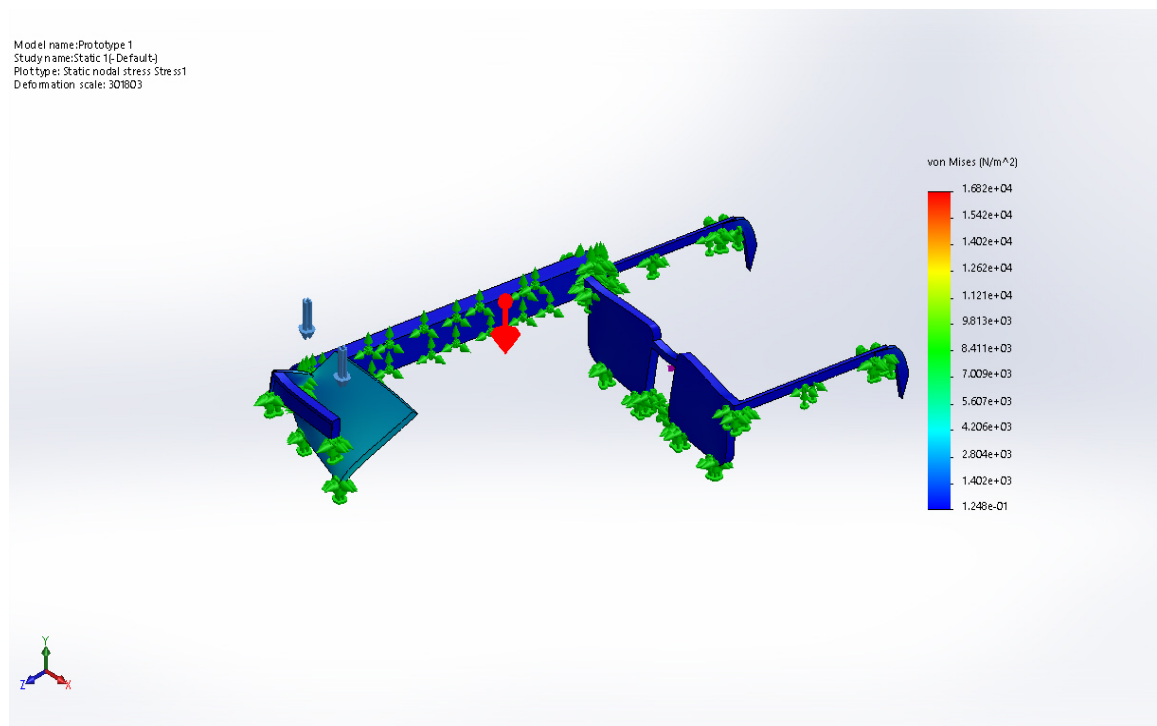


Figure 4.7: Stress Analysis results of Prototype 1

Based on the stress analysis conducted on the Prototype, the maximum stress of  $1.682 \times 10^4 \text{ N/m}^2$  and a minimum of  $1.248 \times 10^1 \text{ N/m}^2$  is exerted on the model. This range of stress is well within the limit of plastic deformation as the maximum tensile strength of

the material is  $5.032 \times 10^7 \text{ N/m}^2$ . The screen of the visual is isolated from the whole design, as a result a very high amount of stress is applied to the joint of the screen section, although the results of the fringe diagram may seem that the object has undergone major displacement due to the loads that were applied, it will be clear that the results are exaggerated for easy analysis. The displacement analysis of the study will be further discussed in the following sections of the development of Prototype 1.

Figure 4.8 shows the maximum stress point that is exerted on the design of prototype 1 of the visual aid. This provides enough information about the stress analysis of the study and information on improvising and optimizing the design for future developments.

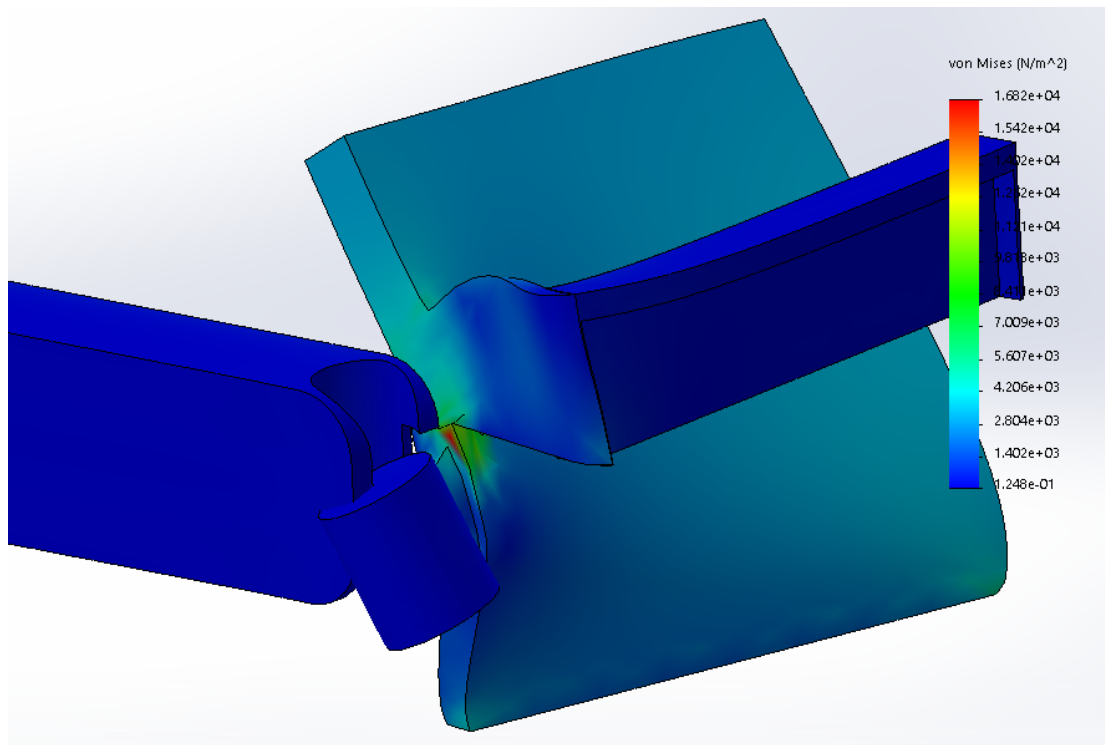


Figure 4.8: Maximum stress point of prototype 1.

As the screen is isolated from the design, and only supported by a bar that is held from the spectacle itself, the screen section of the visual aid needs a thicker and more

supported design to hold the design intact. This part is vital as the microcontroller and other electronic components are housed here as well.

#### 4.4.1.2 Resultant Displacement Study

Figure 4.9 shows the resultant displacement analysis fringe diagram results that were conducted on prototype 1 of the visual aid design.

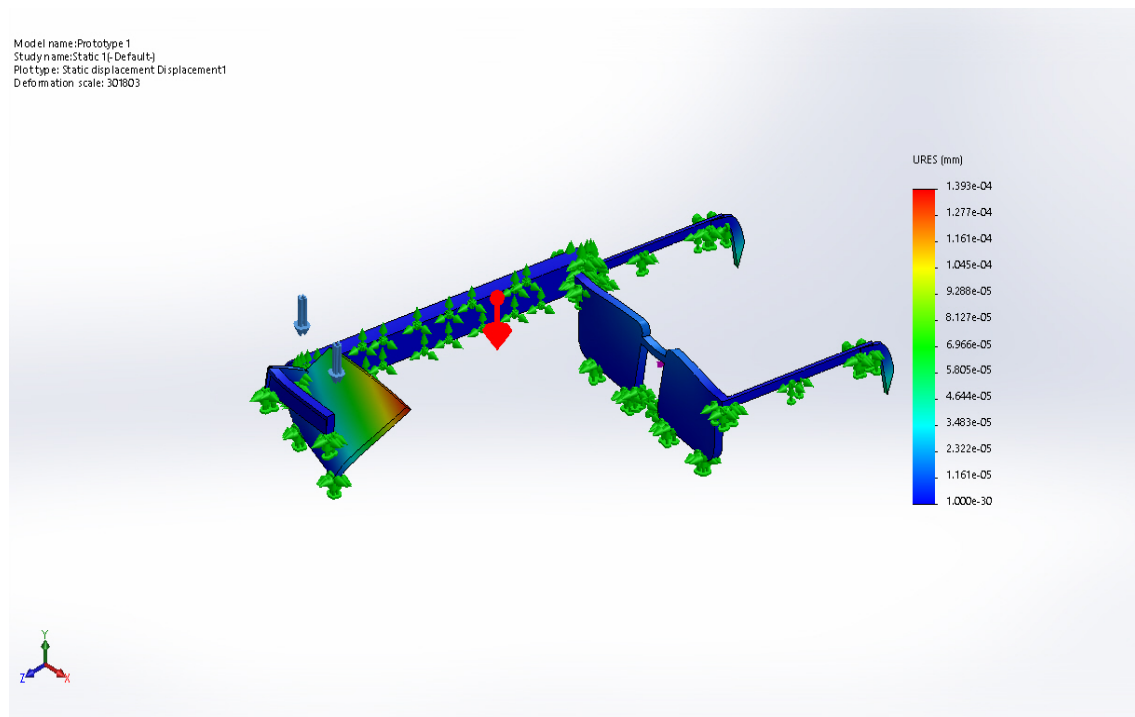


Figure 4.9: Resultant displacement results of prototype 1

The fringe diagram from Figure 4.9 shows a maximum displacement of  $1.393 \times 10^{-4}$  mm. This section is represented by the red colour in the fringe diagram, thus it can be seen that the screen section is part undergoes the maximum displacement. Although the fringe diagram has an exaggerated visual, the displacement is significantly small as it is less than 1.00mm. This area of the entire prototype absorbs most of the load of the visual aid. The screen is the most significant weight in the whole design. It weighs about 0.3 kg, noting also it is the only external component that adhered on the visual aid design.

#### 4.4.1.3 Equivalent Strain Analysis

Figure 4.10 shows the resultant displacement analysis fringe diagram results that were conducted on prototype 1 of the visual aid design.

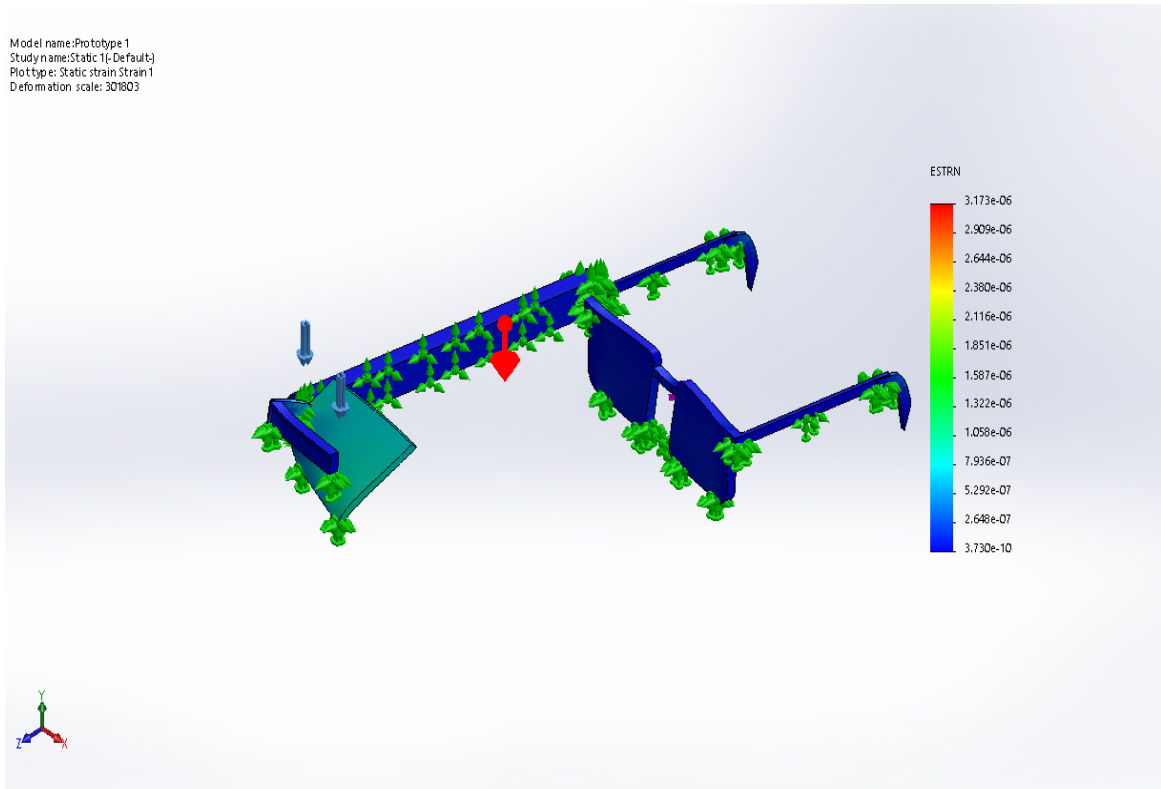


Figure 4.10: Equivalent strain analysis of prototype 1

The fringe diagram results of the equivalent strain analysis justify that this design is within safe limits of plastic deformation as the maximum strain on the visual aid design of prototype 1 is  $3.173 \times 10^{-6}$ . The maximum strain as discussed in the previous sections of this design analysis is a result of the screen which is considered during the design of this prototype.

As discussed in the previous sections. The joint in between the camera holder and the screen holder is the point of maximum strain as loads from opposite sections of the frame are applied on to the design as shown with arrows in Figure 4.11.

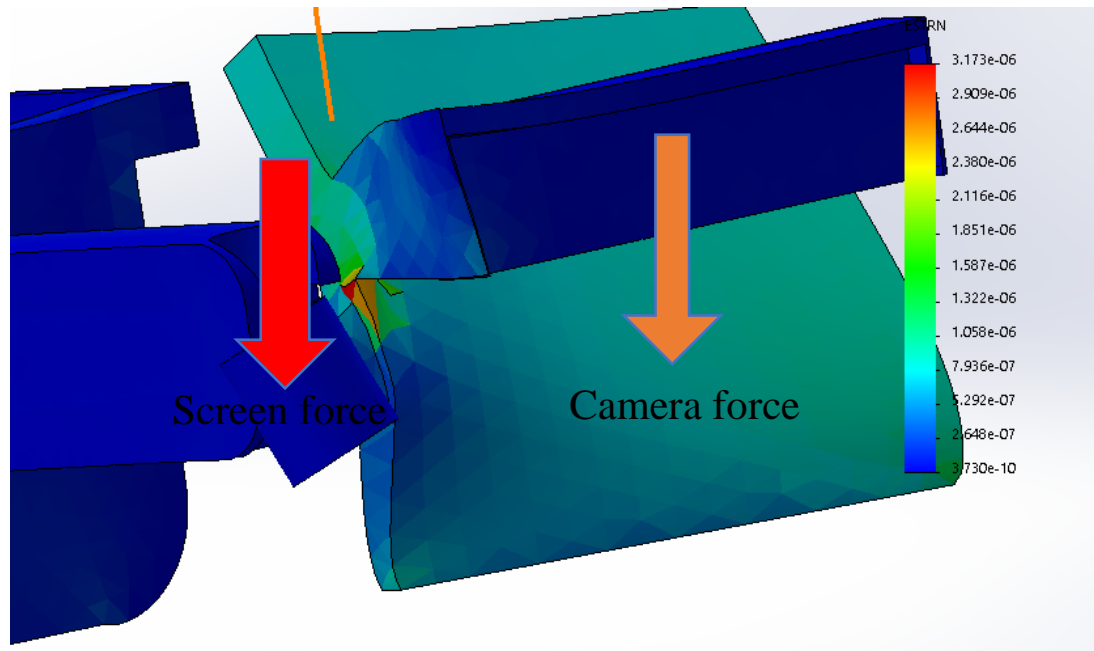


Figure 4.11: Maximum strain points with forces

The imbalance in between the forces of the camera and the screen causes strain to be concentrated on the point as shown in Figure 4.11. There is much modification required to support the screen structure and dissipate the forces equally along with the structure. The slot that is used in this design to whole the screen and the controller together is also not an optimal design for the force that it must endure.

#### 4.4.2 Integration of Visual Aid Design Structure and Stereoscopic camera system

The integration of both the design structure and stereoscopic system of the visual aid features all the electronic components and the 3D printed visual aid design as shown in Figure 4.12. The combined weight of the visual aid was found to be at 320g. Most of the weight of the visual aid is concentrated on the front of the visual aid which comprises of the screen and the camera.



Figure 4.12: Completed assembly Prototype 1

Cost Driver	Quantity	Unit Price (RM)	Price (RM)	Percentage of the total cost (%)
Waveshare Compute Module I/O board	1	275.00	275.00	31.92
Raspberry Pi Compute module	1	175.00	175.00	20.31
Raspberry Pi Wide Angle camera (for stereo vision)	2	60	120.00	13.93
Design Manufacturing (3D-printing) PET-G	60 grams	1.00	60.00	6.96
Interconnecting cables	13	0.50	6.50	0.75
LCD screen 5' inch	1	225.00	225.00	26.13
<b>Total Prototype Cost</b>			<b>861.50</b>	<b>100.00</b>

Table 4.3: Cost Analysis table of Prototype 1

#### 4.4.3 Cost Analysis

The cost analysis is a final and most important phase of a design in a development process. The cost analysis helps us understand the financial implication of this design. Table 4.3 shows the cost analysis table of Prototype 1.

From the above cost analysis, the main cost driver is determined to be the compute module which accounts to 43.21% of the total cost. It is then seconded by the compute module which costs 27.50% of the cost of the visual aid. This analysis is important for the next phases of development where the primary cost driver is reduced to obtain a lower cost of manufacturing. This analysis also falls within the range of optimal costing. Optimal costing is a function-driven cost analysis that prioritizes the function of the parts and costs associated with it. In this prototype, the main component of the visual aid is the Waveshare compute module I/O board and the raspberry pi compute module.

#### 4.4.4 Visual Aid Output

The phase one of the visual aid development did not undergo testing with monocular visual impaired patients, however, it was given to several organizations. The basics of output from the visual aid are as Figure 4.13 (A.) and Figure 4.13 (B.).

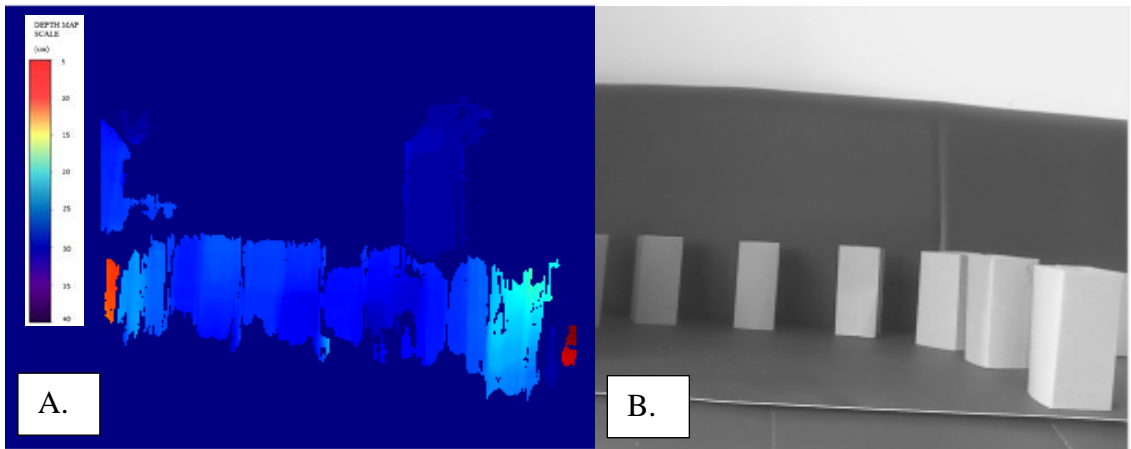


Figure 4.13: (A.) Depth map generated from the prototype of visual aid (B.) Field of vision from visual aid of prototype 1

The depth map in Figure 4.13(A.) is a resultant of the field of vision as seen in Figure 4.13(B.) . From the depth map that is obtained. The depth map does distinguish depth of objects close to it. However, it is not able to distinguish the depth that is far away from the camera and there is also an inconsistency with the depth map translation as it can be seen that the far-right box seems very close to the user, but it doesn't show red mapping. This is due to the limitations of the processor that embedded into it. The field of vision is also deliberately given in grayscale to reduce the processing power required to produce the depth map.

The field of vision as in Figure 4.13(B.), shows a maximum of 7 boxes which translate to 154 ° field of vision. This field of vision is almost the equal field of a

monocular visual impaired person who can see a field of vision in between 120 to 140 ° of vision.

#### **4.4.5 User Feedback**

The customer feedback on this phase of the prototype is provided by three groups namely Tun Hussein Onn Eye Hospital and Society of Blind Malaysia. The medical professionals at these two groups have tested the visual aids on real patients and obtain feedback from them. The feedback form is attached in Appendix F. The feedback from the customer have suggested the design to be lighter as the design is currently front biased which makes the weight of the visual aid act on the nose of the patient, the depth map, however, was found to be very impressive. The medical professionals also conducted a simple test to measure the visual field by placing object out of the natural visual field without the visual aid, the patients were then able to see and grasp that object with the visual aid in place.

In this test, the ophthalmologist from the Tun Hussein Onn Eye Hospital has asked patients to identify steps on a staircase where the depth distinguishes based on its distance from the user. After several minutes of getting used to the visual aid, the users were then able to identify the steps of the staircase, unfortunately, it was found that the visual aid kept dropping as it was frontal biased and have nothing to grip on to the user.

Prototype 1 has many of the theoretical features of the prototype such as depth map generation and visual field indicators working. However there is still much room for improvement as it still costs much to manufacture and has a frontal biased weight.

#### **4.5 Development of Working Prototype 2**

The development of Prototype 2 began with addressing the problems and challenges faced by the previous prototype which is Prototype 1. This prototype primarily focused on the visual aid to evenly distribute its weight. A three-point was added to the design, enabling it to grip to the user holding the visual aid firmly. A common design principle is the more moving parts in an object, the more critical stress points are identified.



Figure 4.14: Slot design on Prototype 2

This design also focused on making the visual aid to be fitted on to any spectacle making it more versatile. This visual aid design has a slot as shown in Figure 4.14, the slot is made to accommodate any spectacle frame into it and holds it within. This makes the visual aid stay in place on the spectacle without slipping on its axis. The advantage of this design is that it enables the user to choose whether to use visual aid while using the same spectacle for common daily usage. An orthographic and exploded view drawings with dimensions of Prototype 2 are attached in Appendix G

### 4.5.1 Design Analysis

The design analysis shows the mesh analysis that was conducted on the design of Prototype 2 as shown in Figure 4.15. A solid mesh type was used to conduct this analysis. The element size that was used to conduct this analysis is 4.65641mm with a tolerance of 0.232821mm. A total of 87189 nodes were found on this model resulting in a total element of 50762. This analysis was accomplished with a much denser element size as the design is different compared to the previous one.



Figure 4.15: Mesh analysis of Prototype 2

The element size of this analysis is increased as this design is more static compared to the previous designs. The screen and camera frame have been made thicker due distribute the forces equally. Besides, as this design is featured with a three-point gripping belt. The stress and strain analysis on the belt has to be studied in detail as it helps the user to grip the visual aid in place. The design was inspired by current virtual reality glasses which normally are equipped with a three-point belt to strap on the head.

#### 4.5.1.1 Von Misses Stress Study

Figure 4.16 below shows the fringe diagram results of the stress analysis results that were conducted on Prototype 2.

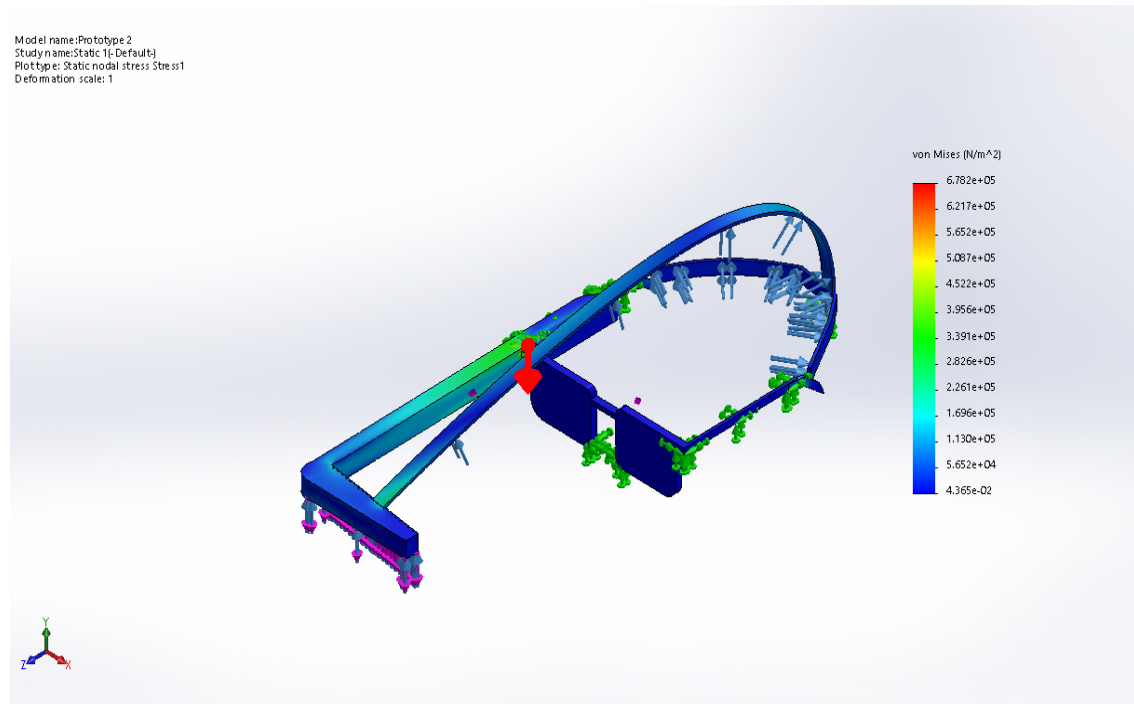


Figure 4.16: Stress analysis of Prototype 2

The fringe diagram results above show the stress analysis conducted on the prototype. The range of stress that was exerted on the design is between  $4.365 \times 10^{-2} \text{ N/m}^2$  and  $6.782 \times 10^5 \text{ N/m}^2$ . The material with the lowest tensile strength in the design was chosen as an analysis benchmark material. In this design, the ABS material has a tensile strength of  $4.07 \times 10^7 \text{ N/m}^2$ . With that, it can be concluded that this design does not have plastic deformation based on all the forces applied on to it. The critical stress point area on the design is the area of union between the visual aid and the spectacle as shown in Figure 4.17.

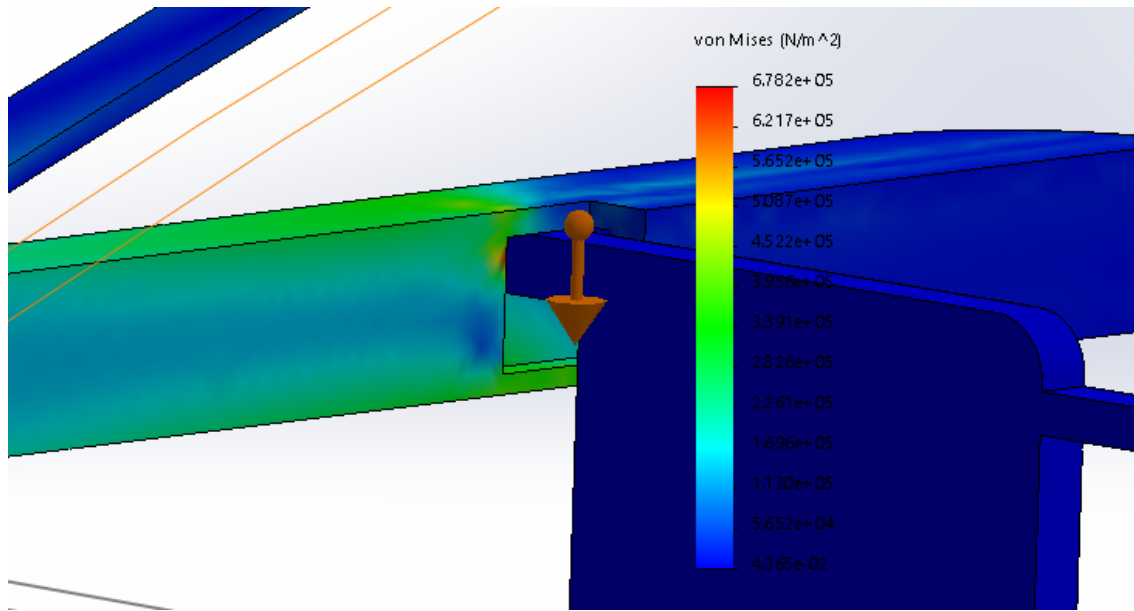


Figure 4.17: Maximum stress area on Prototype 2

The maximum stress occurs at the area due to the force of the three-point gripping belt that occurs at that area. This is however accounted in the design process and helps with ensuring the visual aid does not frontal or backward bias by keeping its centre of gravity (COG) in the appropriate range. If the design was made in such way that the frame of the spectacle does not fit into the frame of the visual aid. There is a tendency for the visual aid to be slipping front and back during motion making the user to be confused by the blurry and unfocused view of the depth map and field of vision.

### 4.5.1.2 Resultant Displacement Study

The Figure 4.18 shows the resultant displacement fringe diagram based on the analysis conducted on Prototype 2 of the visual aid design.

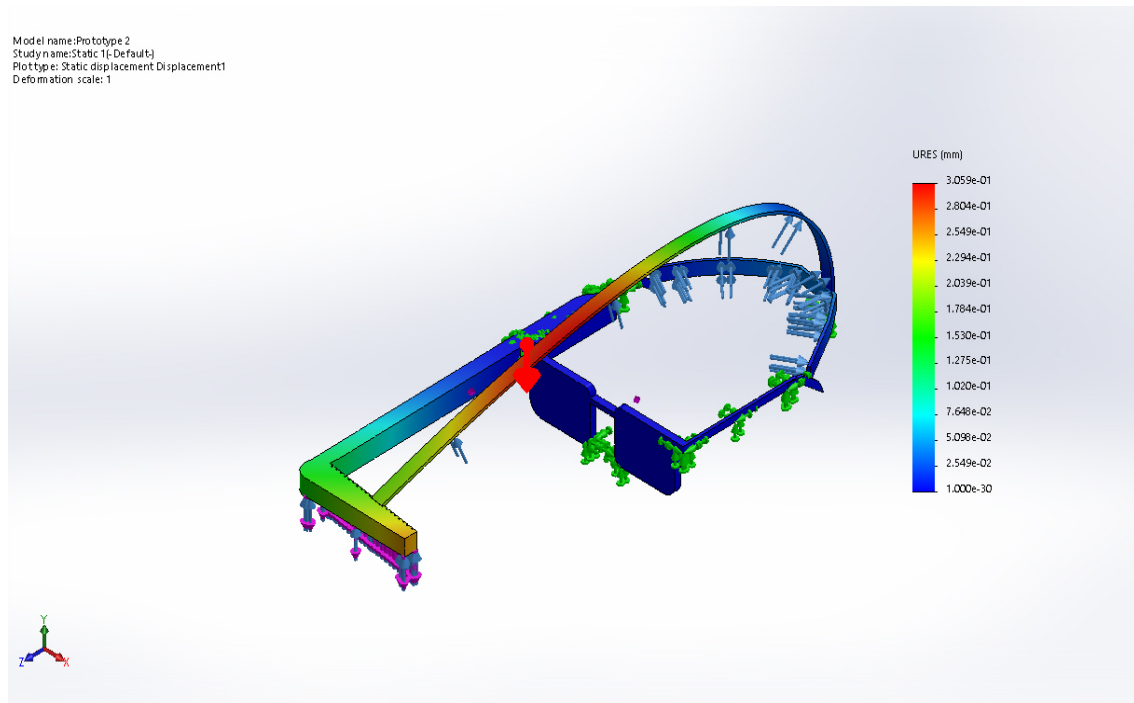


Figure 4.18: Displacement analysis on Prototype 2

From the fringe diagram results above, the maximum displacement seen on the design is  $3.059 \times 10^{-1}$  mm. As an optimization to the previous design, this design consists of a three-point gripping belt, a gripping effect most commonly has the highest displacement due to the opposing force which holds the visual aid in place for the user. Also as seen in the image above, the overhead belt, holds the visual aid at an anchoring point on it, this causes a slight displacement on the visual aid design. As a summary, it

can be said that this analysis has completed within acceptable ranges as all displacement that has been analysed in this design is calculated and accommodated for.

#### 4.5.1.3 Equivalent Strain Study

Figure 4.19 shows the equivalent strain analysis fringe diagram results that were conducted on Prototype 2 of the visual aid design.

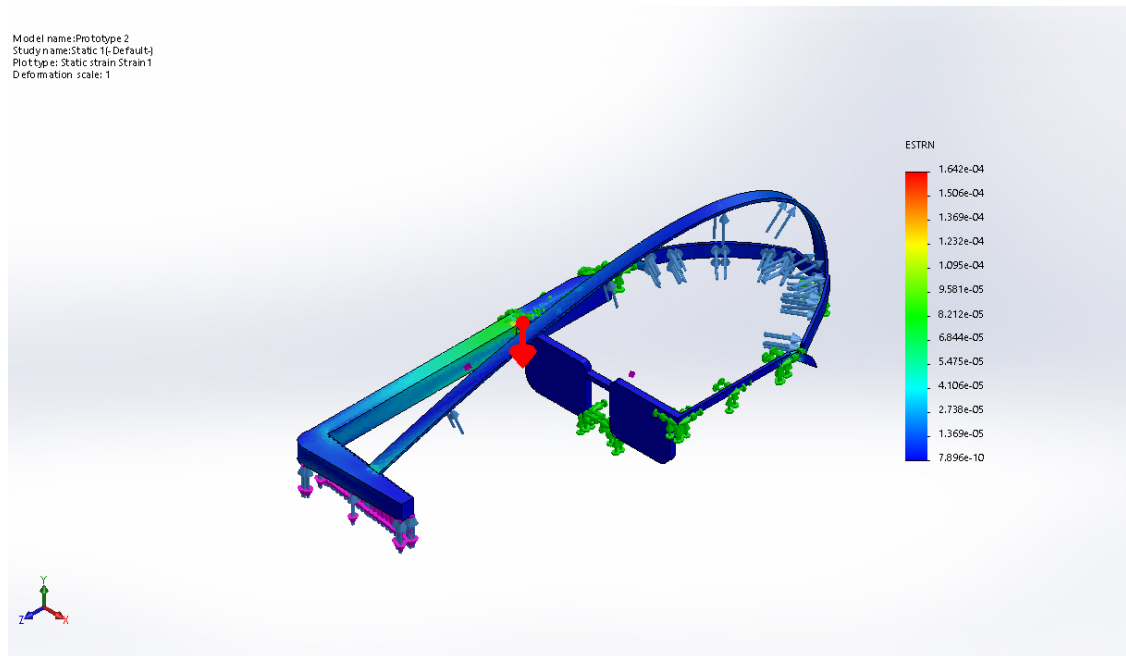


Figure 4.19: Equivalent strain study

The equivalent strain study on Prototype 2 of the object shows a maximum strain of  $1.642 \times 10^{-4}$  and a minimum of  $7.896 \times 10^{-10}$ . This range of strain analysis ensures this design does not elongate or undergo plastic deformation. The stress that is undergone by the visual aid is at the point union between the visual aid and the spectacle. The spectacle on the design analysis is pre conditioned to be static, to simplify the analysis and reduce the processing time of the design.

#### 4.5.2 Integration of Visual Aid Design Structure and Stereoscopic camera system

At the completion of the integration of the second prototype, a field of vision and depth perception test was conducted at the Taiping Hospital as shown in Figure 4.20 (More pictures of the research conducted are attached in Appendix H) . The Prototype 2 of the visual consists of the islanded microprocessor system which is dependant on external power source. However, the integration also consist of an overhead strap which is to assist the frontal biased weight of the visual aid. The overall weight of the visual aid is 227g which is lighter than prototype 1 as it has a much smaller LCD screen.

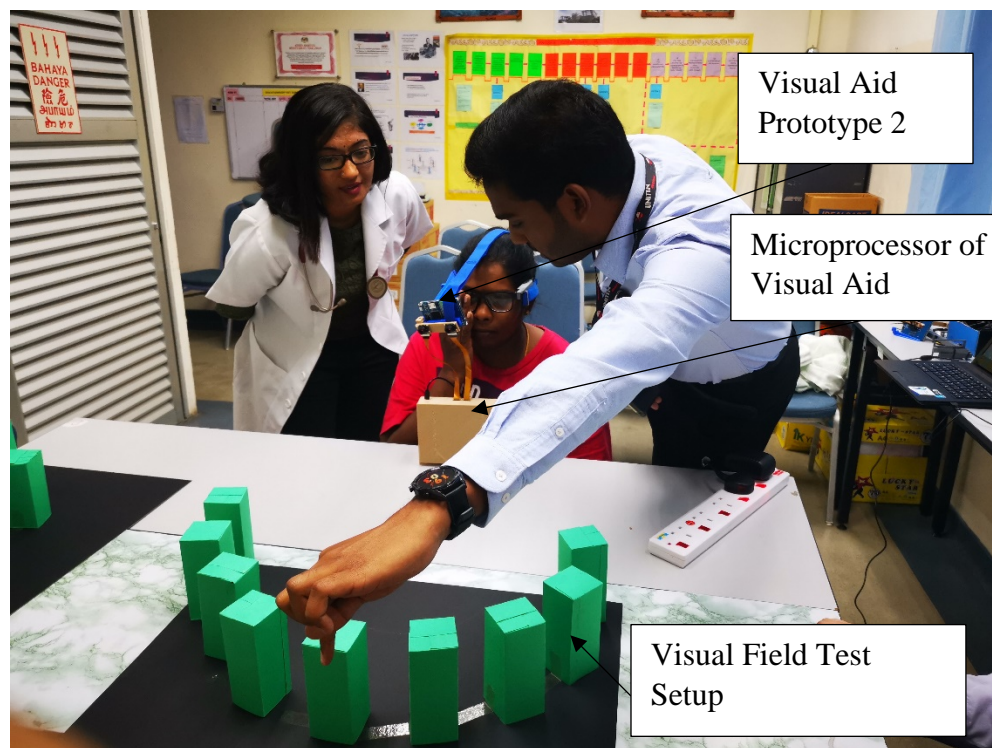


Figure 4.20: Test being conducted on the integrated complete visual aid of prototype 2 as looked on by a doctor at Taiping Hospital

### 4.5.3 Cost Analysis

The Table 4.4 shows the cost analysis conducted on Prototype 2 of the visual aid to lower the cost objectively from the previous version of the prototype.

Table 4.4 Cost Analysis table for Prototype 2

Cost Driver	Quantity	Unit Price (RM)	Price (RM)	Percentage of total cost (%)
Waveshare Compute Module I/O board	1	275.00	275.00	37.75
Raspberry Pi Compute Module Lite	1	125.00	125.00	17.16
Raspberry Pi Wide Angle camera (for stereo vision)	2	60	120.00	16.47
Design Manufacturing (3D-printing) PET-G	67 grams	1.00	67.00	9.20
Interconnecting cables	13	0.50	6.50	0.90
LCD screen 3.5 inch	1	135.00	135.00	18.52
<b>Total Prototype Cost</b>			<b>728.5</b>	<b>100.00</b>

Based on the cost analysis for prototype 2, the primary cost driver in this prototype is found to be the Waveshare compute module I/O board. The Raspberry Pi compute module has also been changed to the compute module lite version which is much a bit more cost-efficient to the previous compute module used as this version of the module does not have an internal memory embedded on to it. The processing power of the processors, however, remains unchanged as the same chipset is used.

#### 4.5.4 Visual Aid Output

Based on the depth map produced below, a vast improvement can be seen in terms of the quality. The distance is more distinct compared to the previously generated depth map. The scale of depth is shown in the Figure 4.21(A.) and (B.). With a close analysis, the object closest to the camera is more reddish in colour and as the object is distant the colour progresses to become blue. In this set up, the blocks are arranged in a circular manner, being able to test the field of vision and depth with the depth map.

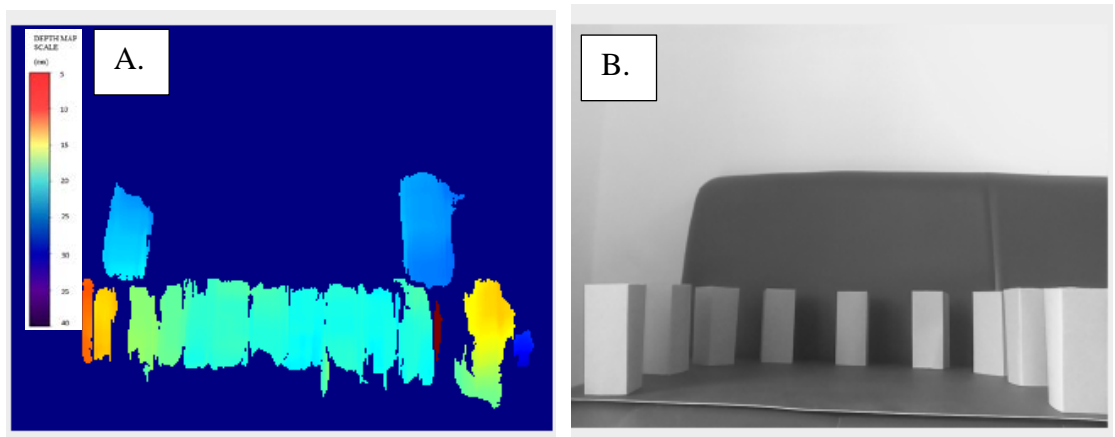


Figure 4.21: (A.) Depth map produced by prototype 2 of the visual aid (B.) Grayscale field of vision output by prototype 2 of the visual aid.

From the field of vision produced by the visual aid, all nine of the boxes can be seen. This proves that the visual aid can increase the field of vision of a monocular visual impaired patient. In contrast with the previous prototype, only 7 boxes were completely seen.

#### 4.5.5 Result of testing Prototype 2

As the Prototype 2 was completed, on-site testing was conducted at the Taiping Hospital to justify the objectives of this research. The test was conducted on real patients with monocular visual impairment. The test was conducted on monocular visual impaired patients with the supervision of Dr Chee Wai , an optometrist at the Taiping Hospital specializing in low vision.

##### 4.5.5.1 Results of Field of vision

The results of the field of vision test are as tabulated in Table 4.6

Table 4.6: Table of results for the field of vision for prototype 2

FIELD OF VISION TEST						
Respondent No	Number of blocks seen without visual aid	Number of blocks seen with the visual aid	Field of vision without visual aid (angle)	Field of vision with a visual aid (angle)	Increment in the field of vision (angle)	Percentage of increase in the field of vision (%)
1	6	8	110	154	44	40.0
2	5	7	88	132	44	50.0
3	5	6	88	110	22	25.0
4	5	7	88	132	44	50.0
5	6	7	110	132	22	20.0
6	6	8	110	154	44	40.0
7	6	7	110	132	22	20.0
8	5	6	88	110	22	25.0
9	5	7	88	132	44	50.0
10	4	5	66	88	22	33.3

Based on the feedback by the patients, they had no complaints about the visual aid as the previously tested prototype was found to be frontal biased and tend to topple off from the head. The patients were also highly satisfied with the depth map produced by the visual aid. The increase in field of vision was also clearly seen and appreciated by the patients. As compared to the previous customer feedback from prototype 1, many parts of the visual aid have been changed to accommodate to the customer feedback, the depth map has been calibrated further for a much-enriched quality of depth map. The depth map has been found to be much clearer and able to differentiate distances at different layers as shown in Figure 4.22 (A.) and (B.)

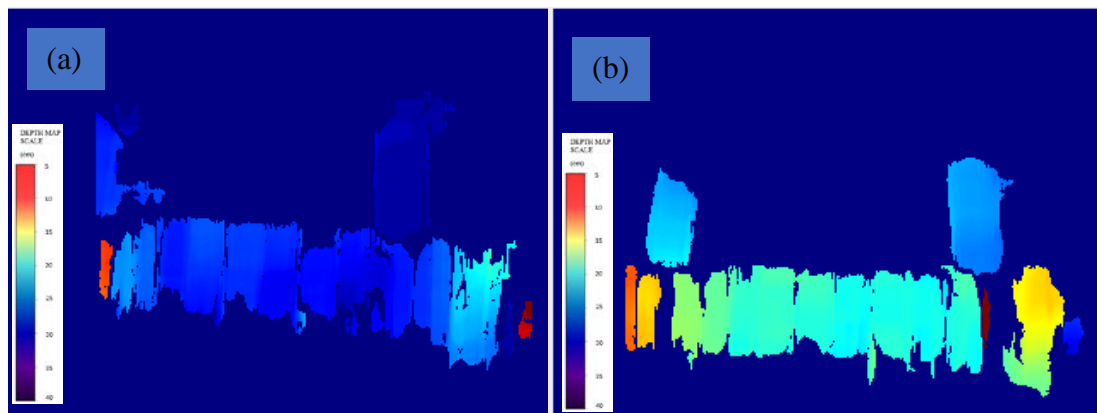


Figure 4.22: (A.) Depth map of prototype 1 (B.) Depth map of prototype 2

However, patients and medical professionals clarified that different patients have distinct field of visions, while some have wide field of vision, some have narrower field of vision, thus it was suggested that the cameras were to be attached on a articulating plate for the user to set his own field of vision. The test was conducted on monocular visual impaired patients with the supervision of Dr Chee Wai, an optometrist at the eye hospital specializing in low vision.

**4.5.5.2 Analysis of field of vision**

Based on the Figure 4.23 below, the minimum of number of blocks seen among all the patients are found to be between 4 and 5, while maximum number of blocks seen is 8. This is clear increase and improvement noted as compared to Prototype 1.

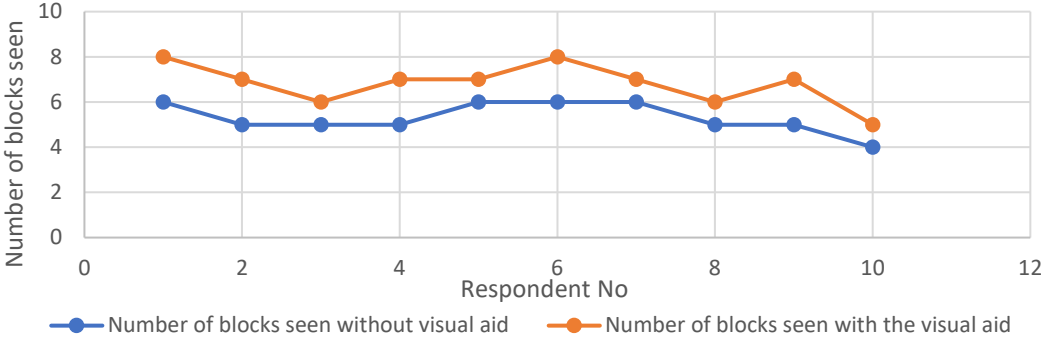


Figure 4.23: Analysis of the blocks seen with and without the visual aid

The Figure 4.24 correlates to Figure 4.23 in terms of angle in from the number of blocks. Hence, the analysis of the figure is typical to Figure 4.23.

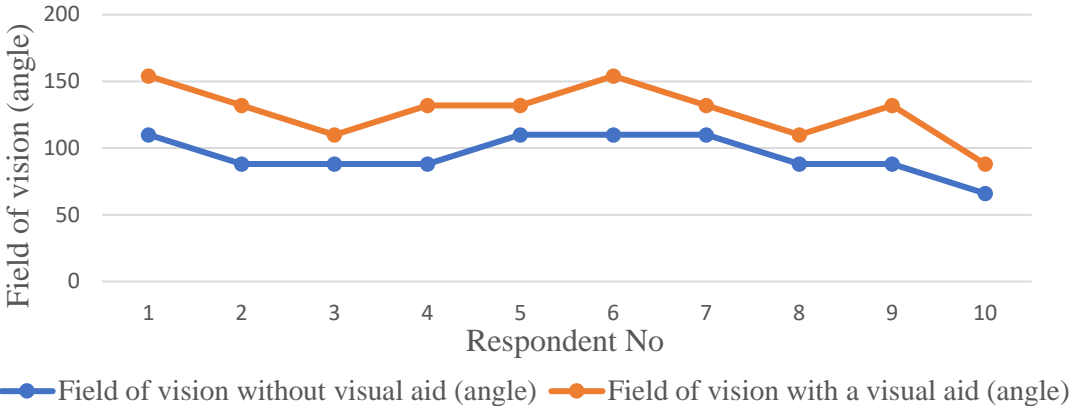


Figure 4.24: Analysis of the field of vision (angle) with and without the visual aid

From the analysis in Figure 4.25 of the test conducted at the Taiping Hospital, it can be seen a minimum of 16.7 % and maximum of 40 % of increase in the field of vision is noted. A minimum angle of 22° has increased among all the patients. This is coherent with the objective of this research to increase the field of vision by at least 20%. However, the increase in field of vision is a variable from patient to another due natural field of vision of the patient itself. There is still however inconsistency with the result that is obtained, thus this prototype is further improved to develop Prototype 3 of the visual aid. However, this test acts as a proof of concept for the visual aid for monocular visual impaired patients.

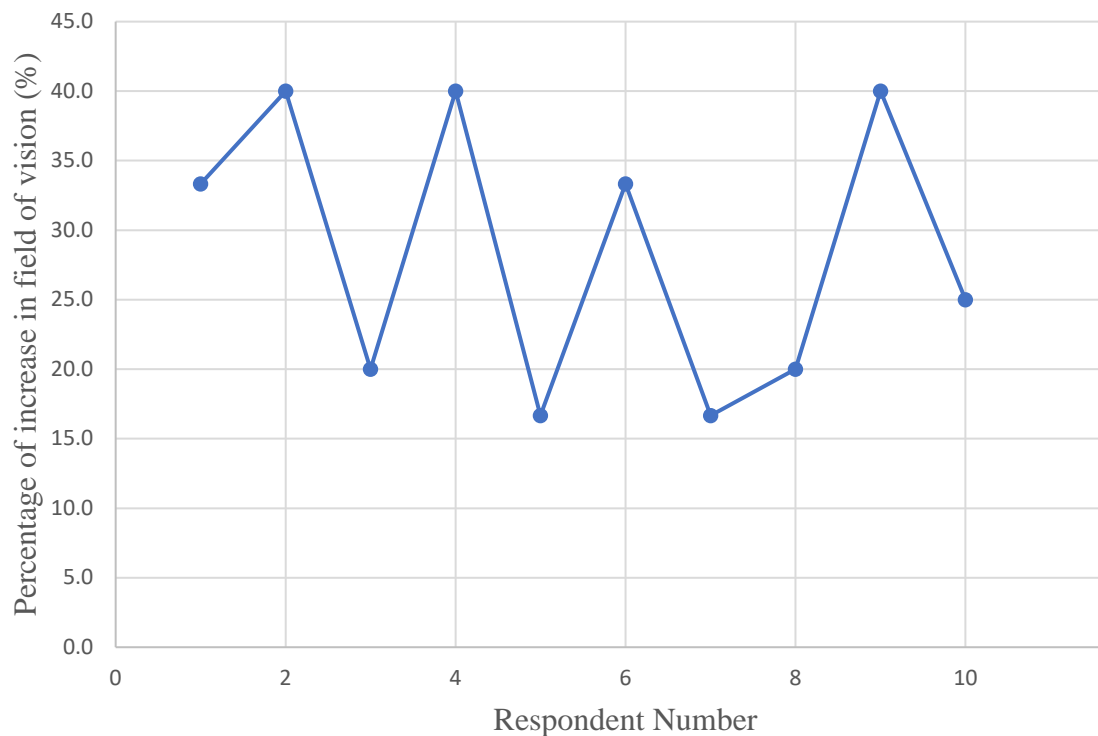


Figure 4.25: Percentage of increase in the field of vision

### 4.5.5.3 Result of Depth Perception

The experimental setup for the depth perception test conducted on monocular visual impaired patients is shown in Figure 4.26 (A.) in grayscale. The results of the test conducted are published in Table 4.6

Table 4.6: Results of depth perception for prototype 2

Respondent No	Block Sequence without visual aid	Block Sequence with the visual aid	Number of blocks with correct sequence without visual aid	Number of blocks with correct sequence with visual aid
1	5,3,1,2	5,1,2,3	2	1
2	3,5,1,2	3,5,1,2	0	0
3	5,3,2,1	5,3,2,1	4	4
4	5,3,1,2	3,5,1,2	2	0
5	3,5,1,2	5,3,2,1	0	4
6	5,3,2,1	5,3,2,1	4	4
7	3,5,1,2	5,3,2,1	0	4
8	3,5,1,2	5,3,2,1	0	4
9	5,3,2,1	5,3,1,2	4	2
10	5,3,1,2	5,3,2,1	2	4

Further test was conducted to test the depth perception of patients with the visual aid as mentioned in Chapter 3. The prototype has aided the patients with depth perception as there is obvious increase of the number of blocks seen before and after using the visual aid. However only 6 of the 10 respondents were able to identify the blocks correctly

with the visual aid. This is due to the inconsistency of the depth map produced by the depth map which was misleading the respondents. This is due to the generation of depth map not being in real-time thus the lag in the depth map causes the respondents to be confused with the order of the boxes thus leading to inconsistency.

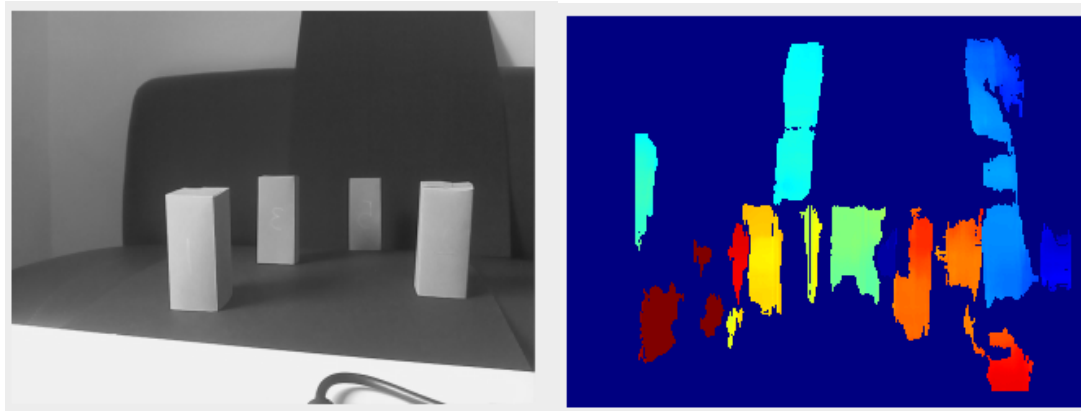


Figure 4.26: (A.) The depth map experimental setup for monocular visual impaired patients (B.) Corresponding Depth Map

From the depth map, it can be analysed that all 4 of the boxes on the setup apparatus is seen clearly in different colours. Although box 1 and two are seen like on the same plane to a monocular visual impaired patient, from the depth map it can be easily distinguishable by “Box 1” in dark red while “Box 2” in orange. With the depth scale shown, it is further analysed that “Box 1” is the closest to the visual aid while “Box 2” is behind it.

Prototype 2 has a significant improvement in terms of increase in field of vision and able to obtain a better depth perception than prototype 1. It also weighs much lesser than prototype 1. However, there is still inconsistency in the depth map and field of vision produced which is a result of poor quality of depth map. These are design specifications which be revised in Prototype 3.

## 4.6 Development of Working Prototype 3

Based on the previous design analysis conducted on Prototype 1 and 2, This design was further optimized in terms of its microprocessors that were used. This design features the StereoPi microprocessor which is much smaller in size and thus be fitted on the visual aid itself. In terms of the design of the visual aid frame itself, a new articulating camera attachment plate in added as an upgrade from the previous customer feedback provided from the analysis in Prototype 2. Besides these two upgrades on the design of Prototype 3, the rest of the design remains the same as Prototype 2. An orthographic and exploded view drawings with dimensions of Prototype 3 are attached in Appendix I.

### 4.6.1 Design Analysis

The mesh analysis was completed with an element size of 9.24482 mm with a tolerance of 1.84896 mm. The total elements that were used in this analysis are 45245 with total nodes amounting to 79630. This analysis required much denser (as shown in Figure 4.27) elements compared to the previous analysis conducted on the previous prototypes as this design has an articulating point which might cause more stress on the joint of it. Thus, it was vital to carefully analyse the design in scrutiny.



Figure 4.27: Mesh analysis of visual aid design prototype 3

#### 4.6.1.1 Von Mises Stress Study

Figure 4.28 shows the stress analysis fringe diagram results conducted on Prototype 3 of the visual aid design.

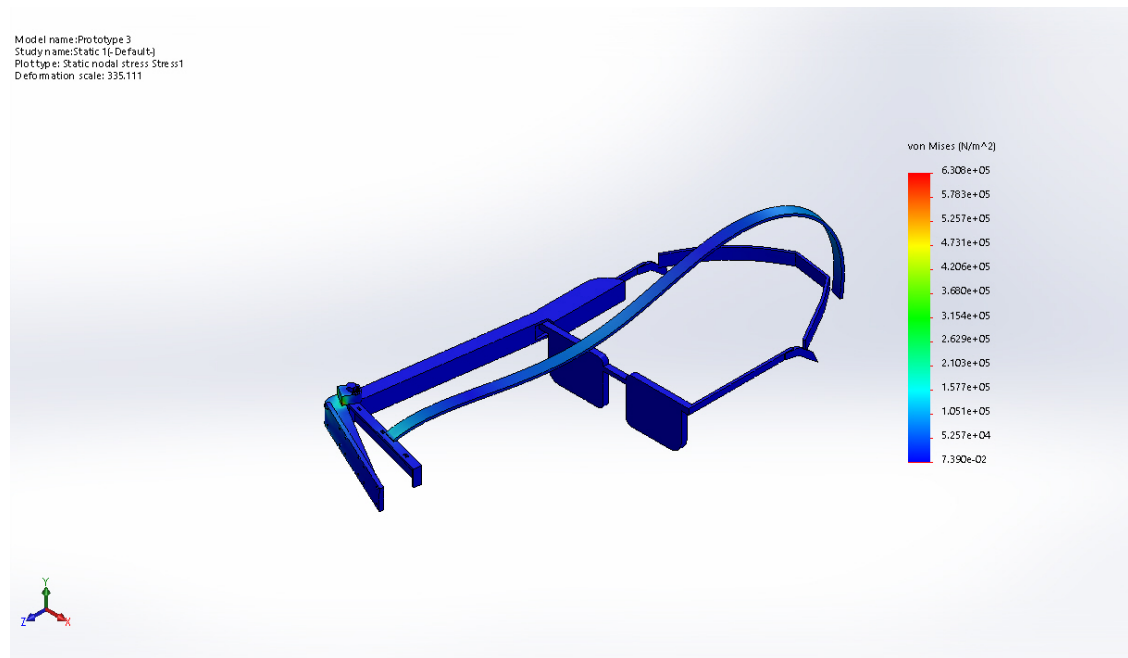


Figure 4.28: Stress Analysis on prototype 3

Based on the fringe diagram results of the stress analysis conducted on Prototype 3 of the visual aid, the maximum stress on the object is  $6.308 \times 10^5 \text{ N/m}^2$  which is well below the minimum tensile strength of the composite, thus this object does not undergo plastic deformation under the preconditioned forces. The maximum stress area is as expected during the design stage which is at the area of articulation of the camera plate. The articulation causes a high stress point as the hinge joint supports the cameras while in motion. A close up of the slot mechanism in Figure 4.29 explains in detail about the hinge and the forces it undergoes.

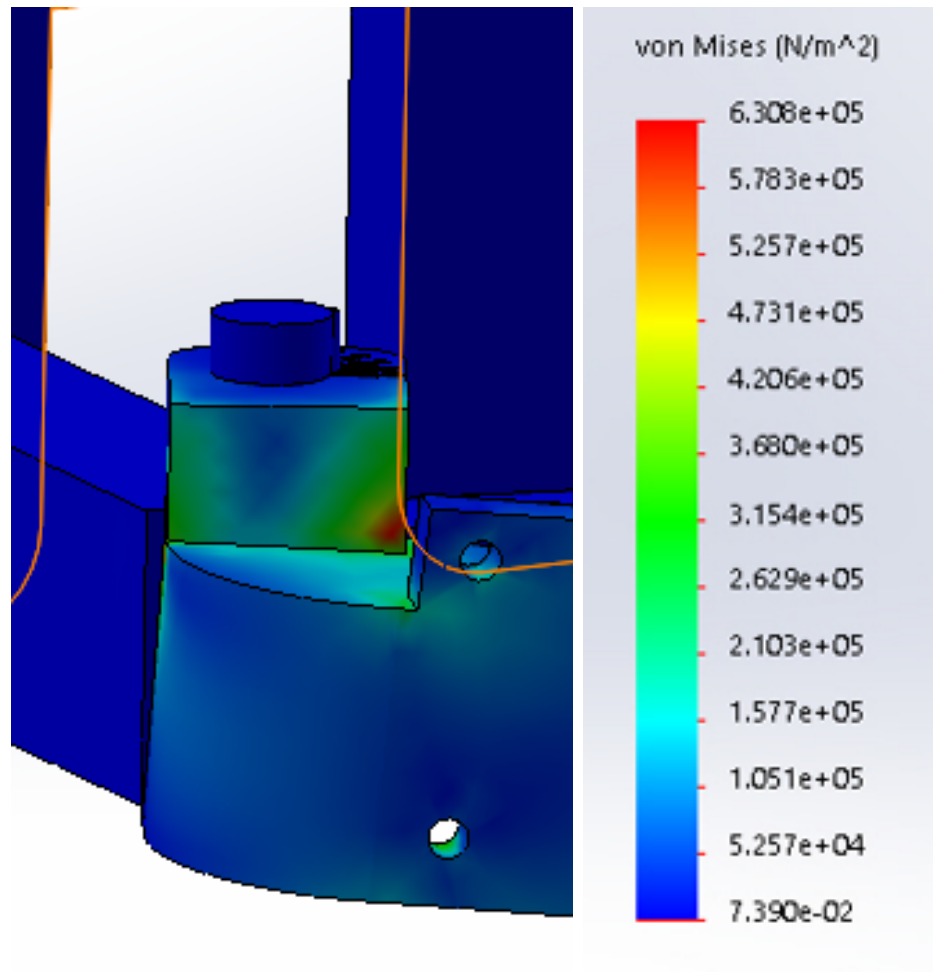


Figure 4.29: Maximum stress area of Prototype 3 of visual aid.

As seen from the Figure 4.29, the maximum stress at the hinge of the camera holding plate of the design, is due to the force of the camera being supported by a single joint. On the contrary, the stress values at the range from the minimum to the maximum range. It also seen that only the edge of the camera plate joint undergoes maximum stress while the midsection of the joint remain at minimum values of  $7.390 \times 10^{-2} \text{ N/m}^2$ .

#### 4.6.1.2 Resultant Displacement Study

The Figure 4.30 shows the displacement analysis fringe diagram result conducted on Prototype 3 of the visual aid design.

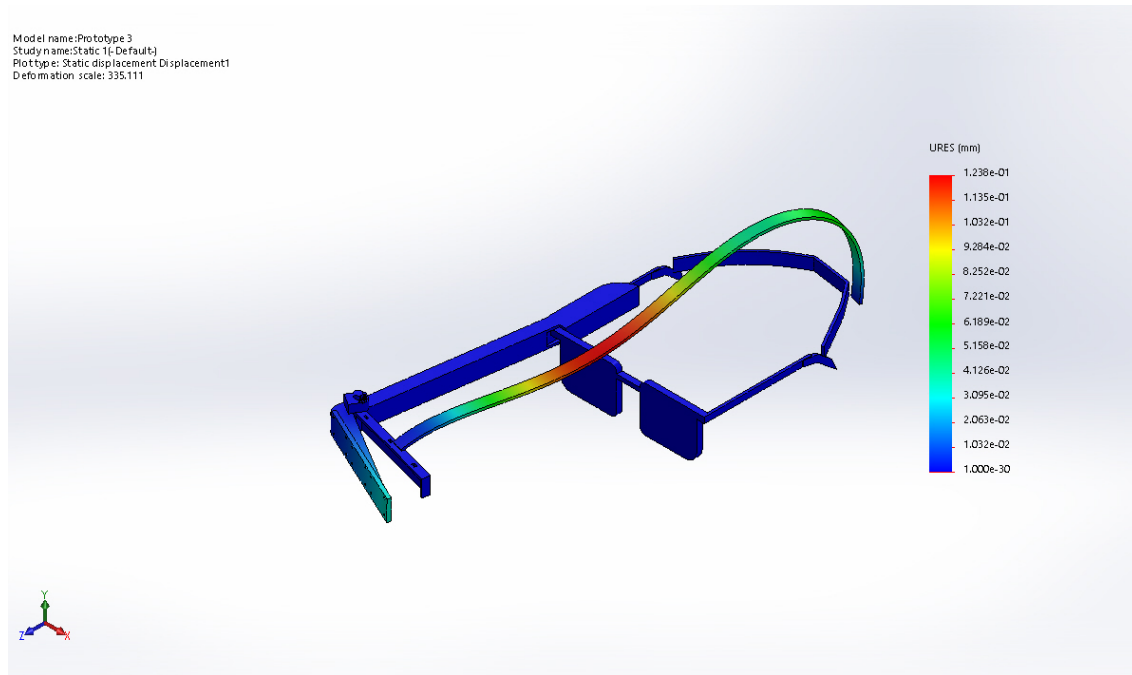


Figure 4.30: Static displacement fringe diagram results of Prototype 3

Based on the analysis conducted of static displacement conducted on Prototype 3 of the visual aid design. It found that statically, there is not much displacement on the design as the maximum displacement was found to be  $1.238 \times 10^{-1}$  mm. This displacement was also only seen in the three-point gripping belt section of the visual aid design. This is because the belt does not have any support in a static displacement analysis, but when the visual aid is used, the belt is attached overhead to a user, thus it grips itself carefully. Some displacement ranging up to  $7.221 \times 10^{-2}$  mm is seen at the end of the camera holding plate, this is due to the force of the camera being fixed to a single rotating joint,

however this displacement is not very significant and not affect the performance of the visual aid.

#### 4.6.1.3 Equivalent Strain Study

The Figure 4.31 below shows the equivalent strain analysis fringe diagram results conducted on Prototype 3 of the visual aid design.

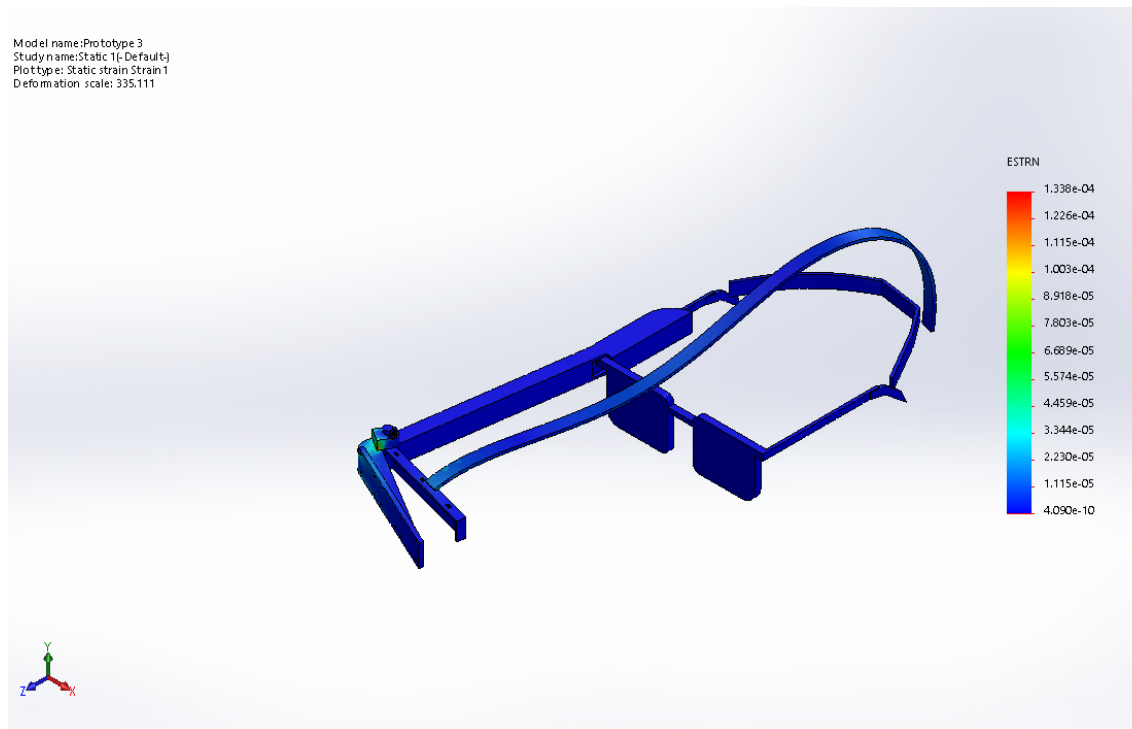


Figure 4.31: Equivalent Strain Analysis Prototype 3

Based on the analysis conducted on Prototype 3 of the visual aid design, the strain analysis concludes there are no major that is occurring on the static design analysis. The strain ranges from  $4.090 \times 10^{-10}$  N/m<sup>2</sup> up to  $1.338 \times 10^{-4}$  N/m<sup>2</sup>. The only area that undergoes minor elongation is at the area of the camera plate hinge where the camera forces act on to it. However, the value of the maximum strain in this design remains

very low thus being insignificant. This visual aid also has been chosen as the final design due to phases of development it has been through in terms of design.

#### 4.6.2 Integration of Visual Aid Design Structure and Stereoscopic camera system

The Figure 4.32 shows the completed model of prototype with the integration of all the design structure with the articulating hinge and the stereoscopic camera system.

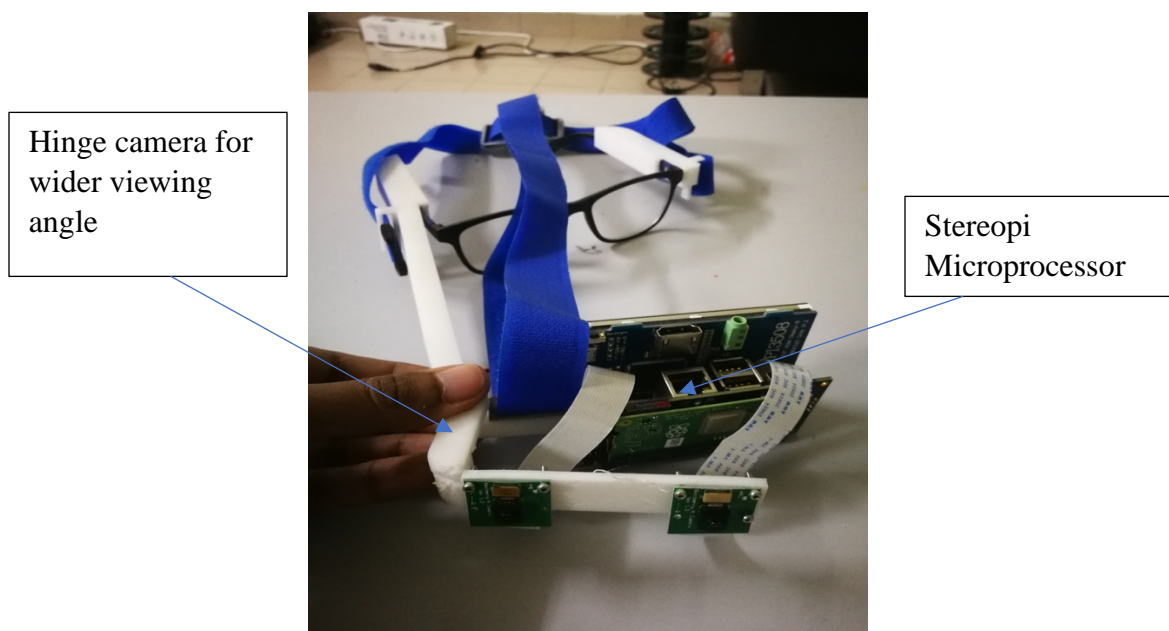


Figure 4.32: Complete Prototype 3 of the visual aid

The overall weight of the model is 254 g which is lighter than Prototype 2 but slightly heavier than Prototype 1. This is because Prototype 2 has its microcontroller isolated compared to this prototype which has it integrated in the visual aid. An analysis in Figure 4.33 shows the comparison of the mass of the visual aids which concludes that prototype 3 has an ideal weight as the weight is held by the strap at the top. The measurement of weight was made three times and no variation was found.

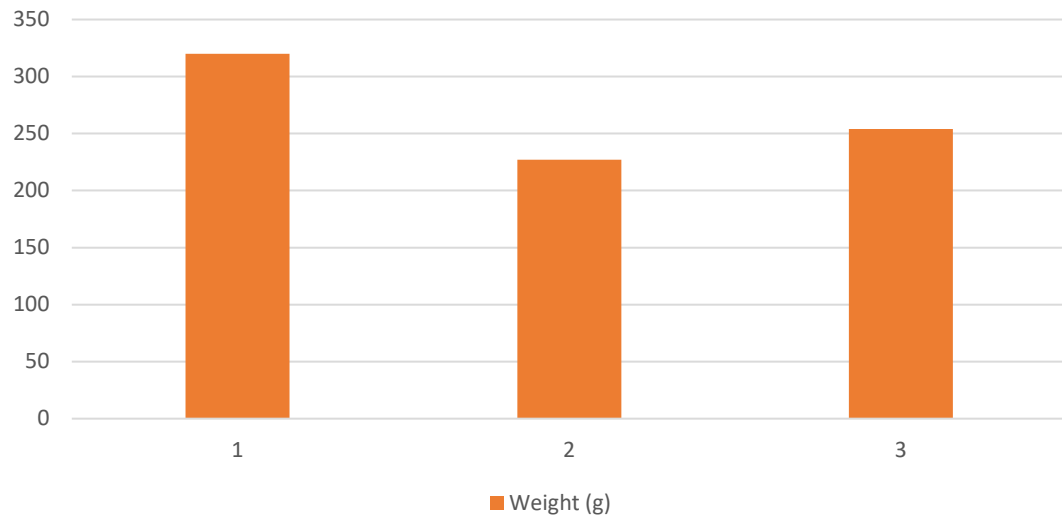


Figure 4.33: Comparison of weight of visual aid from Prototype 1, 2 and 3

#### 4.6.3 Cost Analysis

The Table 4.7 below shows the cost analysis conducted based on the cost drivers on Prototype 3 of the visual aid design.

Table 4.7: Cost Analysis table of Prototype 3

Cost Driver	Quantity	Unit Price (RM)	Price (RM)	Percentage of the total cost (%)
StereoPi module	1	367.00	367.00	51.36
Raspberry Pi Compute Module Lite	1	125.00	125.00	17.50
Wide angle camera v2	2	25.00	50.00	7.00
HDMI cable ribbon (male to male)	1	35.00	35.00	4.90
StereoPi power cable	1	2.50	2.50	0.34
LCD screen	1	135.00	135.00	18.90
<b>Total Prototype Cost</b>			<b>714.50</b>	<b>100.00</b>

The cost analysis that was conducted on the final prototype shows that the primary cost driver is the StereoPi module, which is the microcontroller of the visual aid. It accounts for 51.36% of the total cost of the visual aid. From the analysis, it can also be concluded that most of the major cost is from the electronic components which are the StereoPi module, Raspberry Pi Compute Module Lite, and the LCD screen. With comparison to the previous prototypes, this prototype not only has used much smaller and complex components but also have reduced the cost of the visual aid from RM861.50 in the first prototype to RM728.5 in the second prototype and RM714.50 in the third prototype.

#### 4.6.4 Visual Aid Output

The depth map in Figure 4.34 is the output of the final prototype of the visual aid. From a visual analysis, the map produced is much clearer than the previous outputs which increase the quality of the depth map. The scale of depth is shown by the scale that is shown in the Figure.

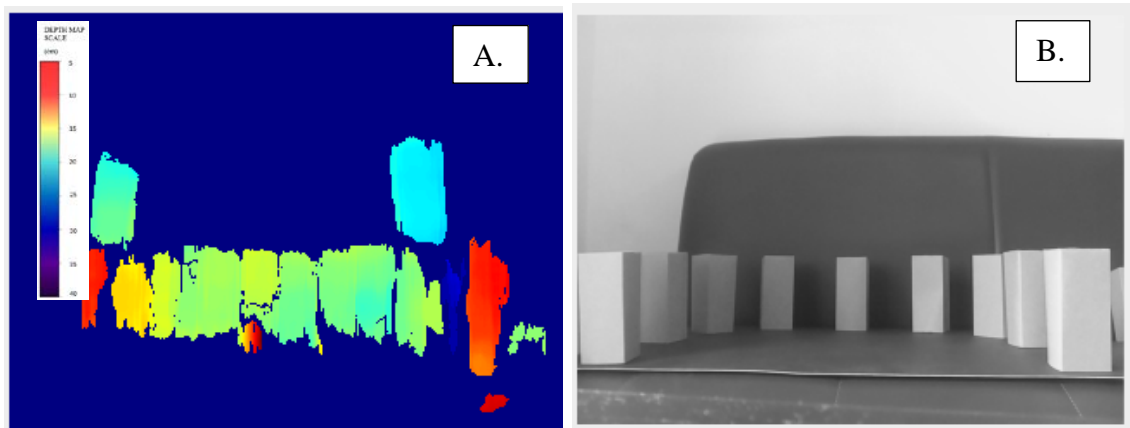


Figure 4.34: (A.) Depth map produced by Prototype 3 of the visual aid (B.) Field of vision produced by the prototype 3 of the visual aid

From the comparison of the depth maps generated from the previous prototypes, more contrast of colours can be seen in this depth map produced by Prototype 3. The contrast of colours on the depth enables us to understand the depth of the image better.

The quality of this depth map has highly improvised due to it using the StereoPi with the compute module.

The advantage of using these hardware's is that it can handle more processing power while working in real-time. The prototypes prior to this have all utilized the Waveshare compute module which also has a similar processing power but in compensation with time thus it cannot handle high processing in real-time.

#### **4.6.5 Result of testing Prototype 3**

As the Prototype 3 was completed, on-site testing was conducted at the Tun Hussein Eye Hospital to justify the objectives of this research. The test was conducted on monocular visual impaired patients with the supervision of Ms Ramakrishnan, an optometrist at the eye hospital specializing in low vision ( Photos of research are attached in Appendix J)

##### **4.6.5.1 Results of Field of vision**

The results of the field of vision test are as tabulated in Table 4.8. The sample size that was used to conduct this test is 10 people out of 27 people who were admitted in ward in the low vision department of the hospital.

The justification for the sample size that was taken in given in chapter 3. The number of respondents that are taken are based on the number of patients of monocular visual impairment that were present on that day. However based on statistical calculation given in Table 3.2 in the previous chapter justifies the obtained results with an acceptable confidence level.

Table 4.8: Table of results for the field of vision for prototype 3

FIELD OF VISION TEST						
Respondent No	Number of blocks seen without visual aid	Number of blocks seen with the visual aid	Field of vision without visual aid (angle)	Field of vision with a visual aid (angle)	Increment in the field of vision (angle)	Percentage of increase in the field of vision (%)
1	6	9	110	176	66	60.0
2	7	8	132	154	22	16.7
3	4	7	66	132	66	100.0
4	5	7	88	132	44	50.0
5	5	9	88	176	88	100.0
6	6	9	110	176	66	60.0
7	4	7	66	132	66	100.0
8	5	9	88	176	88	100.0
9	4	9	66	176	110	166.7
10	6	9	110	176	66	60.0

#### 4.6.5.2 Analysis of field of vision

Based on the Figure 4.35, 6 out of the 10 participants were able to see all 9 of the number of blocks with the visual aid. This is a clearly noted improvement for the field of vision of the visual aid.

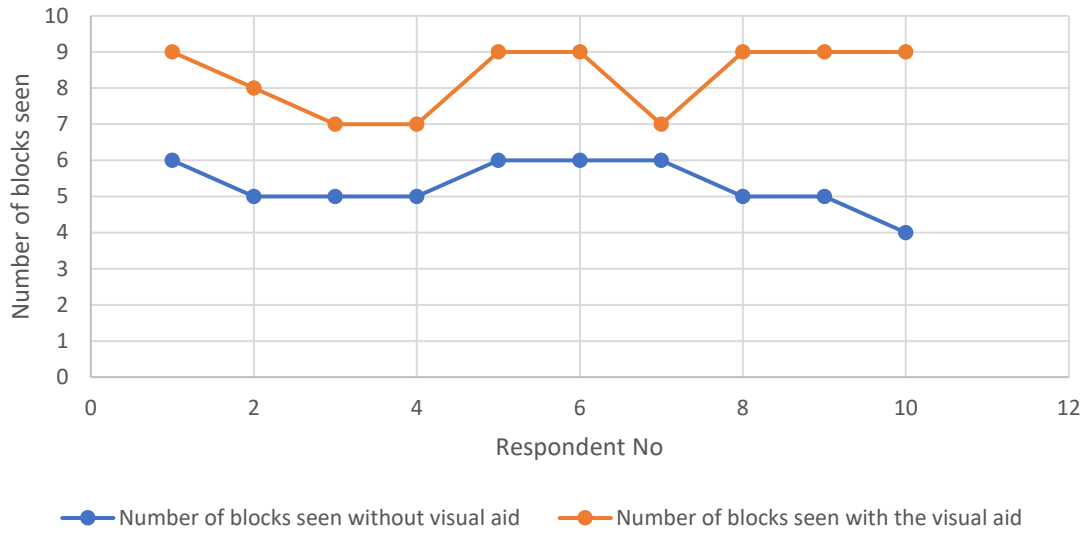


Figure 4.35: Analysis of the blocks seen with and without the visual aid

The Figure 4.36 translates the angle based on the number of blocks seen from Figure 4.35. Hence the analysis is typical to Figure 4.35.

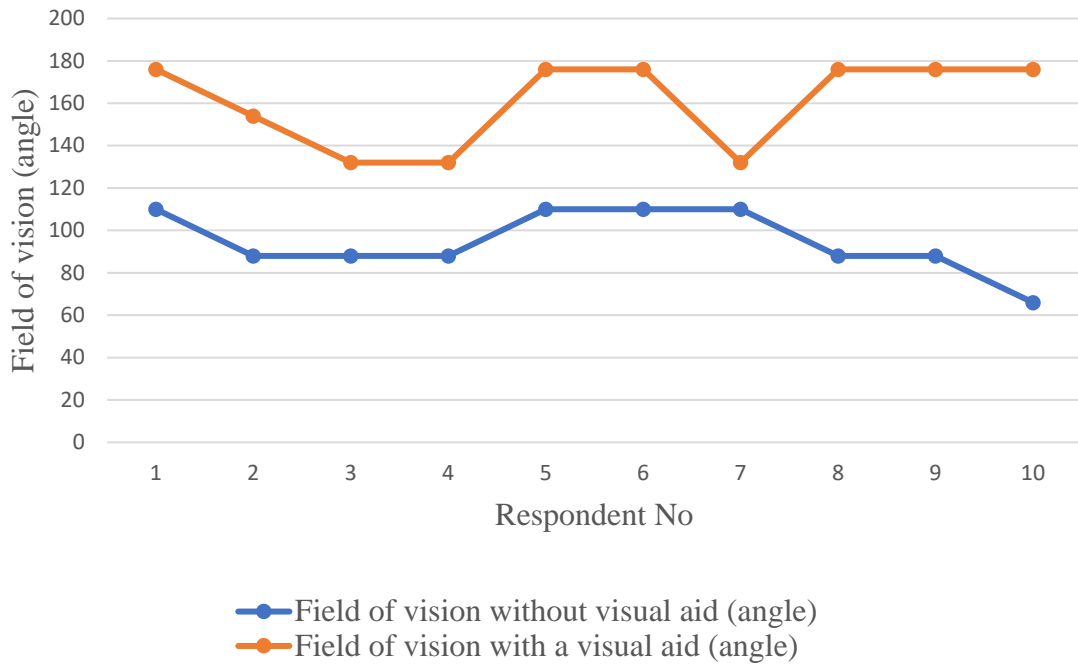


Figure 4.36: Analysis of the field of vision (angle) with and without the visual aid

One of the primary objectives of this research is to increase the field of vision of monocular visual impaired patients. As explained in the methodology, the field of vision test was conducted quantitatively with an experimental setup. The results are analysed as in Figure 4.35 and Figure 4.36, the analysis shows as the number of blocks seen and the increase in the field of vision are the same, this is due to the spacing of each block is arranged with a space of  $22^\circ$  in between them. The objectives of this research are to increase the field of vision by at least 20%, and from the table of results for the conducted experiment, it can be seen that the minimum increase in the field of vision is 28.6%, and the maximum stands at 100%. The analytic representation of the percentage increase in the field of vision can also be seen in Figure 4.37.

The increase in the field of vision, outruns the expected results making the prototype a successful visual aid. As during the conduct of the experiment, many of the monocular visual impaired patients were happy and excited to be able to see a much wider field of field vision with and without the visual aid.

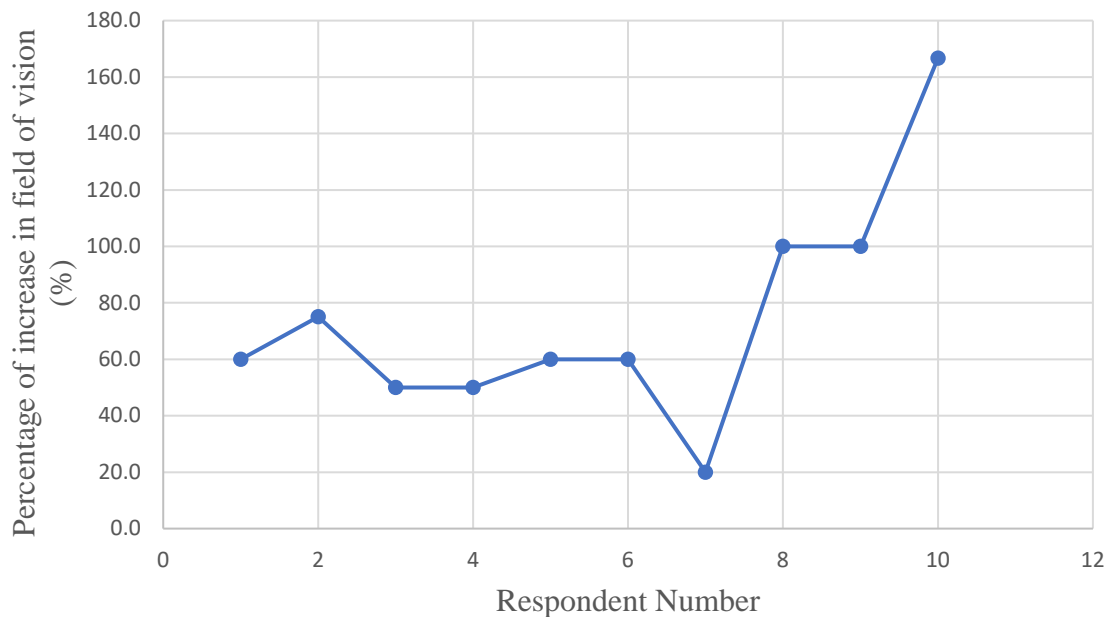


Figure 4.37: Percentage of increase in the field of vision

#### 4.6.5.3 Results of Depth Perception

The experimental setup for the depth perception test conducted on monocular visual impaired patients is shown in Figure 4.38 in grayscale. The results of the test conducted are published in Table 4.9.

Table 4.9: Results of depth perception for prototype 3

Respondent No	Block Sequence without visual aid	Block Sequence with the visual aid	Number of blocks with correct sequence without visual aid
1	5,3,1,2	5,3,2,1	2
2	3,5,1,2	5,3,2,1	0
3	5,3,2,1	5,3,2,1	4
4	5,3,1,2	5,3,2,1	2
5	3,5,1,2	5,3,2,1	0
6	5,3,2,1	5,3,2,1	4
7	3,5,1,2	5,3,2,1	0
8	3,5,1,2	5,3,2,1	0
9	5,3,2,1	5,3,2,1	4
10	5,3,1,2	5,3,2,1	2

Depth perception is the fundamental objectives of this research and visual aid development. As such, the above table shows the block sequence as perceived by the respondents before and after the usage of the visual aid. The block sequence was deliberately sequenced in an unorderedly manner to avoid any sort of tampering during the testing process. Among the participants, 3 out of 10 participants were able to identify the sequence correctly without the visual aid. The results also clearly show that all 10 respondents were able to identify the block sequence clearly with the visual aid. This explains the clarity of the visual aid towards the user. The depth map produced by the visual aid is clearly understood and perceived by the user and thus the user can differentiate the depth in an image clearly.

Some of the respondents were also able to identify the sequence of the visual aid correctly without the aid of the visual aid, this may be due to subjects climatizing to the environment of the experiment making them identify the block sequences correctly.

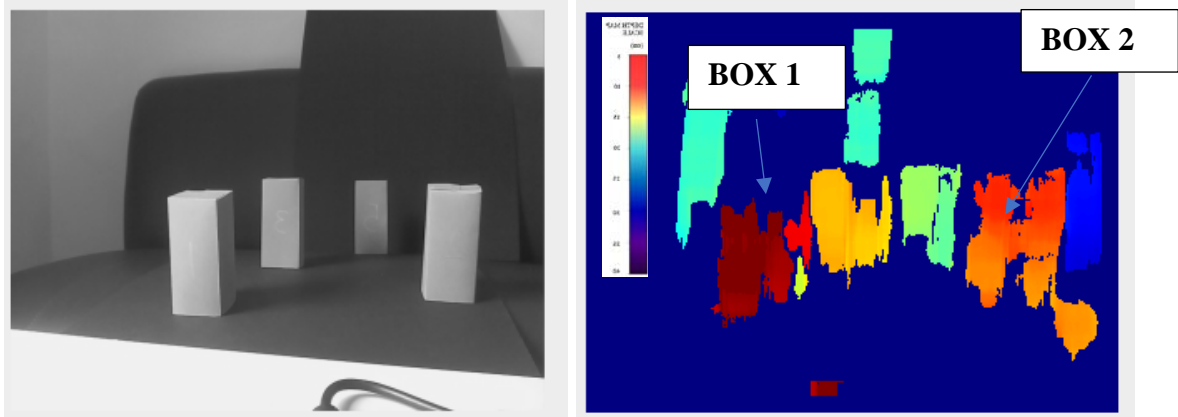


Figure 4.38: (A.)The depth map experimental setup for monocular visual impaired patients (B.) Corresponding Depth Map

From the depth map, it can be analysed that all 4 of the boxes on the setup apparatus is seen clearly in different colours. Although box 1 and box 2 are seen like on the same plane to a monocular visual impaired patient, from the depth map it can be easily distinguishable by “Box 1” in dark red while “Box 2” in orange. With the depth scale shown, it is further analysed that “Box 1” is the closest to the visual aid while “Box 2” is behind it.

#### 4.8 Summary

This chapter has presented all the relevant results pertaining to this research. The survey was conducted with a sample size of 16 patients and 3 medical professionals. The responses of the survey were analysed by using the House of Quality. A total of 16 functional and customer requirements were identified for this purpose. From the analysis, the design and the stereoscopic system of the visual aid was developed simultaneously. These two components were then integrated to form the visual aid. The design phase of

the visual aid comprised of static studies being conducted on the design which consist of stress, strain and displacement studies. A summary of all the 3 prototypes are presented in Table 4.10

Table 4.10: Comparison Table of prototype 1, 2 and 3

<b>Prototype</b>	<b>1</b>	<b>2</b>	<b>3</b>
<b>Maximum Stress (N/m<sup>2</sup>)</b>	$1.682 \times 10^4 \text{ N/m}^2$	$6.782 \times 10^5 \text{ N/m}^2$	$6.308 \times 10^5 \text{ N/m}^2$
<b>Maximum Strain</b>	$3.173 \times 10^{-6}$	$1.642 \times 10^{-4}$	$1.338 \times 10^{-4} \text{ N/m}^2$
<b>Maximum Displacement</b>	$1.393 \times 10^{-4} \text{ mm}$	$3.059 \times 10^{-1} \text{ mm}$	$1.238 \times 10^{-1} \text{ mm}$
<b>Maximum Angle of Vision</b>	No test conducted	176°	176°
<b>Maximum Increase in field of vision (%)</b>	No test conducted	40%	100%
<b>No of people with correct Block Sequence With Visual Aid</b>	No test conducted	60%	100%
<b>Total Cost</b>	RM 861.00	RM 728.40	RM 714.28
<b>Percentage of Cost Reduction compared with prototype 1</b>	0	15.40%	17.04%

The studies were conducted with appropriate materials and forces as stated in chapter 3. The development of the visual aid was consisting of three stages of development. Testing was conducted on the product only after a Minimum Viable Product was obtained which was in prototype 2. The first prototype was provided with only a user feedback from the society of blind Malaysia to improve and achieve a Minimum Viable Product (MVP). The second and third prototypes of the visual aid were tested at the Taiping Hospital and Tun Hussein Eye Hospital low vision departments, respectively.

Two tests were conducted which were the field of vision and depth perception tests as stated in chapter 3. The results of the second prototype were found to be a proof of the concept and its functions, such as the generation of the depth map. The results were however inconsistent due to the selection of components. The third prototype was reiterated with different components, thus producing much prominent and consistent results.

## **CHAPTER 5**

### **CONCLUSION AND RECOMMENDATION**

#### **5.1 Overview**

This chapter encapsulates the development of the visual aid for monocular visual impaired patients with results from the test conducted at various institutions. Further recommendations are also provided for future researchers to develop more in this area.

#### **5.2 Conclusion**

Monocular visual impairment refers to having partial or no vision in either of the two eyes. Monocular visual impaired patients most commonly cannot perceive depth and have a limited field of vision. This research was initiated by designing a survey for face to face interview method with medical professionals and monocular visual impaired patients. This interview was aimed at understanding the causes, challenges and the existing treatment that is available to these patients. A sample size of 16 respondents and 3 medical professionals was chosen to participate in the survey.

The survey has deduced that the most common cause of monocular visual impairment is glaucoma which happens in old age which comprise of 43% of the total respondents. The existing treatment which is common for glaucoma is rehabilitation, these patients lose a sense of confidence due to the challenges they face, such as unable to drive, and walk with stability. Patients were also requested to provide requirements for a visual aid developed for them. From the information that is obtained from the survey, a House

of Quality was generated to analyse the information based on the weightage and mapping of the functional and customer requirements.

Based on House of Quality, it was evident on the features and design of the visual aid was in line with the objective of the research. Simultaneous development of the design and stereoscopic camera system was initiated. In the design phase, static studies were conducted which comprise of stress, strain and displacement analysis of the prototype frame designs. The algorithm used for all three of the designs are similar. The calibration for the stereoscopic system was carried out after the integration of design structure and the stereoscopic system to complete the visual aid.

A total of three prototypes were produced for the purpose of this development, the first prototype was developed with default selection of components. The prototype was given user feedback by the Society of Blind Malaysia, the prototype was found to have poor generation of depth map with high inconsistencies. The weight of the visual aid was also frontal biased thus more pressure was applied on the nose bridge.

With all the user feedbacks from the first prototype, the second prototype was developed. The second prototype was found to be the Minimum Viable Product (MVP) as many of the previous flaws have been improved such as the improved depth map and the overhead belt which reduces the weight on the nose bridge. As this is an MVP, further quantitative tests were conducted on the prototype, it was found that the percentage increase in field of vision was maximum at 40% and a minimum of 16.7%. The depth perception test showed a 50% accuracy rate in terms of the number of respondents which participated in the test. The results obtained from this test remain satisfactory as further optimization was possible on the prototype with the selection of components.

With the upgraded components in prototype 3 of the visual aid, and a change of design with a articulating hinge for the camera for added field of vision, tests were conducted as with prototype 2. The results of the tests shows a percentage increase of field of vision with a minimum of 28.6% and a maximum of 100%. The test on the depth perception shows a consistent results of respondents identifying the order of the boxes

correctly every time. This results satisfy the primary objectives of this research which is to provide depth perception and increased field of vision to a monocular visual impaired patient.

A cost analysis was also conducted at the end of each phase of the prototype development. The cost analysis only consists of the material costs. The first prototype costed a total of RM861 while prototype 2 costs RM 728.40 and prototype 3 costing RM714.28. A clear decline is seen in the cost of the visual aid of almost RM 150.00 which also satisfies the third objective of this research which is to develop a cost effective visual aid.

### **5.3 Recommendation**

The visual aid has been developed to aid monocular visual impaired patients. Although it has undergone three phases of development, there is still in many ways where this development process can be continued to improvise the prototype produced.

The prototype can be developed further with custom made PCB boards which will reduce the amount of wiring on the visual aid. The PCB's would also lighten further the weight of the visual aid. Due to financial constraint, this prototype was made with default microprocessors which require additional wiring to assemble the visual aid. The clarity of the image can also be improvised with use of better microprocessors which are currently unavailable in pocket sized unit.

Furthermore, different types of cameras can be used to experiment the field of vision that can be attained by the visual aid. Other types of cameras that can be used are fish eyed lens and 180° wide angle cameras which would result in much better range of vision. These lenses can also achieve further depth, a pair of far ranged ultrasonic sensors can also be used for precise distance indicators.

The cost of the visual aid can also be decreased in the future with more commercialised and high processing pocket sized processors. The sample size of patients

can also be increased further and more promising results as it would cover a much bigger population of monocular visual impaired patients.

This visual aid can also be used in the future for daily used if it, the weight and the clarity of the image is reduced further making it more robust and user friendly. The user interface can also be made to cater all ages for this purpose. The testing procedures can also be made to be more automated by using sensors on the test rig to capture the field of vision, where as currently the results depend on the respondents feedback which might lead to inconsistency if conducted in small sample sizes.

## REFERENCES

- [1] A. Te Broman, B. Munoce, and J. Rodriguez, "The impact of Visual Impairment and Eye Disease on Vision Related Quality of Life in a Mexican American Population," *Clin. Epidemiol. Res.*, vol. 43, pp. 3393–3398, 2002.
- [2] D. Pascolini and S. P. Mariotti, "Global estimates of visual impairment: 2010," *Br. J. Ophthalmol.*, vol. 96, no. 5, pp. 614–618, 2012.
- [3] D. Rahi and D. Jugnoo, "Risk, causes and outcomes of visual impairment after loss of vision in the non amblyopic eye: a population-based study," *The Lancet*, pp. 597–602, 2002.
- [4] T. Adams and J. Slopper, "Update on squint and amblyopia," *J. R. Soc. Med.*, pp. 3–6, 2003.
- [5] J. A. Ebeigbe and C. M. Emedike, "Parents' awareness and perception of children's eye diseases in Nigeria," *J. Optom.*, vol. 10, no. 2, pp. 104–110, 2017.
- [6] M. C. Leske, A. Heijl, M. Hussein, B. Bengtsson, L. Hyman, and E. Komaroff, "Factors for glaucoma progression and the effect of treatment: the early manifest glaucoma trial," *Arch. Ophthalmol.*, vol. 121, no. 1, pp. 48–56, 2003.
- [7] H. A. Quigley, "Number of people with glaucoma worldwide.," *Br. J. Ophthalmol.*, vol. 80, no. 5, pp. 389–393, 1996.
- [8] A. Iwase, Y. Suzuki, M. Araie, T. Yamamoto, and Abe, "The prevalence of primary open-angle glaucoma in Japanese: the Tajimi Study," *Ophthalmology*, vol. 111, no. 9, pp. 1641–1648, 2004.
- [9] H. A. Quigley, "Neuronal death in glaucoma," *Prog. Retin. Eye Res.*, vol. 18, no. 1, pp. 39–57, 1999.
- [10] D. M. Levi and S. A. Klein, "Vernier acuity, crowding and amblyopia," *Vision Res.*, vol. 25, no. 7, pp. 979–991, 1985.
- [11] National Institute for Rehabilitation Engineering, "Visual Distance Perception & Depth Perception," no. C, pp. 1–12, 2004.
- [12] G. S. Rubin, B. Munoz, K. Bandeen–Roche, and S. K. West, "Monocular versus binocular visual acuity as measures of vision impairment and predictors of visual

- disability,” *Invest. Ophthalmol. Vis. Sci.*, vol. 41, no. 11, pp. 3327–3334, 2000.
- [13] K. N. Ogle, “On the limits of stereoscopic vision.,” *J. Exp. Psychol.*, vol. 44, no. 4, p. 253, 1952.
- [14] J. Rodriguez, R. Sanchez, and Munoz, “Causes of blindness and visual impairment in a population-based sample of US Hispanics,” *Ophthalmology*, vol. 109, no. 4, pp. 737–743, 2002.
- [15] J. van Hof-van Duin, G. Cioni, B. Bertuccelli, B. Fazzi, C. Romano, and A. Boldrini, “Visual outcome at 5 years of newborn infants at risk of cerebral visual impairment,” *Dev. Med. Child Neurol.*, vol. 40, no. 5, pp. 302–309, 1998.
- [16] J. L. Ashton and M. S. Wolfe, “Eye patch for treatment of amblyopia.” Google Patents, 03-Dec-2002.
- [17] K. N. Ogle, “Researches in binocular vision.,” *J. Sci.*, vol. 114, no. 2955, p. 191, 1950.
- [18] G. K. Von Noorden and E. C. Campos, *Binocular vision and ocular motility: theory and management of strabismus*, vol. 6. Mosby St. Louis, 2002.
- [19] C. Lang, T. V Nguyen, H. Katti, K. Yadati, M. Kankanhalli, and S. Yan, “Depth matters: Influence of depth cues on visual saliency,” in *European conference on computer vision*, 2012, pp. 101–115.
- [20] I. P. Howard and B. J. Rogers, *Seeing in depth, Vol. 2: Depth perception*. University of Toronto Press, 2002.
- [21] Department of Social Welfare, “Registrations of People with Disabilities,” *Official Portal Department of Social Welfare*, 2016. [Online]. Available: <http://www.jkm.gov.my/jkm/index.php?r=portal/left&id=UnN2U3dtUHhacVN4aHNPbUIPayt2QT09>. [Accessed: 30-Apr-2018].
- [22] P. Kumar SG, “Visual Impairment and Mental Health Outcomes : Lack of Research Output from India,” *Juniper Online J. Public Heal.*, vol. 2, no. 2, pp. 1–2, 2017.
- [23] T. Arumugam, “One in 10 children in Malaysia has an undiagnosed vision problem,” *News Straits Times*, Kuala Lumpur, 05-Mar-2017.
- [24] R. F. Hess and B. Thompson, “Amblyopia and the binocular approach to its therapy,” *Vision Res.*, vol. 114, pp. 4–16, 2015.
- [25] D. M. Levi, D. C. Knill, and D. Bavelier, “Stereopsis and amblyopia: A mini-

- review,” *Vision Res.*, vol. 114, pp. 17–30, 2015.
- [26] Z. Cattaneo, L. B. Merabet, E. Bhatt, and T. Vecchi, “Effects of complete monocular deprivation in visuo-spatial memory,” *Brain Res. Bull.*, vol. 77, no. 2–3, pp. 112–116, 2008.
- [27] N. W. Daw, “Critical periods and amblyopia,” *Arch. Ophthalmol.*, vol. 116, no. 4, pp. 502–505, 1998.
- [28] R. Sireteanu, M. Fronius, and W. Singer, “Binocular interaction in the peripheral visual field of humans with strabismic and anisometropic amblyopia,” *Vision Res.*, vol. 21, no. 7, pp. 1065–1074, 1981.
- [29] E. Birch, C. Williams, J. Drover, V. Fu, C. Cheng, and Northstone, “Randot® preschool stereoacuity test: normative data and validity,” *J. Am. Assoc. Pediatr. Ophthalmol. Strabismus*, vol. 12, no. 1, pp. 23–26, 2008.
- [30] K. Simons, “A comparison of the Frisby, Random-Dot E, TNO, and Randot circles stereotests in screening and office use,” *Arch. Ophthalmol.*, vol. 99, no. 3, pp. 446–452, 1981.
- [31] M. Schornack and S. O.D, “Prescription and management of contact lenses in patients with monocular visual impairment,” *Optom. J. Am. Optom. Assoc.*, vol. 78, no. 12, pp. 652–656, 2007.
- [32] Y. Chiba, “Bias analysis of the instrumental variable estimator as an estimator of the average causal effect,” *Contemp. Clin. Trials*, vol. 31, no. 1, pp. 12–17, 2010.
- [33] M. X. Repka *et al.*, “Monocular Oral Reading Performance After Amblyopia Treatment in Children,” *Am. J. Ophthalmol.*, vol. 146, no. 6, pp. 942–947, 2008.
- [34] X. Y. Liu and J. Y. Zhang, “Dichoptic training in adults with amblyopia: Additional stereoacuity gains over monocular training,” *Vision Res.*, 2016.
- [35] D. Moganeswari, J. Thomas, K. Srinivasan, and G. P. Jacob, “Test re-test reliability and validity of different visual acuity and stereoacuity charts used in preschool children,” *J. Clin. diagnostic Res. JCDR*, vol. 9, no. 11, p. NC01, 2015.
- [36] S. S. Bhatlawande, J. Mukhopadhyay, and M. Mahadevappa, “Ultrasonic spectacles and waist-belt for visually impaired and blind person,” *2012 Natl. Conf. Commun. NCC 2012*, pp. 8–11, 2012.
- [37] J. B. Peatman, *Design with PIC microcontrollers*. Prentice Hall Englewood Cliffs,

NJ, 1998.

- [38] A. Helal, S. E. Moore, and B. Ramachandran, “Drishti: an integrated navigation system for visually impaired and disabled,” *Fifth Int. Symp. Wearable Comput.*, no. 45, pp. 149–156, 2001.
- [39] N. Molton, S. Se, J. M. Brady, D. Lee, and P. Probert, “A stereo vision-based aid for the visually impaired,” *Image Vis. Comput.*, vol. 16, no. 4, pp. 251–263, 1998.
- [40] M. Cabatuan, E. Dadios, L. Gan Lim, R. K. Billones, and V. I. Carandang, “Feature Driven Development of a Smartphone Based Vision-Aware mHealth Framework,” *Adv. Sci. Lett.*, vol. 12, no. 10, pp. 2762–2769, 2015.
- [41] A. Canessa, M. Chessa, A. Gibaldi, S. P. Sabatini, and F. Solari, “Calibrated depth and color cameras for accurate 3D interaction in a stereoscopic augmented reality environment,” *J. Vis. Commun. Image Represent.*, vol. 25, no. 1, pp. 227–237, 2014.
- [42] D. Zhang, V. Nourrit, and J. L. de Bougrenet de la Tocnaye, “3D visual comfort assessment by measuring the vertical disparity tolerance,” *Displays*, vol. 50, pp. 7–13, 2017.
- [43] Q. Jiang, F. Shao, G. Jiang, M. Yu, Z. Peng, and C. Yu, “A depth perception and visual comfort guided computational model for stereoscopic 3D visual saliency,” *Signal Process. Image Commun.*, vol. 38, pp. 57–69, 2015.
- [44] K. Li, Q. Wang, J. Wu, H. Yu, and D. Zhang, “Calibration error for dual-camera digital image correlation at microscale,” *Opt. Lasers Eng.*, vol. 50, no. 7, pp. 971–975, 2012.
- [45] D. R. Watts, K. L. Tracey, and A. I. Friedlander, “Producing accurate maps of the Gulf Stream thermal front using objective analysis,” *J. Geophys. Res. Ocean.*, vol. 94, no. C6, pp. 8040–8052, 1989.
- [46] M. J. Marín-Jiménez, F. J. Romero-Ramirez, R. Muñoz-Salinas, and R. Medina-Carnicer, “3D human pose estimation from depth maps using a deep combination of poses,” *J. Vis. Commun. Image Represent.*, vol. 55, no. January, pp. 627–639, 2018.
- [47] Y. LeCun, Y. Bengio, and G. Hinton, “Deep learning,” *Nature*, vol. 521, no. 7553, p. 436, 2015.

- [48] S. W. Han, O. Kwon, and L. Lee, “Evaluation of the seismic performance of a three-story ordinary moment-resisting concrete frame,” *Earthq. Eng. Struct. Dyn.*, vol. 33, no. 6, pp. 669–685, 2004.
- [49] M. G. Park and K. J. Yoon, “As-planar-as-possible depth map estimation,” *Comput. Vis. Image Underst.*, vol. 181, no. January, pp. 50–59, 2019.
- [50] P. K. Lai, W. Liang, and R. Laganière, “Additive depth maps, a compact approach for shape completion of single view depth maps,” *Graph. Models*, vol. 104, no. September 2018, p. 101030, 2019.
- [51] O. Krutikova, A. Sisojevs, and M. Kovalovs, “Creation of a Depth Map from Stereo Images of Faces for 3D Model Reconstruction,” *Procedia Comput. Sci.*, vol. 104, no. December 2016, pp. 452–459, 2016.
- [52] D. Lee, Y. Yang, and B. T. Oh, “Pre-/post-processing to improve the coding performance of multiview plus depth map,” *Signal Process. Image Commun.*, vol. 58, no. June, pp. 56–64, 2017.
- [53] C. Yang, P. An, L. Shen, R. Ma, and N. Feng, “Fast depth map coding based on virtual view quality,” *Signal Process. Image Commun.*, vol. 47, pp. 183–192, 2016.
- [54] M. Čadík, D. Sýkora, and S. Lee, “Automated outdoor depth-map generation and alignment,” *Comput. Graph.*, vol. 74, pp. 109–118, 2018.
- [55] R. McNaney, J. Vines, D. Roggen, and M. Balaam, “Exploring the acceptability of google glass as an everyday assistive device for people with parkinson’s,” in *Proceedings of the sigchi conference on human factors in computing systems*, 2014, pp. 2551–2554.
- [56] K. Hoffman and Munchen, “Binocular optical device, in particular electronic spectacles, comprising an electronic camera for automatically setting a focus that includes the correction of different vision defects,” US 2004O1 20035A1, 2004.
- [57] T. L. Brady, “Combined spectacle frame and light,” 2638532, 1953.
- [58] T. Li, D. Thelen, J. A. Martin, S. M. Allen, and S. SA, “Information display device assembled with spectacle frame,” US 20040096078A1, 2004.
- [59] S. Heo, J. Cha, and C. G. Park, “Monocular Visual Inertial Navigation for Mobile Robots using Uncertainty based Triangulation,” *IFAC-PapersOnLine*, vol. 50, no. 1, pp. 2217–2222, 2017.

- [60] M. Kim, K. W. Jang, W. J. Yoo, and B. Lee, “Development of a flexible variable-view angioscopy system using face-angled GRIN lenses to enhance field of vision,” *Sensors Actuators, A Phys.*, vol. 263, pp. 259–263, 2017.
- [61] W. Sankowski, M. Włodarczyk, D. Kacperski, and K. Grabowski, “Estimation of measurement uncertainty in stereo vision system,” *Image Vis. Comput.*, vol. 61, pp. 70–81, 2017.
- [62] R. T. Jose, *Understanding low vision*. American Foundation for the Blind, 1983.
- [63] B. E. K. Klein, R. Klein, W. E. Sponsel, and T. Franke, “Prevalence of glaucoma: the Beaver Dam eye study,” *Ophthalmology*, vol. 99, no. 10, pp. 1499–1504, 1992.
- [64] J. R. Hauser and D. Clausing, “The house of quality,” *Harv. Bus. Rev.*, vol. 5, no. May, p. 291, 1988.
- [65] B. P. Weidema, “Multi-user test of the data quality matrix for product life cycle inventory data,” *Int. J. Life Cycle Assess.*, vol. 3, no. 5, pp. 259–265, 1998.
- [66] S. Owre, J. M. Rushby, and N. Shankar, “PVS: A prototype verification system,” in *International Conference on Automated Deduction*, 1992, pp. 748–752.
- [67] P. Didyk, T. Ritschel, E. Eisemann, K. Myszkowski, and H.-P. Seidel, “Adaptive Image-space Stereo View Synthesis.,” in *VMV*, 2010, no. 1, 2, pp. 299–306.
- [68] R. Barnes, N. King, and P. King, “Raspberry Pi Model B.” Raspberry Pi Trading Ltd, pp. 1–244, 2015.
- [69] V. Vujović and M. Maksimović, “Raspberry Pi as a Sensor Web node for home automation,” *Comput. Electr. Eng.*, vol. 44, pp. 153–171, 2015.
- [70] E. Upton and G. Halfacree, *Raspberry Pi user guide*. John Wiley & Sons, 2014.
- [71] M. Richardson and S. Wallace, *Getting started with raspberry PI*. “O’Reilly Media, Inc.,” 2012.
- [72] M. Maksimović, V. Vujović, N. Davidović, V. Milošević, and B. Perišić, “Raspberry Pi as Internet of things hardware: performances and constraints,” *Des. issues*, vol. 3, no. 8, 2014.
- [73] R. M. Mondor, J. M. Lewis, and S. A. Berke, “Configurable IO subsystem.” Google Patents, 01-Jan-2008.
- [74] I. O. Ogunniyi and M. K. G. Vermaak, “Investigation of froth flotation for beneficiation of printed circuit board comminution fines,” *Miner. Eng.*, vol. 22, no.

- 4, pp. 378–385, 2009.
- [75] A. M. Mohsen, “Field programmable printed circuit board.” Google Patents, 27-Dec-1994.
- [76] M. Wang, Z. Zhang, and G. Wang, “Feasibility Analysis of Baseband Board Based on Field-Programmable Gate Array,” in *Proceedings of the 2019 5th International Conference on Computer and Technology Applications*, 2019, pp. 145–148.
- [77] Waveshare, “Waveshare Compute Module IO board,” 2019. [Online]. Available: <https://www.waveshare.com/compute-module-io-board-plus.htm>. [Accessed: 26-Jun-2019].
- [78] H. Wang, X. I. A. Liming, J. Feng, Q. Wang, N. Qu, and Z. Chen, “Information transmitting method and apparatus in robot operating system.” Google Patents, 19-Feb-2019.
- [79] M. Cashmore, M. Fox, D. Long, and D. Magazzeni, “Rosplan: Planning in the robot operating system,” in *Twenty-Fifth International Conference on Automated Planning and Scheduling*, 2015.
- [80] D. Rosenfeld, Y. Rudich, and R. Lahav, “Desert dust suppressing precipitation: A possible desertification feedback loop,” *Proc. Natl. Acad. Sci.*, vol. 98, no. 11, pp. 5975–5980, 2001.
- [81] M. Quigley, K. Conley, B. Gerkey, J. Faust, T. Foote, and J. Leibs, “ROS: an open-source Robot Operating System,” in *ICRA workshop on open source software*, 2009, vol. 3, no. 3.2, p. 5.
- [82] G. Walsh, “The weight of spectacle frames and the area of their nose pads,” *Ophthalmic Physiol. Opt.*, vol. 30, no. 4, pp. 402–404, 2010.
- [83] T. Tsukada, “State-of-the art of a-Si TFT/LCD,” *Electron. Commun. Japan (Part II Electron.)*, vol. 77, no. 7, pp. 38–45, 1994.
- [84] B. Wittbrodt and J. M. Pearce, “The effects of PLA color on material properties of 3-D printed components,” *Addit. Manuf.*, vol. 8, pp. 110–116, 2015.
- [85] R. Scaffaro, A. Maio, E. F. Gulino, and B. Megna, “Structure-property relationship of PLA-Opuntia Ficus Indica biocomposites,” *Compos. Part B Eng.*, vol. 167, no. December 2018, pp. 199–206, 2019.
- [86] M. G. Aruan Efendy and K. L. Pickering, “Comparison of strength and Young

- modulus of aligned discontinuous fibre PLA composites obtained experimentally and from theoretical prediction models,” *Compos. Struct.*, vol. 208, no. October 2018, pp. 566–573, 2019.
- [87] K. Behera, V. Sivanjineyulu, Y. H. Chang, and F. C. Chiu, “Thermal properties, phase morphology and stability of biodegradable PLA/PBSL/HAp composites,” *Polym. Degrad. Stab.*, vol. 154, pp. 248–260, 2018.
- [88] W. Harrington, *Learning Raspbian*, 1st ed. Birmingham: Packt Publishing Ltd, 2015.
- [89] R. Laganière, *OpenCV Computer Vision Application Programming Cookbook Second Edition*. California, United States of America: Packt Publishing Ltd, 2014.
- [90] G. Bradski and A. Kaehler, *Learning OpenCV: Computer vision with the OpenCV library*. “O’Reilly Media, Inc.,” 2008.
- [91] J.-J. Aguilar, F. Torres, and M. A. Lope, “Stereo vision for 3D measurement: accuracy analysis, calibration and industrial applications,” *Measurement*, vol. 18, no. 4, pp. 193–200, 1996.
- [92] A. Masood, “Stereo Pi: DIY Digital Stereo Camera,” *Digital Media Corporation*, 2018. .
- [93] W. S. Harlan, “Regularization by model reparameterization,” *Citeseer*, 1995.
- [94] Y. Asiedu and P. Gu, “Product life cycle cost analysis: state of the art review,” *Int. J. Prod. Res.*, vol. 36, no. 4, pp. 883–908, 1998.
- [95] E. M. Gramlich and E. M. Gramlich, *A guide to benefit-cost analysis*. Prentice-Hall Englewood Cliffs, NJ, 1990.
- [96] M. M. Mokhtar, M. A. Khairul Anuar, I. H. Aminudin, and S. N. Mohamed Azlan, “Financial Behaviour and State of Financial Well-being of Malaysian Working Adults,” Kuala Lumpur, 2018.
- [97] S. Wild, G. Roglic, A. Green, R. Sicree, and H. King, “Global prevalence of diabetes: estimates for the year 2000 and projections for 2030,” *Diabetes Care*, vol. 27, no. 5, pp. 1047–1053, 2004.
- [98] Z. Hussein, S. W. Taher, H. K. Gilcharan Singh, W. Chee Siew Swee, A. Mohamed, and C. Yang, “Diabetes Care in Malaysia: Problems, New Models, and Solutions,” *Ann. Glob. Heal.*, vol. 49, no. 5, pp. 851–862, 2015.

- [99] D. S. Fong, L. Aiello, and T. W. Gardner, "Retinopathy in diabetes," *Diabetes Care*, vol. 27, no. suppl 1, pp. s84–s87, 2004.
- [100] J. H. Kempen, B. J. O'Colmain, M. C. Leske, and S. M. Haffner, "The prevalence of diabetic retinopathy among adults in the United States.," *Arch. Ophthalmol. (Chicago, Ill. 1960)*, vol. 122, no. 4, pp. 552–563, 2004.

**APPENDIX A**  
**INTERVIEW QUESTIONS (Patient)**

**Respondent Details**

1. What is your name?
2. How old are you?

**Impairment details**

1. What is the type of monocular visual impairment that you're facing?
2. How many years are you facing this impairment?
3. What is the type of treatment that you're undergoing now?
4. What are the challenges that you face daily due to this impairment?

**Visual Aid**

1. Any visual aid used? If, yes what it is and how does it aid?
2. If a visual aid was developed for monocular visual impaired patients, what do you expect from the visual aid?

## **APPENDIX B**

### **INTERVIEW QUESTIONS (Medical Professional)**

#### **Respondent Details**

1. What is your name?
2. How old are you?

#### **Impairment details**

1. What is Monocular Visual Impairment?
2. What is the prevalence monocular visual impairment for a hyperglycaemic patient?
3. What is the type of treatment available for this type of patients?
4. What are the challenges faced by monocular visual impaired patients?

#### **Visual Aid**

1. If a visual aid was developed for monocular visual impaired patients, what do you expect from the visual aid?

## APPENDIX C

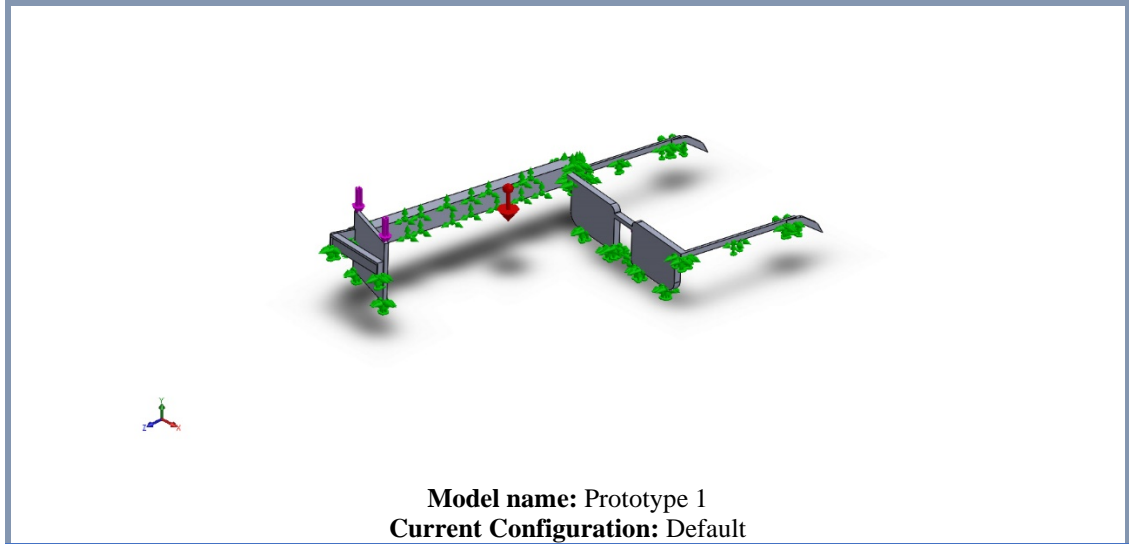
### DETAILED INTERFACE of THE WAVESHARE COMPUTE MODULE IO BOARD

No	Name	Function
1	<b>Compute Module interface:</b>	for connecting Compute Module (CM3 / CM3L / CM3+ / CM3+L)
2	<b>Compute Module GPIO header</b>	breakout all the Compute Module pins
3	<b>Raspberry Pi GPIO header</b>	for connecting Raspberry Pi HATs
4	<b>CSI interface</b>	camera ports, for connecting Raspberry Pi Camera
5	<b>DSI interface</b>	display ports, for connecting Raspberry Pi LCD
6	<b>HDMI Port</b>	
7	<b>USB ports</b>	for connecting USB devices
8	<b>USB SLAVE interface</b>	allows you to burn system image in to Compute Module 3
9	<b>USB TO UART interface</b>	for serial debugging
10	<b>Arduino header</b>	for connecting Arduino shields
11	<b>AD/DA input/output screw terminals</b>	
12	<b>1-WIRE interface</b>	for connecting single-bus devices like DS18B20
13	<b>Sensor interface</b>	
14	<b>Power port</b>	5V 2.5A
15	<b>FE1.1S</b>	USB HUB chip
16	<b>12MHz crystal</b>	

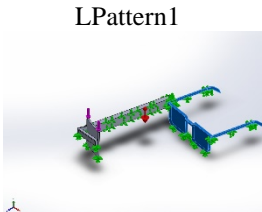
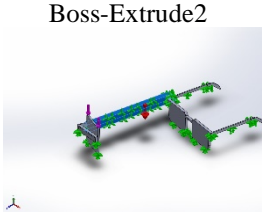
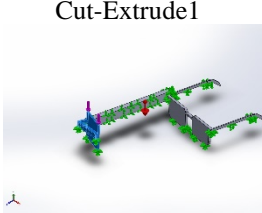
<b>17 CP2102</b>	USB TO UART converter
<b>18 Micro SD card slot</b>	insert a Micro SD card with pre-burnt system, to start up Compute Module 3 Lite
<b>19 TLC1543</b>	AD converter
<b>20 DAC8552</b>	16-bit DAC, 2-ch
<b>21 DS3231</b>	high-precision RTC chip, I2C interface
<b>22 RTC battery holder</b>	supports CR1220 batteries
<b>23 Voltage Regulator</b>	3.3V / 2.5V / 1.8V
<b>24 LFN0038K</b>	IR receiver
<b>25 Buzzer</b>	
<b>26 Power indicator</b>	
<b>27 ACT indicator</b>	indicating the Micro SD card status
<b>28 User LEDs</b>	
<b>29 User Keys</b>	
<b>30 BOOT selection</b>	<ul style="list-style-type: none"> <li>a. EN: enable the PC to access SD card/eMMC through USB SLAVE</li> <li>b. DIS: the Compute Module will boot from SD card/eMMC</li> </ul>
<b>31 VGx power selection</b>	config the I/O level
<b>32 USB HUB enable jumper</b>	HUB enable and USB SLAVE power selection
<b>33 ADC/DAC configuration</b>	config the power supply and reference voltage of ADC/DAC
<b>34 Peripheral configuration</b>	config the control pins of UART, user keys, user LEDs, 1-WIRE interface, IR receiver, and buzzer
<b>35 Arduino AD selection</b>	<ul style="list-style-type: none"> <li>a. connect 1 and 2: Arduino A0-A5 as digital control pin</li> <li>b. connect 2 and 3: Arduino A0-A5 as AD input</li> </ul>

## APPENDIX D

### PRESET STUDY OF PROTOTYPE 1



#### Solid Bodies

Document Name and Reference	Treated As	Volumetric Properties	Document Path/Date Modified
 LPattern1	Solid Body	Mass:0.0245175 kg Volume:2.29136e-05 m <sup>3</sup> Density:1070 kg/m <sup>3</sup> Weight:0.240272 N	C:\Users\Cpt.Nirvenesh\Desktop\Spectacle Frame\Results\Prototype 1\GLASS.SLDPRT Jun 25 23:40:39 2019
 Boss-Extrude2	Solid Body	Mass:0.0390764 kg Volume:3.12751e-05 m <sup>3</sup> Density:1249.44 kg/m <sup>3</sup> Weight:0.382948 N	C:\Users\Cpt.Nirvenesh\Desktop\Spectacle Frame\Results\Prototype 1\Part1 - Copy.SLDPRT Apr 20 19:51:53 2019
 Cut-Extrude1	Solid Body	Mass:0.0136803 kg Volume:1.09492e-05 m <sup>3</sup> Density:1249.44 kg/m <sup>3</sup> Weight:0.134067 N	C:\Users\Cpt.Nirvenesh\Desktop\Spectacle Frame\Results\Prototype 1\Part2.SLDPRT Apr 20 14:42:32 2019

## Study Properties

<b>Study name</b>	Static 1
<b>Analysis type</b>	Static
<b>Mesh type</b>	Solid Mesh
<b>Thermal Effect:</b>	On
<b>Thermal option</b>	Include temperature loads
<b>Zero strain temperature</b>	298 Kelvin
<b>Include fluid pressure effects from SOLIDWORKS Flow Simulation</b>	Off
<b>Solver type</b>	FFEPlus
<b>Inplane Effect:</b>	Off
<b>Soft Spring:</b>	Off
<b>Inertial Relief:</b>	Off
<b>Incompatible bonding options</b>	Automatic
<b>Large displacement</b>	Off
<b>Compute free body forces</b>	On
<b>Friction</b>	Off
<b>Use Adaptive Method:</b>	Off
<b>Result folder</b>	SOLIDWORKS document (C:\Users\Cpt.Nirvenesh\Desktop\Spectacle Frame\Results\Prototype 1)

## Units

<b>Unit system:</b>	SI (MKS)
<b>Length/Displacement</b>	mm
<b>Temperature</b>	Kelvin
<b>Angular velocity</b>	Rad/sec
<b>Pressure/Stress</b>	N/m <sup>2</sup>

## Mesh information

<b>Mesh type</b>	Solid Mesh
<b>Mesher Used:</b>	Standard mesh
<b>Automatic Transition:</b>	Off
<b>Include Mesh Auto Loops:</b>	Off
<b>Jacobian points</b>	4 Points
<b>Element Size</b>	4.02497 mm
<b>Tolerance</b>	0.201249 mm
<b>Mesh Quality Plot</b>	High
<b>Remesh failed parts with incompatible mesh</b>	Off

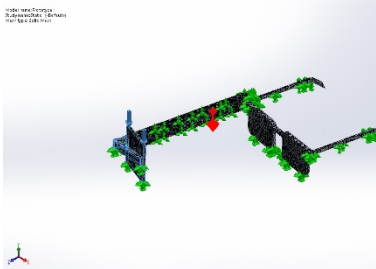
## Mesh information - Details

<b>Total Nodes</b>	89780
<b>Total Elements</b>	56263
<b>Maximum Aspect Ratio</b>	213.87
<b>% of elements with Aspect Ratio &lt; 3</b>	98.9
<b>% of elements with Aspect Ratio &gt; 10</b>	0.0942
<b>% of distorted elements(Jacobian)</b>	0
<b>Time to complete mesh(hh:mm:ss):</b>	00:00:03
<b>Computer name:</b>	NIRVENESH-PC



Mesh Control Information:

Mesh Control Name	Mesh Control Image	Mesh Control Details
Control-1		<b>Entities:</b> 1 Solid Body (s) <b>Units:</b> mm <b>Size:</b> 2.91802 <b>Ratio:</b> 1.5
Control-2		<b>Entities:</b> 1 Solid Body (s) <b>Units:</b> mm <b>Size:</b> 2.01243 <b>Ratio:</b> 1.5

Control-3		<b>Entities:</b> 1 Solid Body (s) <b>Units:</b> mm <b>Size:</b> 2.86771 <b>Ratio:</b> 1.5
-----------	--	---

### Sensor Details

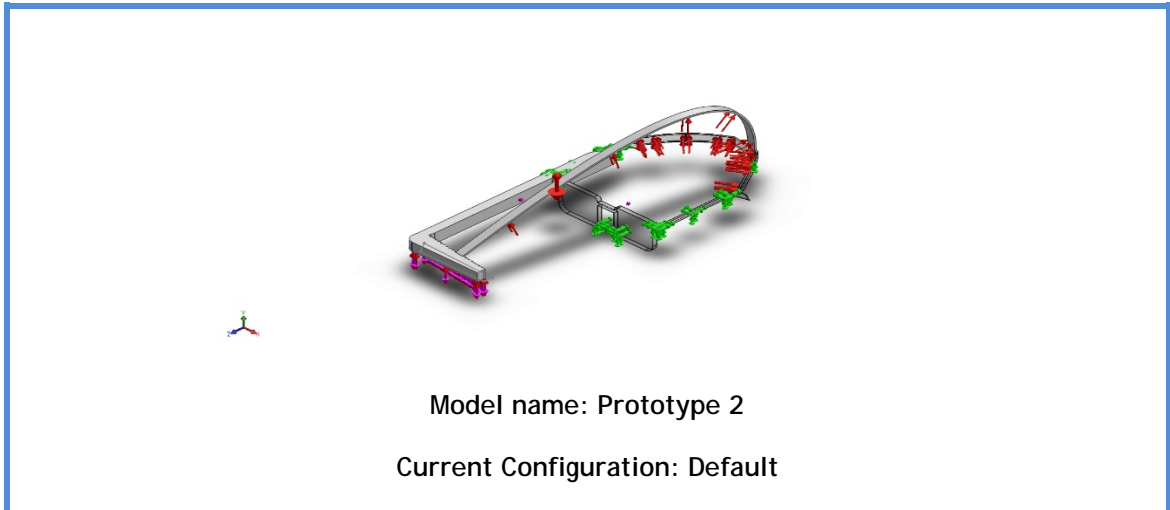
No Data

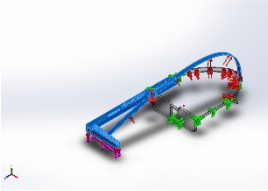
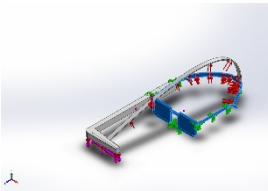
### Resultant Forces

Reaction forces

Selection set	Units	Sum X	Sum Y	Sum Z	Resultant
Entire Model	N	-0.006932	1.23749	-0.022406	1.23771

**APPENDIX E**  
**PRESET STUDY OF PROTOTYPE 2**



Solid Bodies			
Document Name and Reference	Treated As	Volumetric Properties	Document Path/Date Modified
Extrude-Thin1 	Solid Body	Mass:0.0688379 kg Volume:5.47075e-05 m <sup>3</sup> Density:1258.29 kg/m <sup>3</sup> Weight:0.674612 N	C:\Users\Cpt.Nirvenesh\Desktop\Spectacle Frame\Results\Prototype 2\By Nirvenesh.SLDPRT Jun 26 00:29:33 2019
Extrude-Thin3 	Solid Body	Mass:0.0286948 kg Volume:2.68175e-05 m <sup>3</sup> Density:1070 kg/m <sup>3</sup> Weight:0.281209 N	C:\Users\Cpt.Nirvenesh\Desktop\Spectacle Frame\Results\Prototype 2\GLASS.SLDPRT Jun 26 00:32:28 2019

## Study Properties

<b>Study name</b>	Static 1
<b>Analysis type</b>	Static
<b>Mesh type</b>	Solid Mesh
<b>Thermal Effect:</b>	On
<b>Thermal option</b>	Include temperature loads
<b>Zero strain temperature</b>	298 Kelvin
<b>Include fluid pressure effects from SOLIDWORKS Flow Simulation</b>	Off
<b>Solver type</b>	FFEPlus
<b>Inplane Effect:</b>	Off
<b>Soft Spring:</b>	Off
<b>Inertial Relief:</b>	Off
<b>Incompatible bonding options</b>	Automatic
<b>Large displacement</b>	On
<b>Compute free body forces</b>	On
<b>Friction</b>	Off
<b>Use Adaptive Method:</b>	Off
<b>Result folder</b>	SOLIDWORKS document (C:\Users\Cpt.Nirvenesh\Desktop\Spectacle Frame\Results\Prototype 2)

## Units

<b>Unit system:</b>	SI (MKS)
<b>Length/Displacement</b>	mm
<b>Temperature</b>	Kelvin
<b>Angular velocity</b>	Rad/sec
<b>Pressure/Stress</b>	N/m <sup>2</sup>

Mesh information

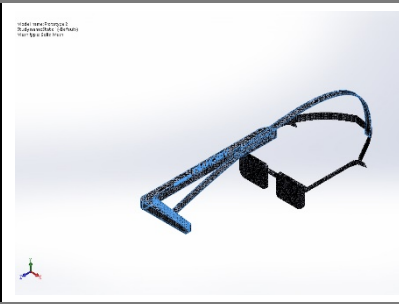
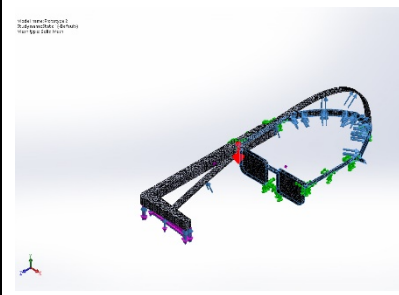
<b>Mesh type</b>	Solid Mesh
<b>Mesher Used:</b>	Standard mesh
<b>Automatic Transition:</b>	Off
<b>Include Mesh Auto Loops:</b>	Off
<b>Jacobian points</b>	4 Points
<b>Element Size</b>	4.65641 mm
<b>Tolerance</b>	0.232821 mm
<b>Mesh Quality Plot</b>	High
<b>Remesh failed parts with incompatible mesh</b>	Off

Mesh information - Details

<b>Total Nodes</b>	87189
<b>Total Elements</b>	50762
<b>Maximum Aspect Ratio</b>	77.519
<b>% of elements with Aspect Ratio &lt; 3</b>	94.5
<b>% of elements with Aspect Ratio &gt; 10</b>	0.201
<b>% of distorted elements(Jacobian)</b>	0
<b>Time to complete mesh(hh:mm:ss):</b>	00:00:04
<b>Computer name:</b>	NIRVENESH-PC



Mesh Control Information:

Mesh Control Name	Mesh Control Image	Mesh Control Details
Control-1		<b>Entities: 1 Solid Body</b> <b>(s)</b> <b>Units: mm</b> <b>Size: 3.60875</b> <b>Ratio: 1.5</b>
Control-2		<b>Entities: 1 Solid Body</b> <b>(s)</b> <b>Units: mm</b> <b>Size: 2.27073</b> <b>Ratio: 1.5</b>

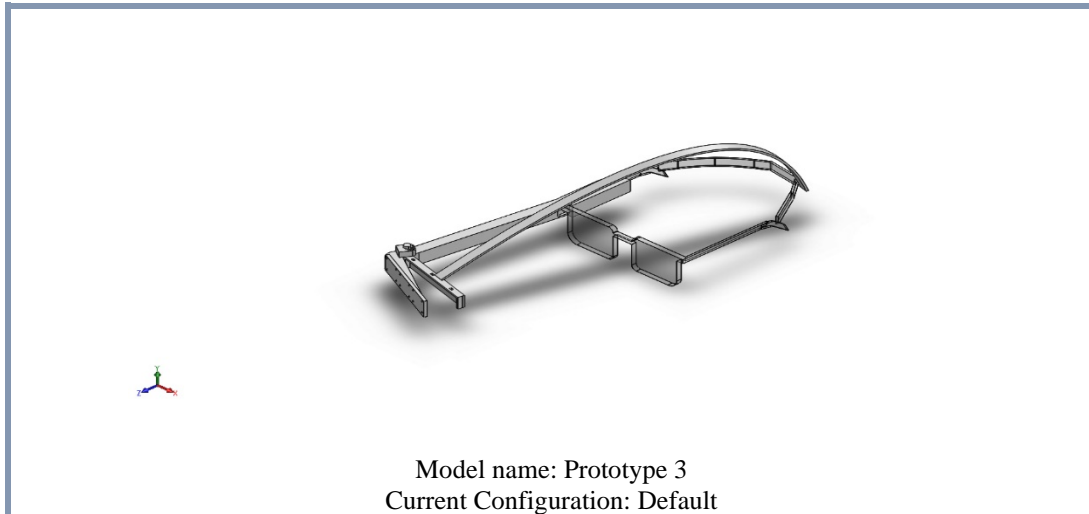
Resultant Forces

Reaction forces

Selection set	Units	Sum X	Sum Y	Sum Z	Resultant
Entire Model	N	-0.000124954	1.42847	0.00165574	1.42847

Reaction Moments

**APPENDIX F**  
**PRESET STUDY OF PROTOTYPE 3**



**Solid Bodies**

Document Name and Reference	Treated As	Volumetric Properties	Document Path/Date Modified
 Cut-Extrude20	Solid Body	Mass:0.0112777 kg Volume:9.02622e-06 m <sup>3</sup> Density:1249.44 kg/m <sup>3</sup> Weight:0.110522 N	C:\Users\Cpt.Nirvenesh\Desktop\Spectacle Frame\Results\Prototype 3\Front New.SLDPRT Jun 19 21:02:59 2019
 Extrude-Thin3	Solid Body	Mass:0.0286948 kg Volume:2.68175e-05 m <sup>3</sup> Density:1070 kg/m <sup>3</sup> Weight:0.281209 N	C:\Users\Cpt.Nirvenesh\Desktop\Spectacle Frame\Results\Prototype 3\GLASS.SLDPRT Jun 26 00:32:28 2019
 Extrude-Thin3	Solid Body	Mass:0.0593382 kg Volume:4.74891e-05 m <sup>3</sup> Density:1249.51 kg/m <sup>3</sup> Weight:0.581514 N	C:\Users\Cpt.Nirvenesh\Desktop\Spectacle Frame\Results\Prototype 3\New1.SLDPRT Jun 25 14:54:40 2019

## Study Properties

<b>Study name</b>	Static 1
<b>Analysis type</b>	Static
<b>Mesh type</b>	Solid Mesh
<b>Thermal Effect:</b>	On
<b>Thermal option</b>	Include temperature loads
<b>Zero strain temperature</b>	298 Kelvin
<b>Include fluid pressure effects from SOLIDWORKS Flow Simulation</b>	Off
<b>Solver type</b>	FFEPlus
<b>Inplane Effect:</b>	Off
<b>Soft Spring:</b>	Off
<b>Inertial Relief:</b>	Off
<b>Incompatible bonding options</b>	Automatic
<b>Large displacement</b>	Off
<b>Compute free body forces</b>	On
<b>Friction</b>	Off
<b>Use Adaptive Method:</b>	Off
<b>Result folder</b>	SOLIDWORKS document (C:\Users\Cpt.Nirvenesh\Desktop\Spectacle Frame\Results\Prototype 3)

## Units

<b>Unit system:</b>	SI (MKS)
<b>Length/Displacement</b>	mm
<b>Temperature</b>	Kelvin
<b>Angular velocity</b>	Rad/sec
<b>Pressure/Stress</b>	N/m <sup>2</sup>

Mesh information

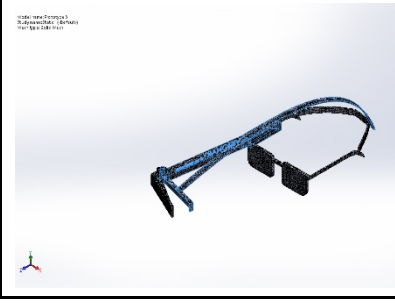
<b>Mesh type</b>	Solid Mesh
<b>Mesher Used:</b>	Standard mesh
<b>Automatic Transition:</b>	Off
<b>Include Mesh Auto Loops:</b>	Off
<b>Jacobian points</b>	4 Points
<b>Element Size</b>	9.24482 mm
<b>Tolerance</b>	1.84896 mm
<b>Mesh Quality Plot</b>	High
<b>Remesh failed parts with incompatible mesh</b>	Off

Mesh information - Details

<b>Total Nodes</b>	79630
<b>Total Elements</b>	45245
<b>Maximum Aspect Ratio</b>	841.7
<b>% of elements with Aspect Ratio &lt; 3</b>	91
<b>% of elements with Aspect Ratio &gt; 10</b>	1.01
<b>% of distorted elements(Jacobian)</b>	0
<b>Time to complete mesh(hh:mm:ss):</b>	00:00:06
<b>Computer name:</b>	NIRVENESH-PC



Mesh Control Information:

Mesh Control Name	Mesh Control Image	Mesh Control Details
Control-1		<b>Entities: 1 Solid Body (s)</b> <b>Units: mm</b> <b>Size: 2.65789</b> <b>Ratio: 1.5</b>
Control-2		<b>Entities: 1 Solid Body (s)</b> <b>Units: mm</b> <b>Size: 3.06235</b> <b>Ratio: 1.5</b>
Control-3		<b>Entities: 1 Solid Body (s)</b> <b>Units: mm</b> <b>Size: 3.00457</b> <b>Ratio: 1.5</b>

Resultant Forces

Reaction forces

Selection set	Units	Sum X	Sum Y	Sum Z	Resultant
Entire Model	N	-8.22915e-05	1.45091	0.00127087	1.45091





## APPENDIX H

### FEEDBACK FORMS

 <b>YUSGAM CANGELOR</b>	<b>Feedback Analysis of Visual Aid for Monocular Visual Impaired Patients</b>
<i>Funded by : YCU UNITEN</i>	
<b>Name :</b>	<b>Dr Ahmad Shamsuri Muhamad</b>
<b>Organisation:</b>	<b>Society of Blind Malaysia</b>
<b>Position:</b>	<b>Senior Member Society of Blind Malaysia (SBM)</b>
<b>Date :</b>	
<b>How is the visual aid Beneficial to your organization?</b>	<p>Being a visually impaired or blind myself, I think this prototype would help a lot of monocular visually impaired patients out there. We have a lot of monocular visually impaired patients in our organization and most of them find this visual aid to be useful as most of them have experienced this visual impairment from trauma</p>
<b>Does the visual aid meet the expectations of the subjects at your organization? (Comments)</b>	<p>The visual aid has clearly met its objectives, as subjects themselves feel very pleased especially with the field of vision which has drastically improved with the visual aid</p>
<b>Recommendation and Comments</b>	<p>The visual is light and comfortable compared to its earlier versions of it. A recommendation would be to commercialize it soon</p>

**Signature** 

**(Ahmad Shamsuri Muhamad)**  
Pertubuhan Orang Cacat Penglihatan Malaysia  
Society of Blind Malaysia (SBM)  
(ROS368/51)  
24, Jalan Tun Sambanthan 3,  
Brickfields, 50470 Kuala Lumpur,  
Malaysia.



**Feedback Analysis of Visual Aid for Monocular Visual Impaired Patients**

Funded by : YCU UNITEN

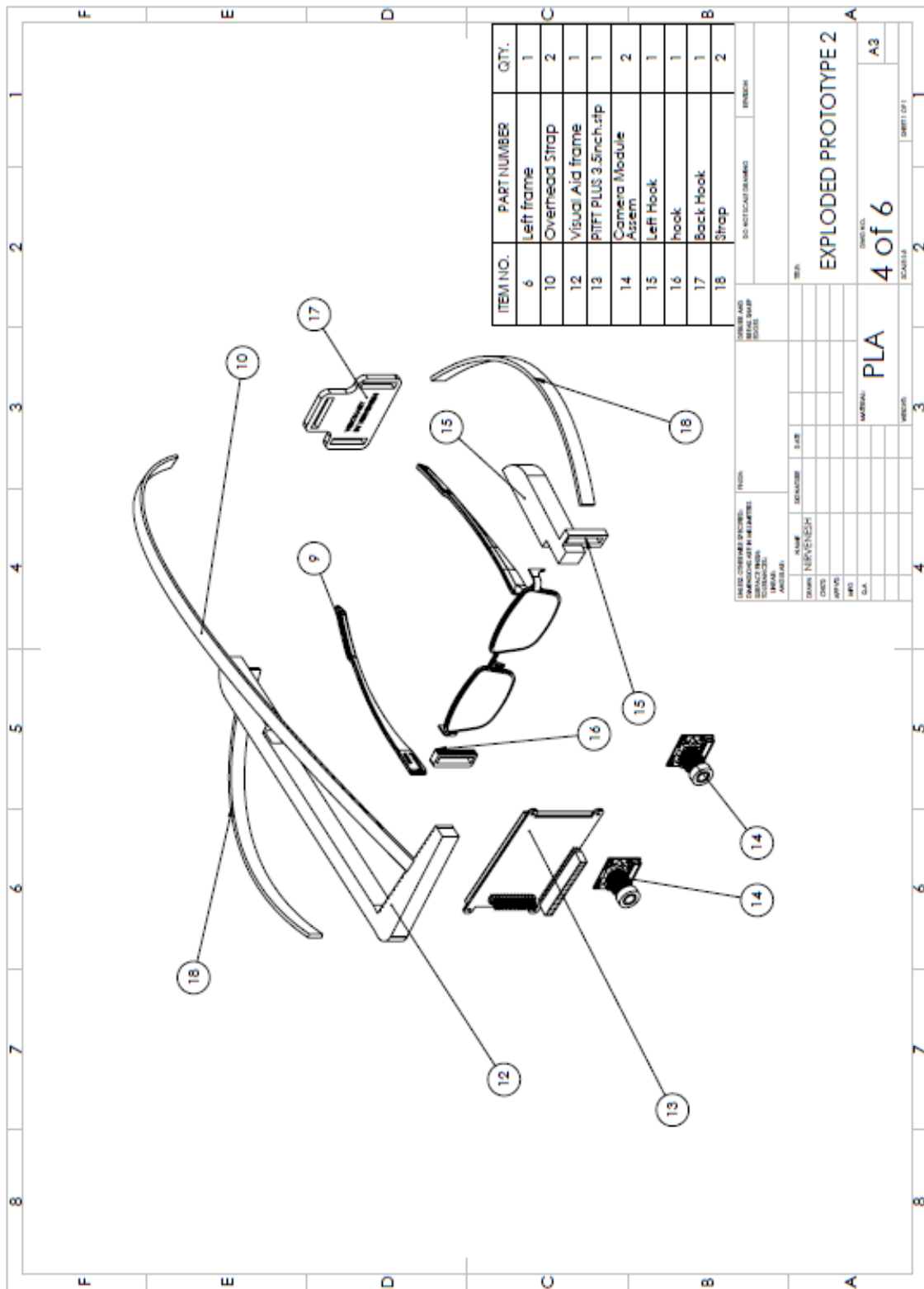
<b>Name :</b>	Ms Geetha Ramakrishnan
<b>Organisation:</b>	Tun Hussein Eye Hospital (THONEH)
<b>Position:</b>	Optician (Low Vision Specialist)
<b>Date :</b>	
<b>How is the visual aid Beneficial to your organization</b>	<p>The visual aid produced by Nirvenesh and his team at UNITEN provisions as a great tool for us to train new monocular visual impaired patients at the hospital. Normally, patients would initially have a tough to grasp and estimate distance with one eye as any of us would. The first prototype which was presented to us had a coloured map to differentiate distances. This is very sufficient for us to train patients here especially after glaucoma or truma çases.</p>
<b>Does the visual aid meet the expectations of the subjects at your organization ? (Comments)</b>	<p>The visual aid does meet the expectation as it meets the criterias when we initially mentioned the problem during the initial meetings</p>
<b>Recommendation and Comments</b>	<p>We expect the visual aid to have smaller screens as the current prototype has a big one. We also hope to be a bit lighter on the patient.</p>

Signature

(Geetha Ramakrishnan)

Ms. Geetha Ramakrishnan  
Head Optician (Low Vision)  
The Tun Hussein Onn National Eye Hospital  
Petaling Jaya, Kuala Lumpur





DESIGNER AND CHECKER		DATE	
DESIGNER	CHECKER	DATE	DATE
NAME: NIKHIL	NAME:	DATE:	DATE:
DESIGN NO:	DESIGN NO:	DATE:	DATE:
APP'D:	APP'D:	DATE:	DATE:
DATE:	DATE:	DATE:	DATE:
SCALE:	SCALE:	DATE:	DATE:

NO. NOTIFICATION DURING DESIGN

EXPLODED PROTOTYPE 2

MATERIAL: PLA

4 of 6

SCALE: 1:1

SHEET NO: 2

SHEET OF: 1

## APPENDIX J

### RESEARCH PHOTOS AT TAIPING HOSPITAL



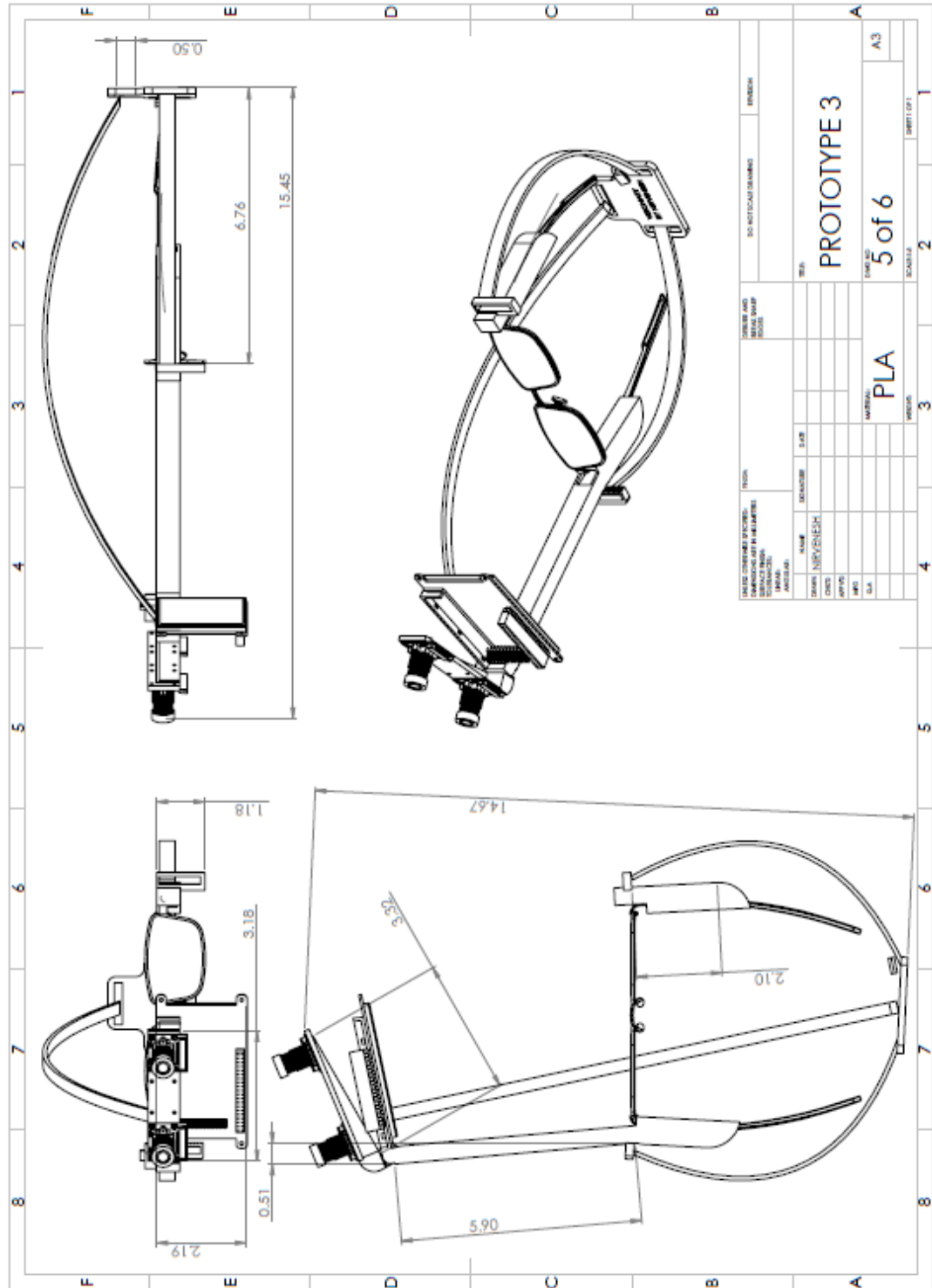
Figure 1 : Testing of Prototype 2 at Taiping Hospital



Figure 2 : Testing of Prototype 2 at Taiping Hospital with (from left) Prof Lee & Dr Sanggari

## APPENDIX K

### ORTHOGRAPHIC AND EXPLODED VIEW DRAWINGS OF PROTOTYPE 3





## APPENDIX L

### RESEARCH PHOTOS AT TUN HUSSEIN ONN EYE HOSPITAL (THONEH)



Figure 3 (from left) Ms Geetha Ramakrishnan and Nirvenesh during Visual Aid testing at THONEH



Figure 4 Testing of Visual Aid at THONEH with test subjects and setup

## **BIOGRAPHY OF AUTHOR**

Nirvenesh Ravindran was born in the mainland city of Penang on the 20<sup>th</sup> of December 1995, obtaining his early education in one of the oldest schools of the town Sekolah Kebangsaan St Mark's Butterworth. Throughout his journey in his secondary school at Sekolah Menengah Kebangsaan Dato Onn Butterworth, he has participated in many international events organised by the British Council of which he was accredited with a bronze award. He was also a state level debater representative at the time in 2011.

Upon entry for his tertiary studies at University Tenaga Nasional Putrajaya, for his Foundation in Engineering and Bachelor of Mechanical Engineering (Hons.), he has participated and organised many social and charitable events as the Head of Welfare for the Student representative Council of UNITEN. He was also chosen as the National Youth Representative to Japan on a delegation to the Mayor of the City of Hokkaido.

Upon completion of his Bachelor's degree, he was motivated to pursue further on for his love electronics and mechanical design, and hence pursued his post graduate studies in research while working as a Research Officer for a project with the collaboration of the Ministry of Energy, Science, Technology, Environment and Climate Change (MESTECC). He is now a Mechanical Engineer in one of the world's leading offshore engineering procurement and commissioning consultancy, McDermott Inc.